

THE UNIVERSITY OF MANITOBA

ULTIMATE TORSIONAL STRENGTH
OF PRESTRESSED RECTANGULAR CONCRETE BEAMS
REINFORCED PARTLY WITH DEFORMED STEEL BARS

by

Jeremiah A.N. M o r a

A THESIS

SUBMITTED TO THE FACULTY OF GRADUATE STUDIES
IN PARTIAL FULFILMENT OF THE REQUIREMENTS FOR THE DEGREE
OF MASTER OF SCIENCE

DEPARTMENT CIVIL ENGINEERING

WINNIPEG, MANITOBA

October 1974

ULTIMATE TORSIONAL STRENGTH
OF PRESTRESSED RECTANGULAR CONCRETE BEAMS
REINFORCED PARTLY WITH DEFORMED STEEL BARS

by

JEREMIAH A.N. MORA

A dissertation submitted to the Faculty of Graduate Studies of
the University of Manitoba in partial fulfillment of the requirements
of the degree of

MASTER OF SCIENCE

© 1974

Permission has been granted to the LIBRARY OF THE UNIVERSITY OF MANITOBA to lend or sell copies of this dissertation, to the NATIONAL LIBRARY OF CANADA to microfilm this dissertation and to lend or sell copies of the film, and UNIVERSITY MICROFILMS to publish an abstract of this dissertation.

The author reserves other publication rights, and neither the dissertation nor extensive extracts from it may be printed or otherwise reproduced without the author's written permission.



TABLE OF CONTENTS

	<u>PAGE</u>
I INTRODUCTION AND REVIEW	1
1.1 Introduction	1
1.2 Object of the tests	4
1.3 Dr. Hsu's theory	5
1.3.1 The effect of prestressing	8
1.4 Dr. Lampert's theory	9
1.4.1 The effect of prestressing	11
1.5 Illustrative example	12
II SPECIMENS AND TESTING EQUIPMENT	14
2.1 The test specimens	14
2.2 Reinforcement	15
2.3 Concrete for the test beams	19
2.4.1 The testing equipment	20
2.4.2 Instrumentation	20
III TEST OF MODELS AND RESULTS	32
3.1 The test set up	32
3.2 Testing of the specimens	34
3.2.1 Characteristic behaviour of the specimens	34
3.3 Evaluation of the strain gauge readings (Beam IV)	38
3.4 Strain Computation	40
3.5 Prestressing force	49
3.5.1 Initial prestressing	49

TABLE OF CONTENTS CONTINUED

	<u>PAGE</u>
3.5.2 Area of composite section	49
3.5.3 Computation of the losses in prestress	49
3.5.4 Creep factors	51
3.5.5 Prestressing force on Beam IV determined from the strain gauge readings	51
3.5.6 Loss in prestress from April 20 to Sept. 19	53
3.6 Experimental results	54
3.6.1 Torque twist	54
3.6.2 Ultimate torsional moment	58
3.6.3 Ultimate torsional moment computed in accor- dance with the equations of Hsu and Lampert	59
IV CONCLUSION	62
4.1 The effect of a void central core	62
4.2 Influence of the longitudinal reinforcement	64
4.3 Influence of transverse reinforcement	64
4.4 Effect of prestress on the angle of twist	65
4.5 Strain in the stirrups	66
4.6 Comparison with previous investigations	67
4.7 Suggestions for further research	75
V HISTORICAL BIBLIOGRAPHY	78
VI APPENDIX A: DESIGN OF THE FORM WORK FOR THE CASTING OF THE CONCRETE BEAMS	82

TABLE OF CONTENTS CONTINUED

	<u>PAGE</u>
A 1 Concrete pressure on the form work	82
A 2 Details of the form work	84
A 3 Composite section properties	86
A 4 Computation of the stresses	
System with loading	86
A 5 Deflection	87
VII APPENDIX B: DESIGN OF THE STEEL YOKE	89
B 1 Introductory remark	89
B 2 Analysis of the yoke	94
B 3 Check for stresses	100
VIII APPENDIX C: CROSS-SECTION AREAS FOR	
STRESS COMPUTATION	112
IX APPENDIX D: DETERMINATION OF THE CREEP FACTORS	113
X APPENDIX E: ULTIMATE TORSIONAL STRENGTHS OF 4	
BEAMS DETERMINED IN ACCORDANCE WITH	
THE EQUATIONS OF DR. HSU AND DR. LAMPERT	117
XI APPENDIX F: ULTIMATE TORSIONAL MOMENT OF THE TEST	
BEAMS COMPUTED IN ACCORDANCE WITH THE	
EQUATIONS OF DR. HSU AND DR. LAMPERT	123

SUMMARY

A laboratory investigation was undertaken to determine the ultimate strength of four 12" x 24" prestressed concrete beams subjected to pure torsion. The results obtained are reported and certain factors which proved to have significant influence on the torsional strength of structural concrete members are discussed. The ultimate torsional moments obtained by test are compared with those predicted by the equations of some previous investigators, and certain discrepancies are reported.

The test results show that the longitudinal reinforcement makes a considerable contribution to the ultimate torsional strength of the reinforced beam. The results also indicate that prestressing reduces the pre-cracking angle of twist of the test beam and increases the pre-cracking torsional load.

Suggestions for further research are made, which could lead to a better understanding of the mechanism of the torsional resistance of prestressed concrete beams.

ACKNOWLEDGEMENTS

I wish to acknowledge the assistance and advice received from Professor A.M. Lansdown, Ph.D., M.E.I.C., M.I.A.B.S.E., under whose direction this investigation was carried out. I also wish to express my thanks to Dr. K.R. McLachlan for the good suggestions he made expecially with regard to the instrumentation of the test specimen.

LIST OF TABLES

<u>TABLE</u>	<u>PAGE</u>
1 Properties of steel reinforcement	17
2 Reinforcement of the beams	17
3 Concrete compressive strength for the concrete of Beams No. I to IV	19
4 Calibration of the hydraulic jacks	23
5 Shrinkage strain (Beam IV)	43
6 Creep and shrinkage strain (Beam IV)	44
7 Strain in the stirrups of (Beam III)	46
8 Initial prestressing; area of composite sections	49
9 Creep factors	51
10 Angle of twist vs. loading	54
11 Ultimate forces and moments	59
12 Ultimate torsional moments	60
13 Comparison of the test results with the results predicted by Hsu/Hognestad and Lampert equations	61
14 Contributions to the ultimate torque	69
B 1 Member end forces for the yoke adjusted for 12" x 24" test specimen	94
B 2 Member end forces for the yoke adjusted for 24" x 24" test specimen	95
E 1 Properties of the non-prestressed reinforcement	117
E 2 Reinforcement of the beams	118

LIST OF FIGURES

<u>FIGURE</u>	<u>PAGE</u>
1 The Proposed Failure Surface (Hsu)	6
2 Force diagram	7
3 Diagram to illustrate the truss theory	10
4 Graphical Representation of the Ultimate torsional Moments	13
5 Test Beams: cross-sections and reinforcement	16
6 Test set-up	21
7 Calibration graph of the hydraulic jacks	24
8 Chart for the reading of the angle of twist	27
9 Large scale angle of twist chart	27
10 Position of the strain gauges on the longi- tudinal bars and tendons in Beam IV	30
11 Position of the strain gauges on two stirrups in Beam III	31
12 Structural System of the yoke for the 12" x 24" beam	33
13 Chart for loading jack 1	39
14 Chart for loading jack 2	39
15 Changes in the length of Beam IV due to the influences of shrinkage and creep	47
16 Tensile strain in the prestressing tendons	48
17 Increase in concrete compressive strain versus decrease in tendon tensile strain due to creep and shrinkage	48

LIST OF FIGURES CONTINUED

<u>FIGURE</u>	<u>PAGE</u>
18 Torque vs Twist diagram for Beam I	56
19 Torque vs Twist diagram for Beam II	56
20 Torque vs Twist diagram for Beam III	57
21 Torque vs Twist diagram for Beam IV	57
22 System for the computation of the ult. moment	58
23 Cross sections, reinforcement and ultimate torsional strengths of the test beams	63
24 Influence of the wall surface friction on the lateral concrete pressure	82
25 Form work (elevation)	84
26 Form work (plan)	84
27 A portion of the wall with stiffner (plan)	85
28 Loading of the wall	85
29 Yoke set-up for large test specimen	90
30 Yoke adjusted for smaller test specimen	91
31 Yoke and supporting system for the 12" x 24" test specimen	92
31a Structural System of the yoke for the 12"x24" beam	93
32 Joints for detailed design	97
E 1 Beam cross section	117

LIST OF PLATES

<u>PLATE</u>	<u>PAGE</u>
1 Reinforcement cage with tendons for Beam IV	18
2 Set up for prestressing	18
3 Calibration of hydraulic jack	25
4 Test set up: a hydraulic jack in position on the yoke at the middle of the beam	25
5 Test set up: apparatus for the reading of the angle of twist mounted on the beam	29
6 Test set up: yoke at the end of a test beam in position	29
7 Test set up: all three yokes in position	35
8 Some pieces of apparatus used for obtaining strain gauge information: (a) car battery, (b) data acquisition system	36
9 Typical torsion cracks	37
10 Beam I just before failure occurred	37

NOTATION

- A_o = area enclosed by the stringers. A stringer is the longitudinal bar or tendon at each corner of the beam
- A_t = cross-sectional area of one stirrup leg
- b = smaller overall dimension of a rectangular cross section
- b_1 = smaller centre to centre dimension of a closed rectangular stirrup
- B_y = yield force in one leg of stirrup
- d = larger overall dimension of rectangular cross section
- d_1 = larger centre to centre dimension of a closed rectangular stirrup
- f'_c = compressive strength of 6 x 12 - in concrete cylinder
- f_{ly} = yield strength of longitudinal bars
- f_{pa} = average effective prestress after all losses
- f_{ty} = yield strength of stirrup
- m = ratio of volume of longitudinal bars to volume of stirrups; $0.7 \leq m \leq 1.5$
- M_{tp} = contribution of the concrete to the torsional strength of a member with web reinforcement
- M_{tp}^* = ultimate torsional moment of a prestressed beam
- p_l = volume of longitudinal reinforcing bars per length s
- p_t = volume of a rectangular stirrup
- s = spacing of stirrup in the direction parallel to the longitudinal axis of beam

T_u = ultimate torque of reinforced concrete member

T_{up} = ultimate torque of a prestressed member with web reinforcement and longitudinal reinforcing bars

T_{uo} = ultimate torque of a member subjected to pure torsion

u = perimeter of the rectangle formed by the stringers

Z_y = total yield force of the longitudinal reinforcement (bars and tendons)

CHAPTER I

INTRODUCTION AND REVIEW

1.1 Introduction

Structural soundness had always been a major concern of design engineers. Such forces as the bending moment, shear, thrust and torsion resulting from the design load must be effectively resisted by the structure. In the past it was assumed that the torsional effects were minor. In some cases the torsional effects were accounted for by the large factors of safety used in flexural designs. The shear stress determined by elastic or plastic analysis was added to the torsional stress, and the total was compared with the specified allowable stress. This practice was found to be unsatisfactory (15,27). In addition to structural adequacy, economy also exerts a considerable influence on the design. There is an increasing tendency to refine the design methods. Increasing use is being made of structures in which the torsional moment resulting from the applied load can no longer be regarded as minor in comparison with the flexural moment. Curved bridge beams, spandrel beams and spiral staircases are a few examples. Even in the structures in which the torsional moment remains comparatively low, the influence of the torsion on the flexural

capacity of the member could be considerable. It is necessary to give explicit consideration to torsion when its magnitude in a structural member is great or when its influence on the flexural capacity of the member is significant. These considerations call for more attention to the study of torsion in structural design.

Systematic study of the behaviour of structural concrete subjected to torsion is relatively new, in comparison with the study of the behaviour under such forces as bending moment and shear. The amount of research work and the publications available in this area of concrete technology are comparatively small. The earliest major contributions to the literature of torsion in structural concrete (1,2,5) dealt almost exclusively with plain concrete.

In the 1920's some investigators started to direct their attention to torsion in reinforced concrete. Reinforced concrete members subjected to pure torsion were the first to be investigated (2). In 1945 an investigation on reinforced concrete subjected to torsion and bending was conducted (3). This was followed later by similar experiments (7,8,9,11). The scope of these experiments gradually widened to include the effect of shear (3,12,13,14,15,16).

One of the earliest investigations in torsion in structural concrete that took the effect of prestressing into consideration was the work of H . Nylander (3), 1945. Similar experiments on pure torsion of prestressed concrete were carried out at later dates (17,18,19). The behaviour of prestressed concrete members in combined torsion and bending was gradually receiving the attention of investigators (17,20,21,22). More recently published materials on prestressed concrete beams subjected to torsion with bending and shear have become available (23,24,25,26).

Controversies and differences of opinion sometimes arose when a subject was investigated by different people, each working under different conditions and making assumptions he considered pertinent to the particular cases under investigation. Such was the case with the study of torsion in structural concrete. The majority of the experiments were aimed at determining the ultimate strength of concrete under the influence of pure torsion, torsion with bending or torsion with combined bending and shear. From their investigations some authors were able to develop equations which, they claimed, could predict the ultimate torsional strength of concrete. A concluding remark of one of the investigators (28) quoted below indicated the existence of differences in the torsional strength of reinforced concrete beams as predicted by theories put forward by some of the authors.

"Torsional theories developed by Rausch, Cowan, and Lessig have been reviewed. Presently, these theories are the basis for the German, Australian and Soviet Codes, respectively. When compared with test results each of these three approaches was found to significantly overestimate the torsional strength of many reinforced concrete beams."

In one of the recent publications (23) Lampert claimed to have developed equations which provided accurate predictions for the torsional strength of both reinforced and prestressed concrete beams.

1.2 Object of the tests

To help to shed some light on the differences existing between some of the existing theories, it was concluded that laboratory tests of selected concrete beams would be required.

In order to keep the number of parameters involved in such tests as small as possible, investigation of the ultimate strength of the beams for pure torsion was considered appropriate. To take all major forms of concrete

reinforcement into consideration, the effect of prestressing was also included in the investigation.

The writer selected the work of two authors, each of them having published a number of articles on torsion in structural concrete, as a basis for the present investigation. Each of the chosen authors, Dr. Thomas T.C. Hsu and Dr. Paul Lampert, have received recognition in technical circles, but their theories show substantial discrepancies in the predicted ultimate torsional strength of reinforced and prestressed concrete beams. The writer therefore decided to carry out laboratory tests on a group of concrete beams reinforced with intermediate grade deformed bars and prestressing tendons, with the aim of clarifying some discrepancies between the two theories. A brief summary of the two theories is given below.

1.3 Dr. Hsu's theory (28,29)

The equation for the ultimate torque of a reinforced concrete beam according to Hsu was derived using a failure surface, the plane of which was perpendicular to the wider face of the cross section and inclined at 45° to the axis of the beam. This failure surface did not intersect the shorter legs of the stirrups (Fig. 1). The indications

shown in Fig. 1 were defined as follows:

$A_t f_{ty}$ = yield force in the stirrups

Q_{1x}, Q_{1y} = dowel force in x and y directions
respectively of the corner bars outside
the shear compression zone.

a = depth of shear compression zone

P = vertical force at the concrete compression zone of the failure plane to balance the force of the stirrups.

P is provided by the shear strength of the concrete element between cracks in the shear compression zone, and by the resistance of the bars.

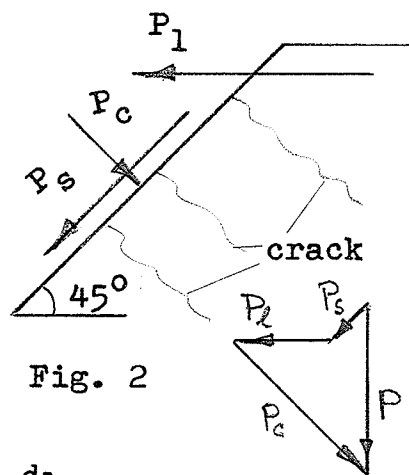


Fig. 2

From Fig. 2,

$$P = \sqrt{2} P_s + P_1$$

P_1 = longitudinal force in the bars

P_c = compressive force in concrete

P_s = shear in compression zone

$$T_{us} = \frac{d_l}{s} A_t f_{ty} X_{lt} = \text{ultimate moment contributed by stirrups on the tension side of the beam.}$$

Based on the foregoing forces the following equation for ultimate torque was derived:

$$T_u = \frac{2.4}{\sqrt{b}} \cdot b^2 d \sqrt{f'_c} + (0.66m + 0.33 \frac{d_1}{b_1}) \frac{b_1 d_1 A_t f_{ty}}{s} \text{ -----(1)}$$

$$\frac{2.4}{\sqrt{b}} \cdot b^2 d \sqrt{f'_c} = \text{contribution made by concrete.}$$

$$(0.66 + 0.33 \frac{d_1}{b_1}) = \text{slope of the curve of equation (1).}$$

m = ratio of the volume of longitudinal bars to volume of stirrups.

s = spacing of stirrup in the direction parallel to the longitudinal axis of beam.

1.3.1 The effect of prestressing

For a prestress of less than 0.7 of the compressive strength of the concrete, a prestressed beam is predicted to fail in the same manner as a non-prestressed beam. The bending mechanism of torsional failure for non-prestressed beams could be applied to prestressed beams also. The ultimate torsional strength of a prestressed beam ^{is} was given by the equation

$$M_{tp}^* = M_{tp} \sqrt{1 + 10 \frac{f_{pa}}{f'_c}} \text{ ----- (2)}$$

where M_{tp}^* = ultimate torsional moment of a prestressed beam;

M_{tp} = contribution of the concrete to the strength of a member with web reinforcement (26);

f_{pa} = average effective prestress after all losses;

f'_c = compressive strength of concrete.

1.4 Dr. Lampert's theory (23,24)

Dr. Lampert's approach was based on the truss theory. In a reinforced concrete beam subjected to pure torsion tensile stress occurred in the reinforcement and compressive stress in the compression diagonals in the concrete. Thus a truss model resulted (Fig. 3). For beams which were not over reinforced, both the longitudinal and the transverse reinforcements yielded before the concrete compression diagonals were crushed. These compression diagonals were not always inclined at 45° . It was observed that they adjusted their inclination in such a way that the longitudinal and transverse reinforcement both reached their yielding point. Sometimes adjustment in the proportion of force resisted by the particular reinforcement resulted. There was no transfer of force in the case of equal volume reinforcement, where the volume of the longitudinal reinforcing bars per unit length of beam was equal to that of stirrups in the unit length assuming similar yield strengths. In such cases the compression diagonals were inclined at 45° to the longitudinal axis of the beam.

The reinforcement at the corners served as support for the compression diagonals and enhanced their resistance to crushing. In solid beams the core was assumed to contribute little or nothing to the torsional capacity of the beam.

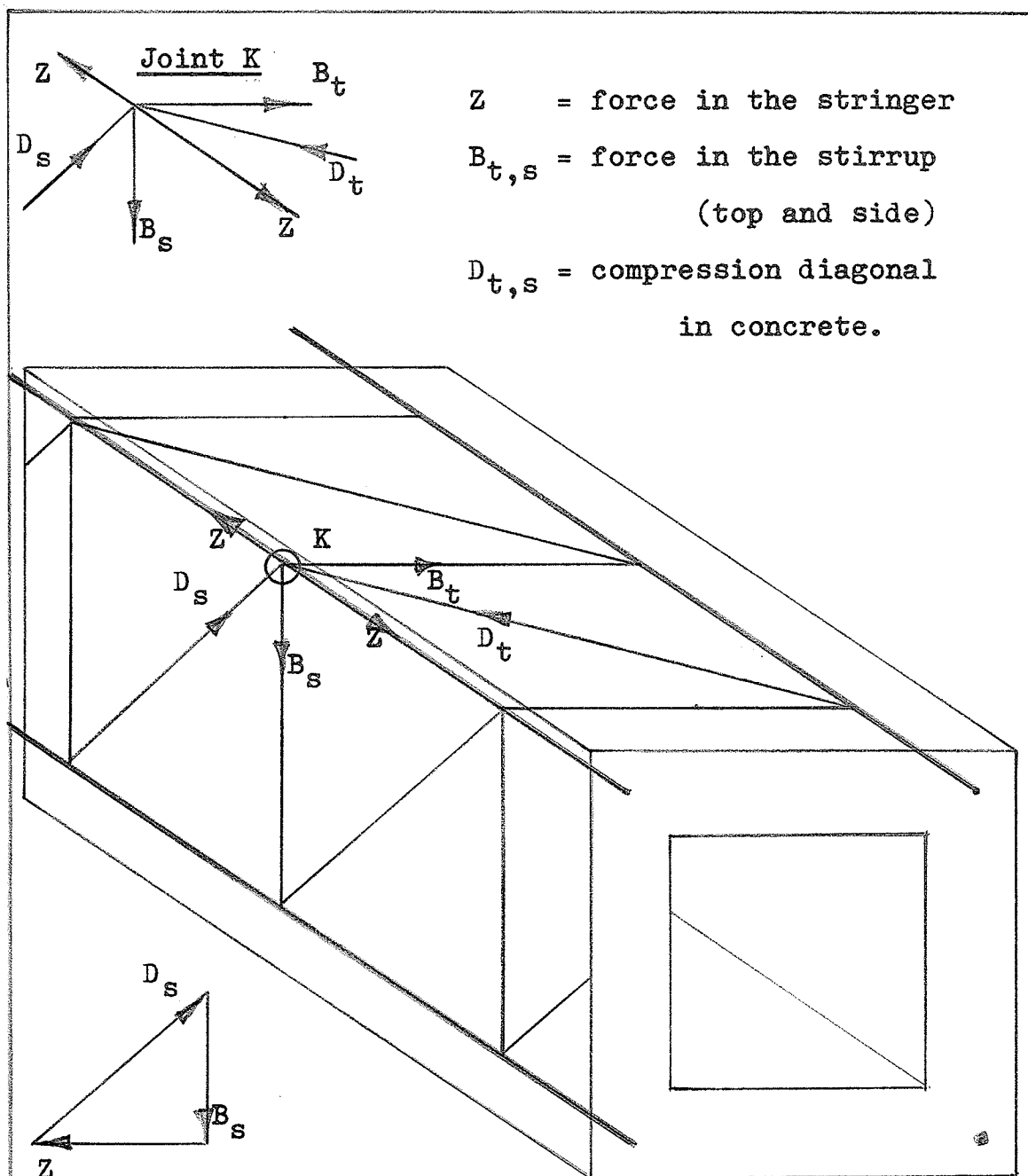


Fig. 3 Diagram to illustrate the truss theory

It made no difference whether the longitudinal reinforcement was concentrated at the corners or was distributed through the perimeter of the cross section.

The equation for the ultimate capacity of a beam under pure torsion was given by

$$T_{uo} = 4A_o \sqrt{\frac{B_y \cdot Z_{fo}}{s \cdot u}} \text{-----} (3)$$

For pure torsion Z_{fo} was defined as the yield force of the longitudinal reinforcement concentrated at each corner of the beam. $Z_{fo} = \frac{1}{4} Z_y$

$$T_{uo} = 4A_o \sqrt{\frac{1}{4} \frac{B_y \cdot Z_y}{s \cdot u}}$$

$$\text{therefore } T_{uo} = 2A_o \sqrt{\frac{B_y \cdot Z_y}{s \cdot u}} \text{-----} (4)$$

where A_o = area enclosed by the stringers. A "stringer" was defined as the longitudinal bar or tendon at each corner of the beam;

Z_y = total yield force of the longitudinal reinforcement (bars and tendons);

B_y = yield force in one leg of stirrup;

s = stirrup spacing;

u = perimeter of the rectangle formed by the stringers.

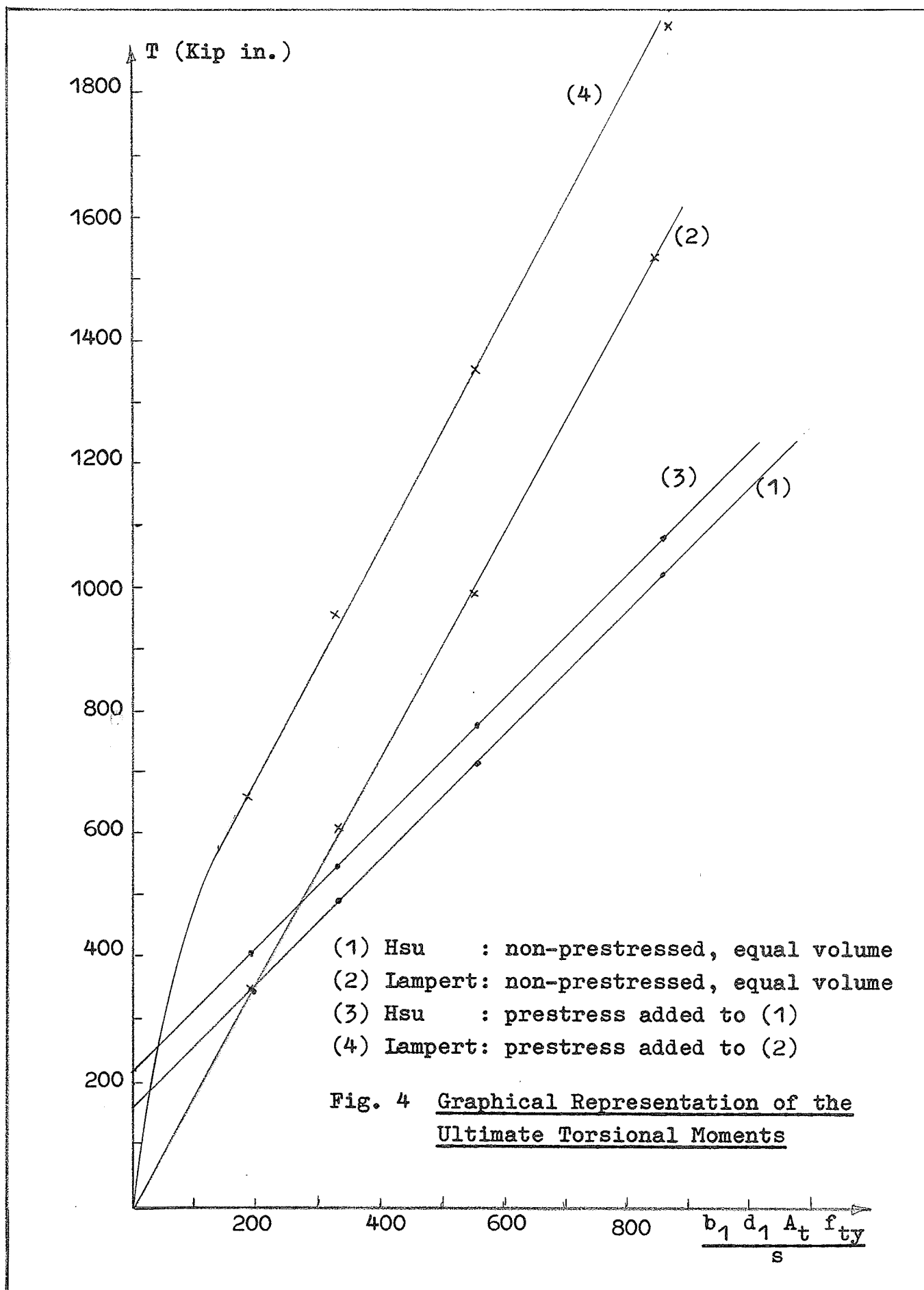
1.4.1 The effect of prestressing

In prestressed beams the prestressing tendons were assumed to behave like longitudinal reinforcing bars with

higher yield strength. Their yield force became included in Z_y of equation (4), enabling the equation to be used for both reinforced and prestressed beams.

1.5 Illustrative example

To illustrate the difference between the two theories, computations of the ultimate torsional strengths of a group of reinforced concrete beams based on the theories have been carried out, Appendix E. The computed ultimate torsional moments so obtained are represented graphically in Fig. 4. The differences in the predicted ultimate strengths of the beams as indicated in the example were of such a proportion that an investigation into the possible factors responsible for these differences could be justified.



CHAPTER II

SPECIMENS AND TESTING EQUIPMENT

2.1 The test specimens

According to the two theories described in the preceding chapter the torsional capacity of a rectangular reinforced concrete beam, as predicted by the equations (1) and (4), is a function of the geometry of the cross section and the quantity and the properties of the reinforcement. The test beams chosen for the present investigation were similar in size to some of the beams tested by Dr. Hsu and Dr. Lampert for the verification of their theories. By keeping the size of the four test beams constant and varying the amount of longitudinal and transverse reinforcement, the influence of the reinforcement on the torsional capacity could be given closer study. Moreover Dr. Hsu's experimental results (29) have challenged the validity of the law of similitude by which, according to Hsu, the ultimate torque of a model was usually assumed to be linearly related to that of its prototype. Further investigation of the size effect, which would necessitate the testing of a series of beams of different sizes is outside the scope of the present work. The only variation in the geometry of the concrete cross section employed

was the inclusion of the hollow beam. The primary purpose of this was to investigate the effect of the absence of concrete core on the torsional strength of a reinforced concrete beam. To this effect, Beams III and IV were identically reinforced. But whereas Beam III was solid, Beam IV had a rectangular void filled with a material of negligible stiffness in comparison with that of concrete.

2.2 Reinforcement

Not only were the overall dimensions of the four test beams kept constant, but also identical transverse reinforcement was adopted for Beam I and Beam II. Each had $\frac{3}{8}$ " ϕ stirrups at 4.75" spacing. However, Beam I contained twice as many longitudinal reinforcing bars and thrice as many prestressing tendons as Beam II. This arrangement provided the means of estimating the influence of longitudinal reinforcement on the torsional capacity of the beams. The beams were not designed with any specific ultimate strength in view, since the primary purpose was to determine the effect of the longitudinal reinforcement. From this a better study of the ultimate strengths predicted by the two theories could be made.

The cross sections of the four test beams are shown in Fig. 5 (page 16). Each beam had a total length of 19.5 ft. $\frac{3}{8}$ " ϕ deformed bars having a yield strength of 56.4 Ksi were used for both the longitudinal and for the transverse reinforcement of each beam. Each of the

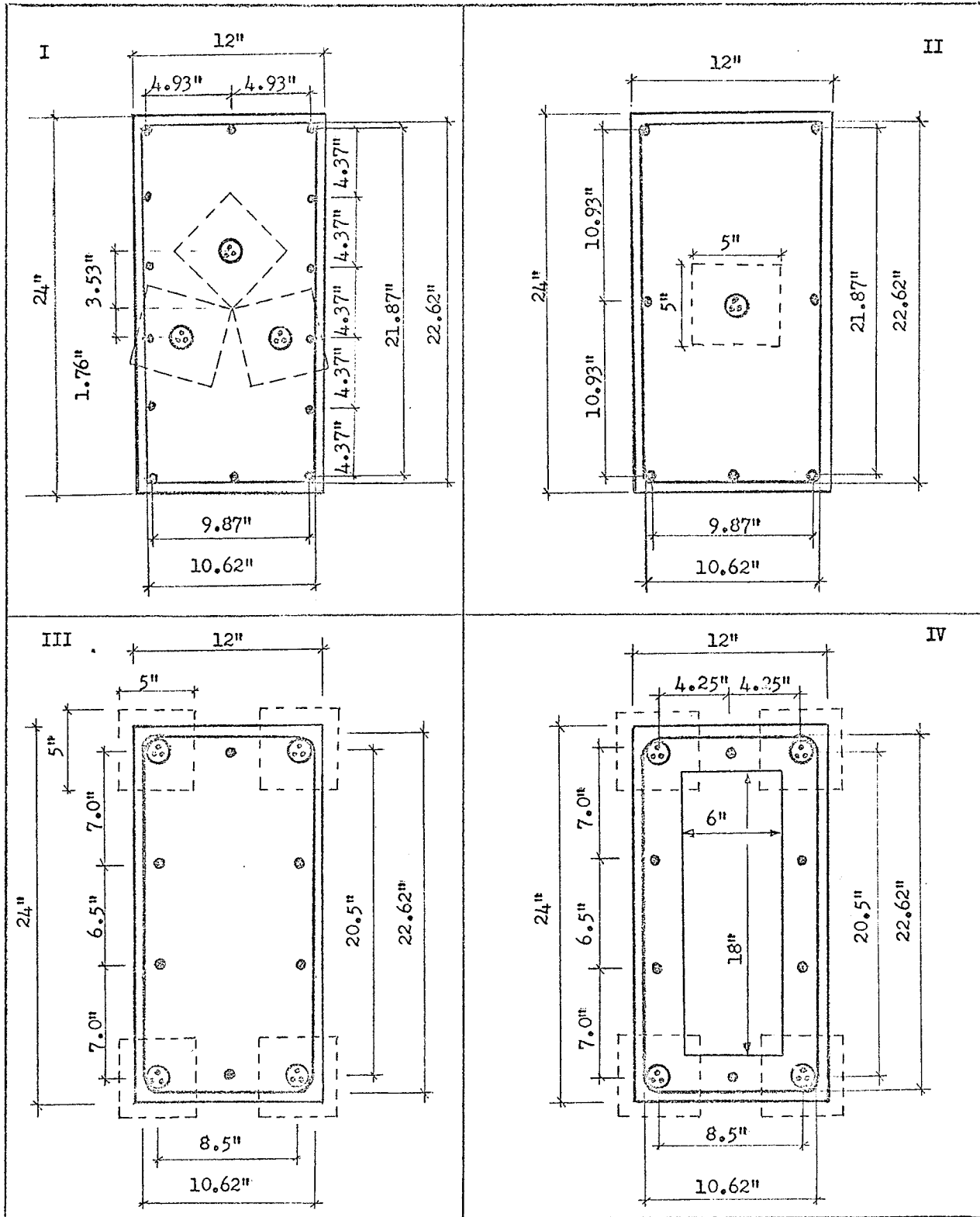


Fig. 5 Test Beams : cross-sections and reinforcement

prestressing tendons consisted of three wires with button heads (BBR System), each wire having a diameter of 0.275 inch and a yield strength of 241.3 Ksi. The three wire tendons were each encased in a 1.5 inch diameter metal duct which provided space for grouting in cases where grouting was employed. At each end of the beam a 5 inch square steel plate one inch thick provided the necessary bearing and anchorage for the heads of each post-tensioned tendon. Plate No. 1 shows the reinforcement cage for Beam IV. The set up for prestressing is shown in Plate No. 2.

Table 1 Properties of steel reinforcement

Reinforcement	Diam.(in)	Area(in ²)	f _y (ksi)
Longitudinal bars	3/8	0.11	56.4 [*]
Stirrups	3/8	0.11	56.4 [*]
Prestressing wires	0.275	0.0594	241.3 ^{**}

* Average of 6 tests in laboratory

** Supplied by manufacturer

Table 2 Reinforcement of the beams

Beam	Longitudinal reinforcement		Transverse reinforcement
	Number of $\frac{3}{8}$ " ϕ bars	Number of pre-stressing wires	Spacing of $\frac{3}{8}$ " ϕ stirrups
I	14	9	4.75 in.
II	7	3	4.75 in.
III	6	12	5.5 in.
IV	6	12	5.5 in.

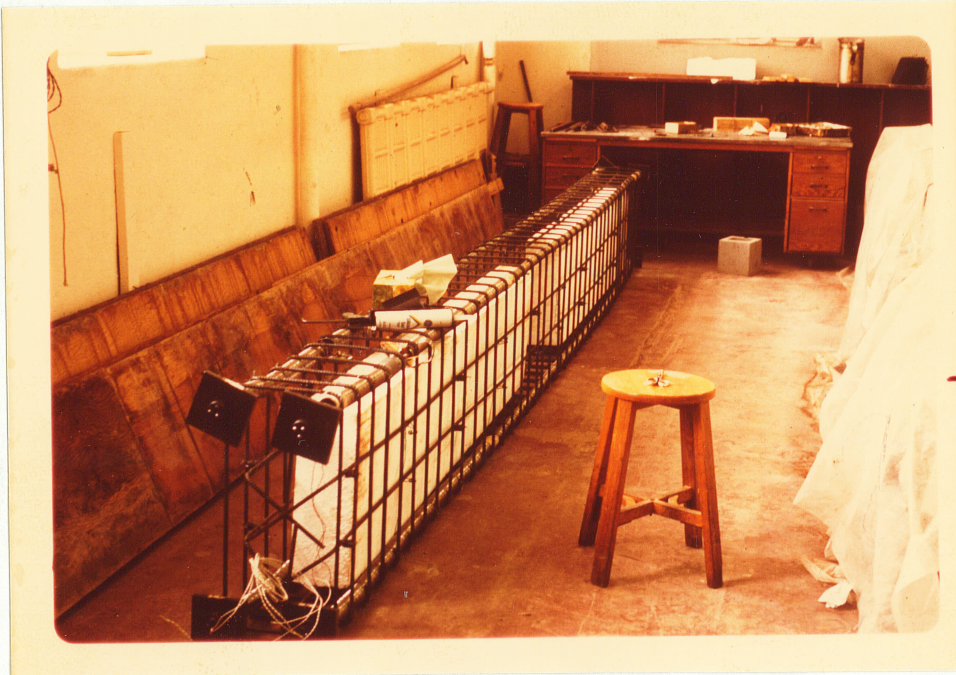


Plate No. 1

Reinforcement cage with tendons for Beam IV

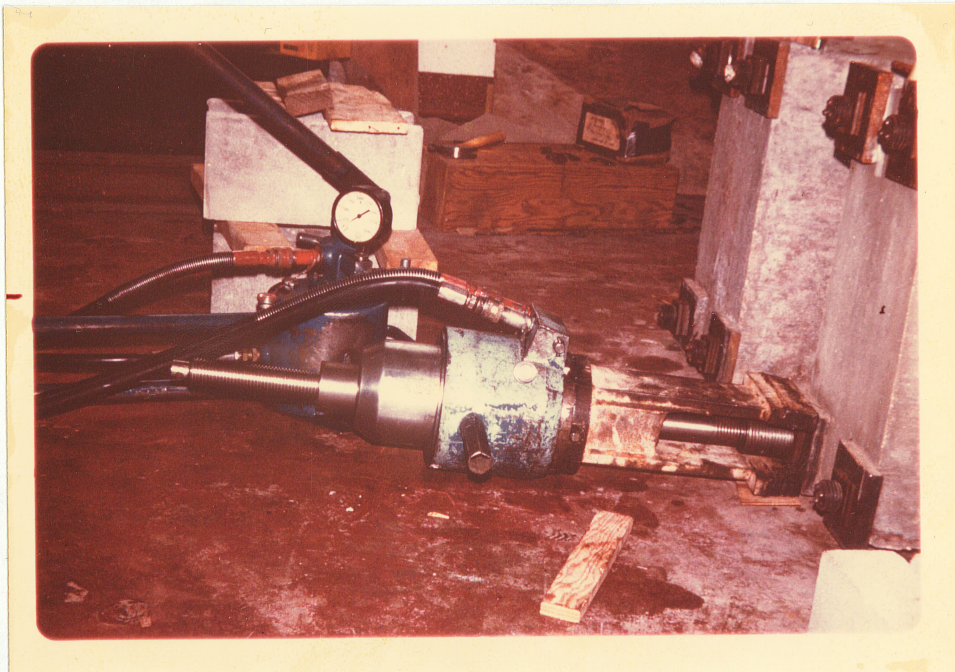


Plate No. 2 Set up for prestressing

2.3 Concrete for the test beams

About 41 cu.ft. of unvibrated concrete was required for the manufacture of each of the solid beams. The concrete mixing machine in the Civil Engineering laboratory produces only 3.5 cu.ft. in one batch. The use of this machine to provide the concrete necessary for one beam would require many operations. Even with exercise of great care, this could result in differential hardening and inhomogeneity of the concrete in each beam. To avoid such occurrences, the concrete required for the beams was obtained from a commercial firm. The compressive strengths of the concrete for the Beams I to IV as determined by cylinder tests are shown in Table 3.

Table 3 Concrete compressive strength for the
concrete of Beams No I to IV (psi)

I	II	III	IV
5220	4840	6520	4860
5930	4910	7220	5240
6160	4170	7050	4900
Average compressive strength			
5770	4640	6930	5000

To prevent bulging and therefore ensure that the desired overall dimensions of the beams cross sections were achieved, a careful and detailed design of the timber form work

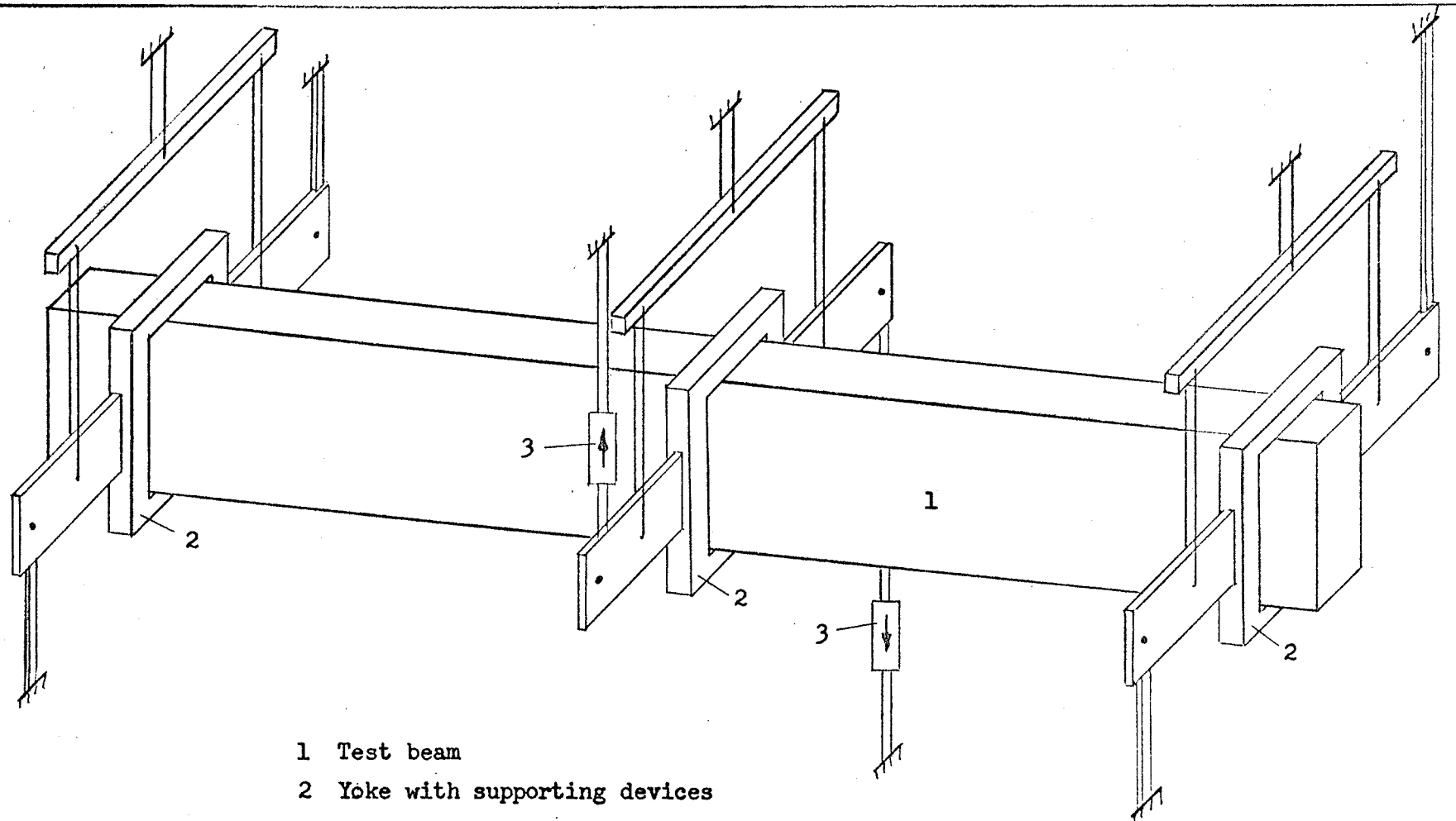
for the beams was necessary. The design details are contained in Appendix A.

2.4.1 The testing equipment

In the absence of a complete testing rig suitable for torsional tests of large sized reinforced concrete beams, the manufacture of some specialized equipment was undertaken. These consisted essentially of three steel yokes. Two of them were employed to constrain the ends of each beam, while the third, mounted at the middle of the beam, provided the means of applying the necessary torsional moment. The detailed design of the yoke is shown in Appendix B. Other pieces of apparatus needed for the tests included two hydraulic jacks. These, together with the necessary connecting parts and the already existing testing frames constituted the system for the application of the torsional force (Fig. 6).

2.4.2 Instrumentation

For the interpretation and compilation of the test results, the collection of some pieces of information about the behaviour of the test specimens was necessary. Accurate information about the creep and shrinkage of the concrete was necessary in order to determine their effect on the prestressing force applied to the beams. It was necessary to know the amount of force applied to



- 1 Test beam
- 2 Yoke with supporting devices
- 3 Loading jack

Fig. 6 : Test set-up

the two hydraulic jacks in order to be able to compute the magnitude of the applied torsional moments. A knowledge of the state of strain in the reinforcement at different stages of the experiment would provide some information for the evaluation of the test results.

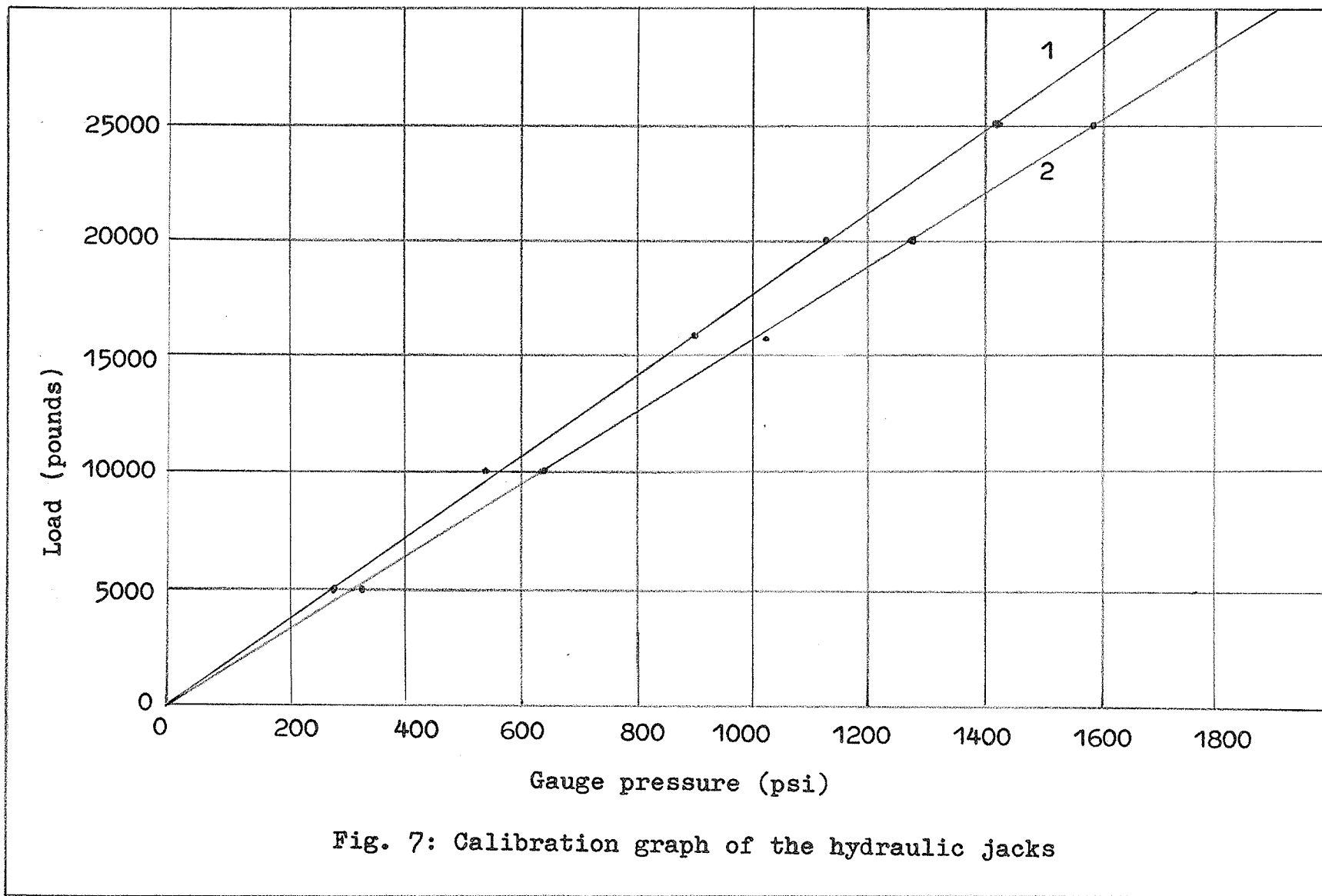
The calibration of the two jacks is shown in Table 4. The applied load versus the gauge pressure is represented by the linear graphs in Fig. 7. Any load which is applied by the calibrated jack and which is determined on the basis of load linearly related to gauge pressure could be subject to some degree of error. Due to imperfection such as leakage through the valves of the hydraulic jacks, the load versus gauge pressure coordinates obtained by calibration do not lie exactly on a straight line. Differences in the order of 500 pounds could occur between the actual applied load and that determined on the basis of load linearly related to gauge pressure. For an applied load in the order of 12000 pounds such difference would produce an error of about 4 %. Plate No. 3 shows the set up for the calibration. The position of a jack on the middle yoke is shown in Plate No. 4.

A group of metal film strain gauges was used in the test, by means of which the creep and shrinkage effects were determined. These gauges also provided the means of comparing the prestressing force indicated by

Table 4: Calibration of the hydraulic jacks

-23-

Loading Stage	Applied Force (lb)	Gauge Pressure (psi)	
		Jack 1	Jack 2
1	5000	280	320
2	10000	560	640
3	12000	680	770
4	14000	790	890
5	16000	910	1020
6	18000	1020	1140
7	19000	1070	1210
8	20000	1130	1270
9	20500	1160	1300
10	21000	1190	1340
11	21500	1220	1370
12	22000	1250	1400
13	22500	1275	1430
14	23000	1300	1460
15	23500	1330	1490
16	24000	1360	1530
17	25000	1418	1590
18	26000	1470	1650
19	27000	1530	1720



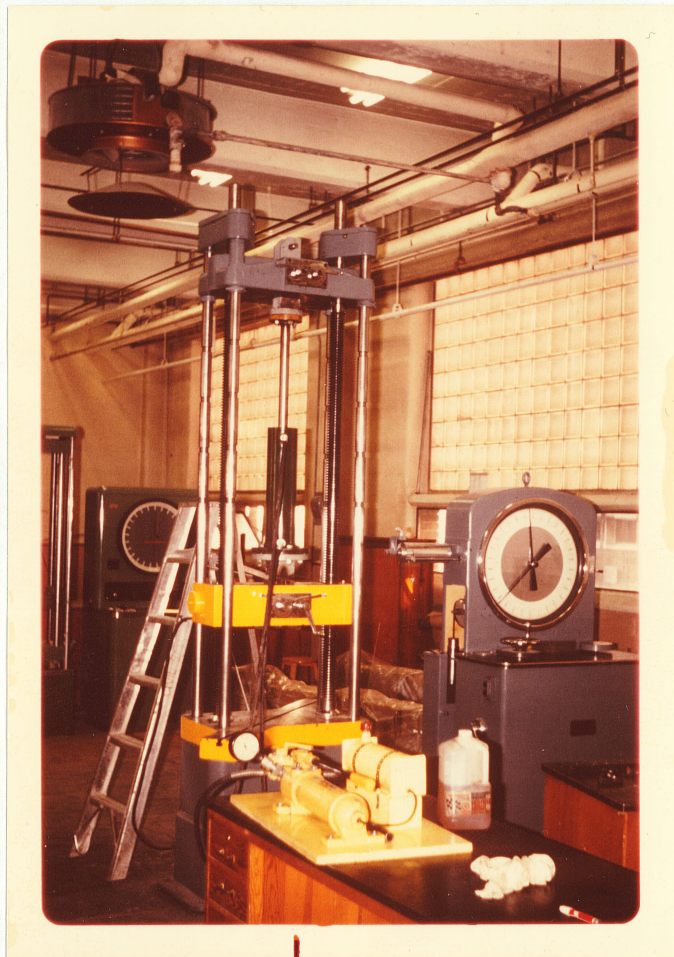
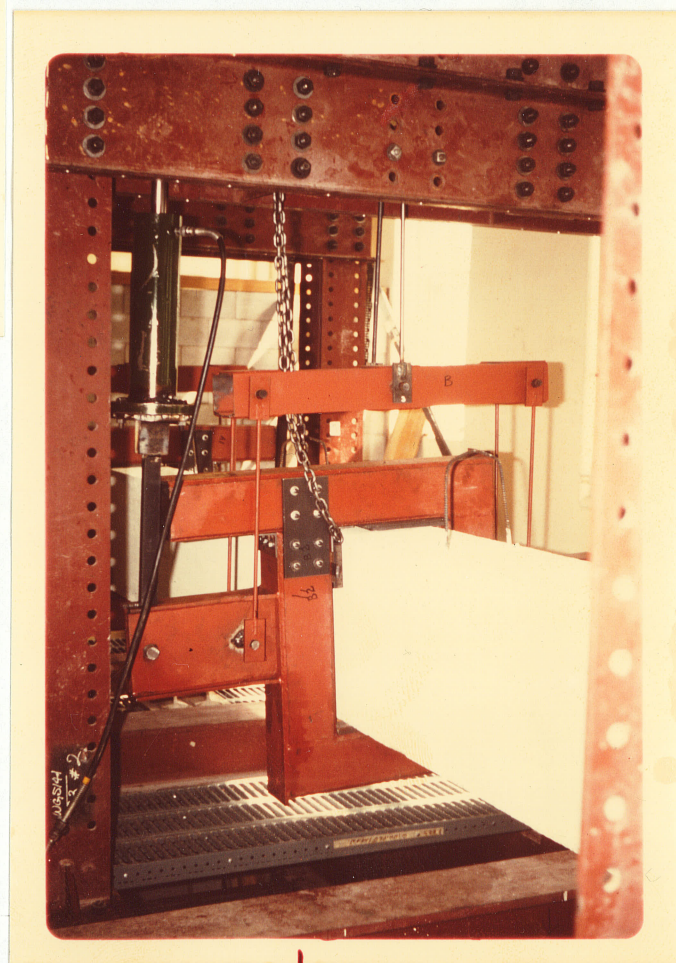


Plate No. 3
Calibration of the
hydraulic jack

Plate No. 4
Test set up: a hydraulic jack
in position on the yoke at
the middle of the beam



the readings on the dial gauge on the prestressing jack with that computed from the known stress-strain relation of the prestressing tendons supplied by the manufacturers.

Apparatus for determining the angle of twist of the beams under the influence of torsional loading was not readily available. However a device was improvised which crude as it appeared, did serve the purpose well. The principle of angle of twist method of measurement is shown in Fig. 8. A chart (A) graduated in degrees was attached to each end and also to the middle of each test beam. Each was so placed that the plane of the chart was perpendicular to the longitudinal axis of the beam, and there was no relative movement between the beam and the chart. A very thin string attached to a plumb bob (B) was fixed onto the point (C) from which the calibration lines radiated. As the beam was twisted about its axis the graduation lines rotated relative to the vertical plumb line. The actual chart used in the experiment is shown in Fig. 9. By means of the chart, the angle of rotation could be read to one fifth of a degree. The difference between the rotations at one end of the beam and at the middle of the beam determined the angle of twist for one half of the beam length. Plate No. 5

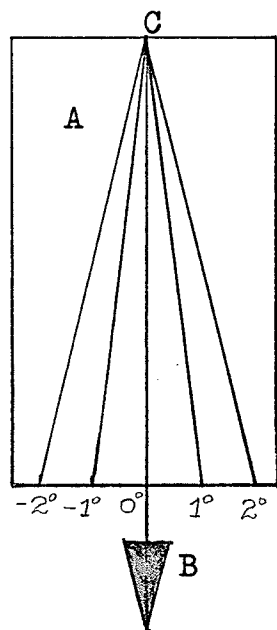


Fig. 8 Chart for the reading of the angle of twist

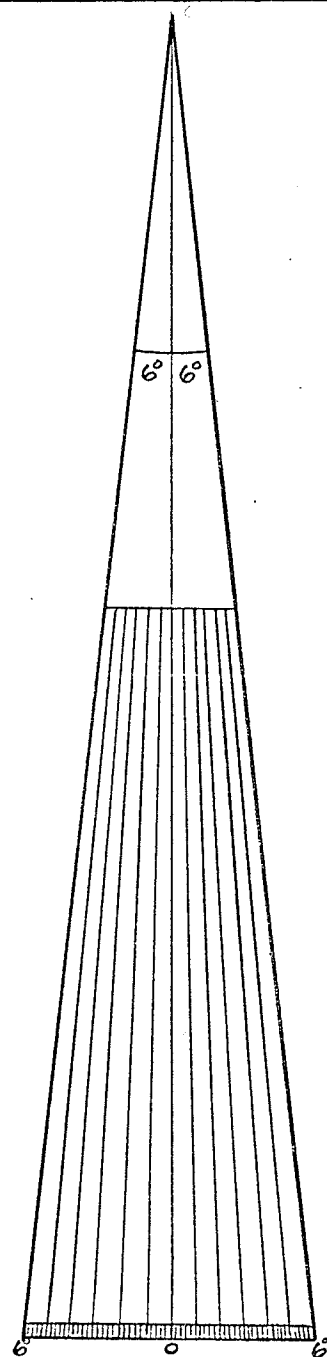


Fig. 9 Large scale chart
(2/3 the original
size)

shows the device mounted at the middle of a test beam for the measurement of the angle of twist. The constraint yoke at the end of a test beam is shown in Plate No. 6.

In order to determine the strain in the reinforcing bars and in the prestressing tendons, 5 mm metal film strain gauges were attached on some of the reinforcing bars, stirrups and prestressing wires. A couple of high elongation strain gauges were also attached on two of the prestressing wires (Fig. 10).

An accurate determination of the losses in the prestressing force due to such important factors as creep and shrinkage in the concrete was necessary. There were no frictional losses since the prestressing tendons were straight. The creep and shrinkage losses were determined by strain losses in the prestressing tendons and checked or compared with the shortening in the length of the beam under the influence of prestress.

The strain gauges numbered 8, 19, 20, 21, 22 and 23 were attached on reinforcing bars (Fig. 10). All of the $\frac{3}{8}$ " ϕ reinforcing bars were fully bonded to the concrete. Should the moisture-proofing of the strain gauges develop some fault, the moisture in the concrete could re-

Plate No. 5

Test set up: apparatus for
the reading of the angle of
twist mounted on the beam

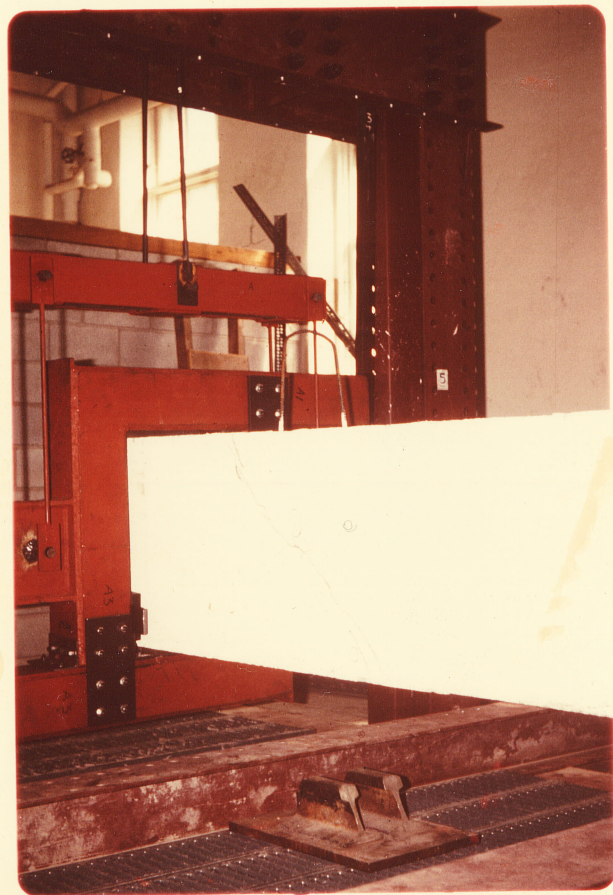


Plate No. 6

Test set up: yoke at the
end of a test beam in
position

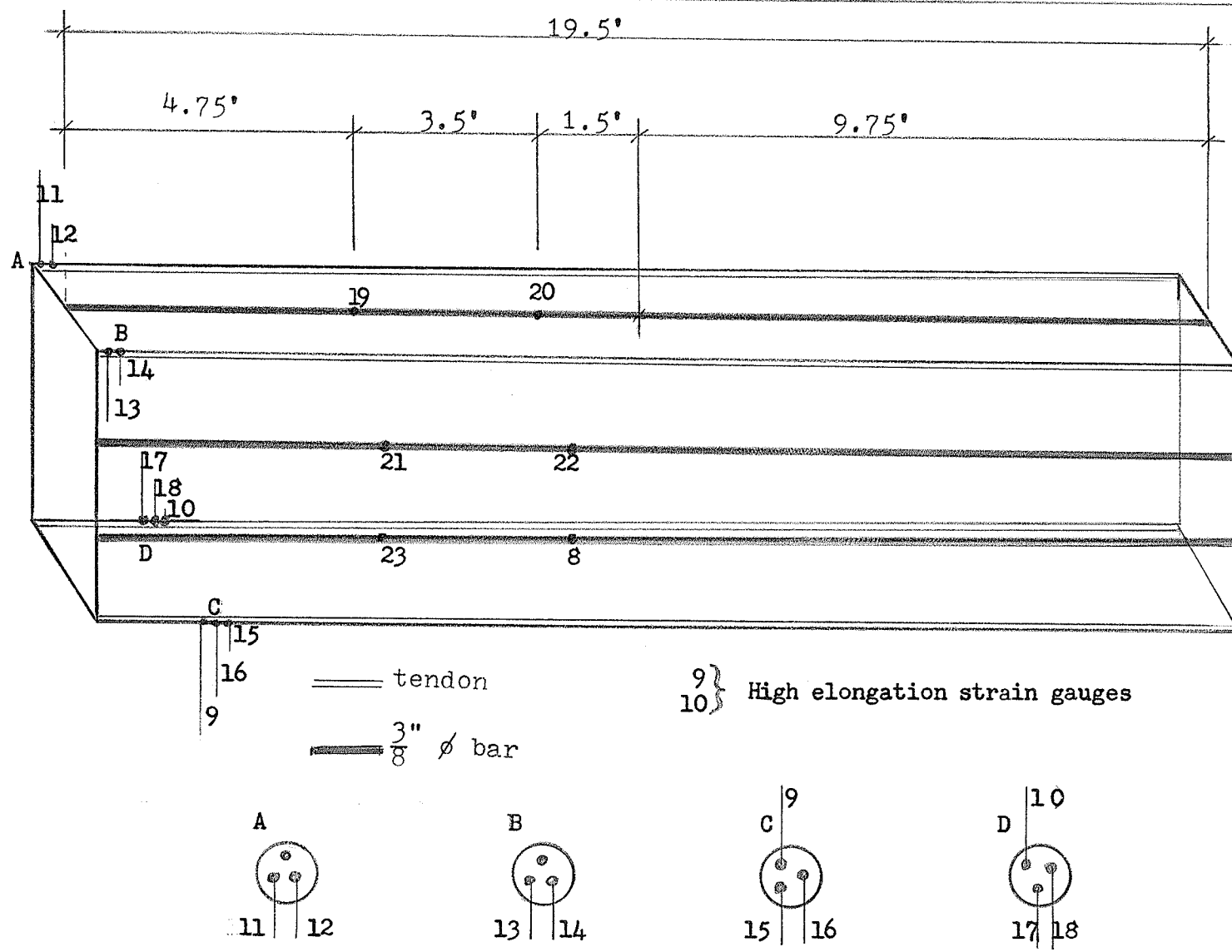


Fig.10 : Position of the strain gauges on the longitudinal bars and tendons in Beam IV

duce the gauge-to-surface resistance of the strain gauges affixed on the reinforcing tendons or bars bonded to the concrete. As a result the strains indicated by the strain gauges could be unreliable. In order to determine the strain losses in the tendons with a good degree of accuracy, the tendons with gauge numbers 9 to 18 affixed were kept free from any direct influence of the concrete. That is, the ducts were not grouted, and therefore there was no bond between the tendons and the concrete. This arrangement not only made a reasonably accurate evaluation of the creep and shrinkage strain in the tendons possible, but also provided a means for a check on the strain of the deformed bars due to creep and shrinkage. In such a case, creep and shrinkage strain losses indicated by the tendon strain gauges must be the same as the creep and shrinkage losses (shortening of the beam) in the bars bonded with concrete.

The strain gauges attached on two of the stirrups in Beam III were for estimating the state of strain at different position on a stirrup in a reinforced concrete beam subjected to pure torsion (Fig. 11).

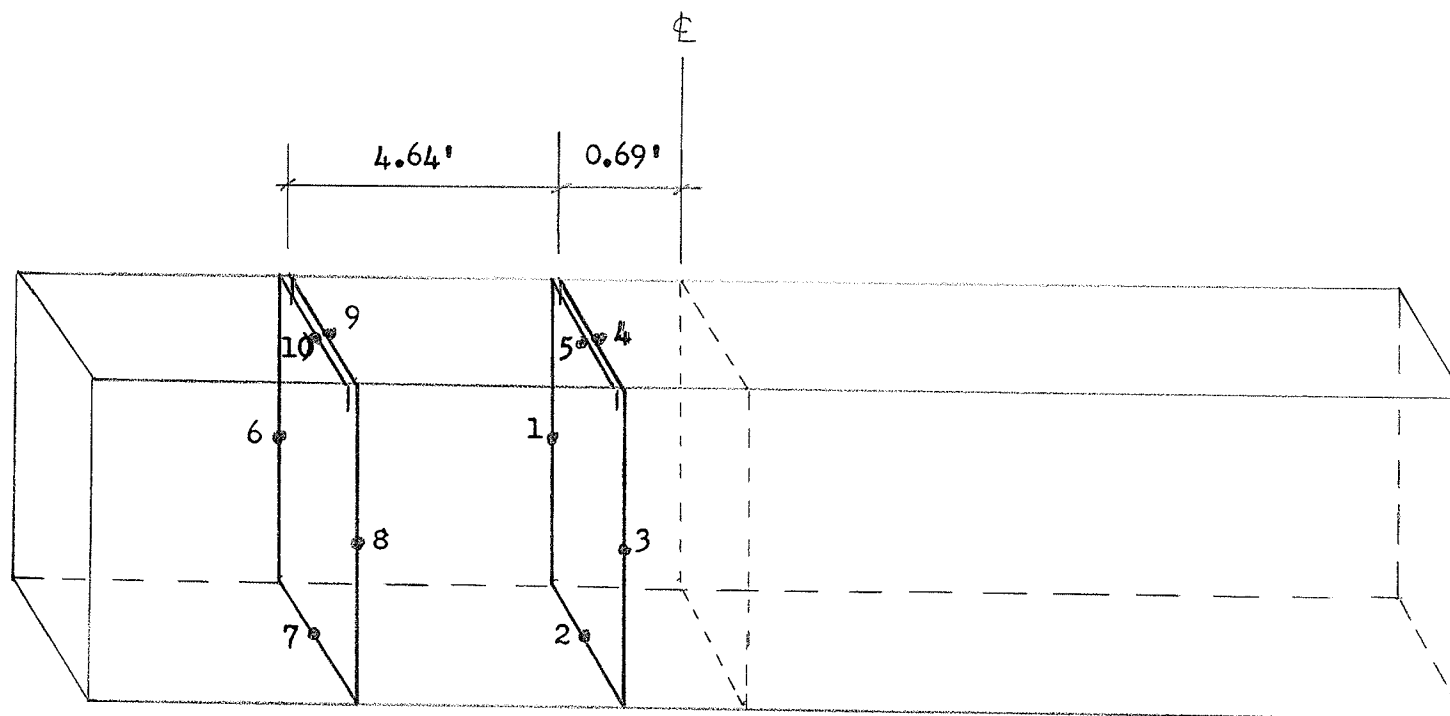


Fig. 11 : Position of the strain gauges on two stirrups in Beam III

CHAPTER IIITEST OF MODELS AND RESULTS3.1 The test set up

The three yokes were attached to the beam, one at each end and one at the middle of the beam, with 9 ft. spacing between the centre lines of the middle and each end yoke. The three yokes, which also served as the support for the concrete beam, were then hung onto the testing frame by means of short steel cross beams with pin-connected rods (Fig. 6). Steel shims were placed between the yokes and the test beams at the point of support. For example, A, B, C and D in Fig. 12 indicate the support positions for the middle yoke. The two loading jacks (numbered 3 in Fig. 6) were then fitted to the two pulling rods of the middle yoke. One of these tension rods was pin-supported on the cross beam of the testing frame and the other was also pin-supported on a beam attached to the testing frame below floor level. Similar beams also provided pinned support for the pulling rods of the end yokes. With this arrangement the test beam could resist any torsional moment resulting from the loads applied to the jacks up to the torsional capacity of the beam. Since moments cannot be transmitted through the pinned supports of the connecting rods, and since the stiffness of the rods is very small in comparison with that of the frame or the girder of the test rig, any influence of the structural indeterminacy of the rig on the magnitude of the applied torsional moment would be negligible. The charts for the reading of the angle of twist were attached at the middle and at each end of the beam. Where applicable, the strain gauge leads were con-

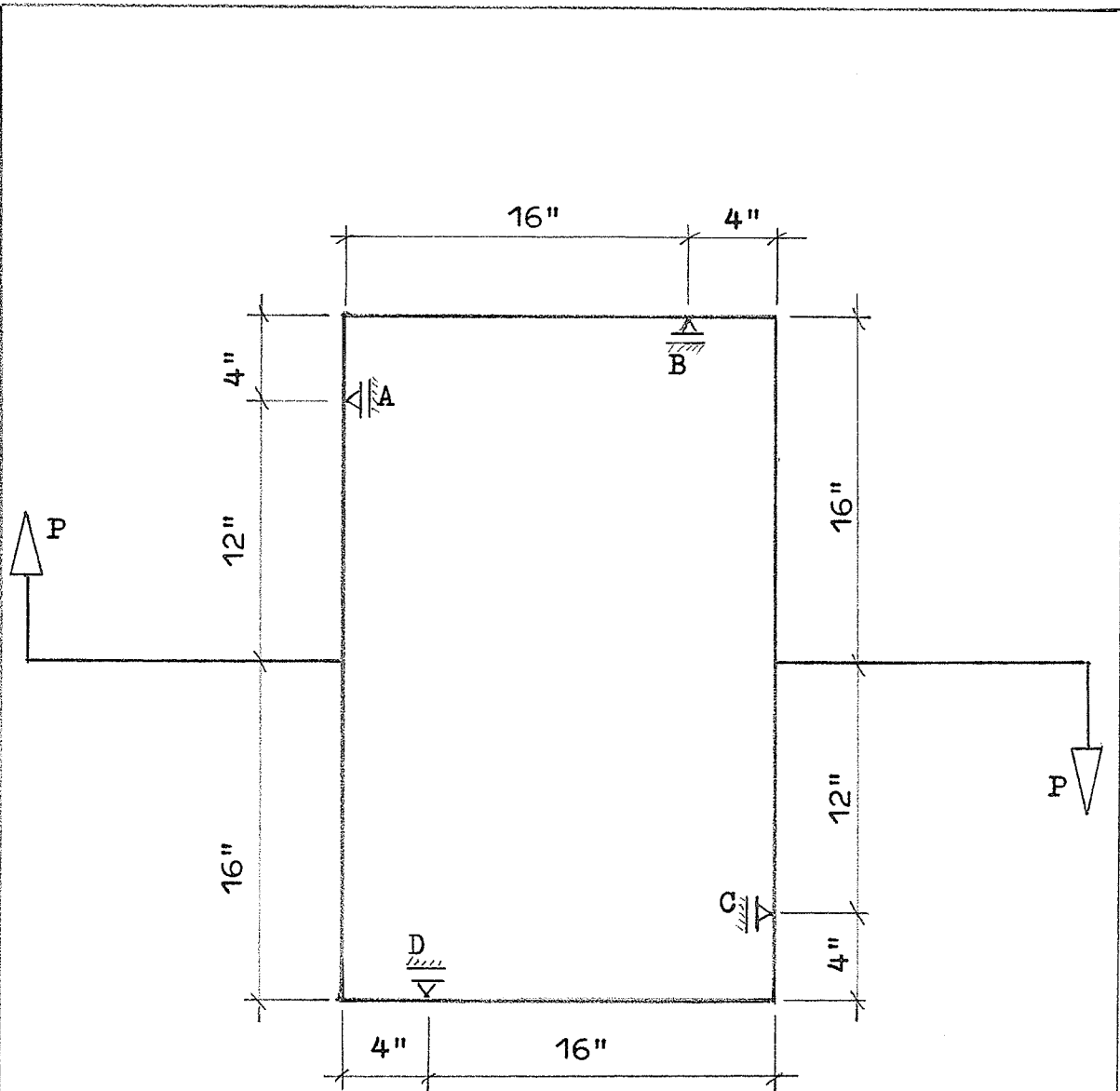


Fig. 12 Structural System of the yoke for the
12" x 24" beam

The applied forces P cause reactions at the supports A, B, C and D. These support reactions provided by the test specimen produce couples for the torsional loading.

nected to a 6-volt car battery and to a Hewlett Packard Data Acquisition System with the following model numbers and brief description: 2402A Integrating Digital Voltmeter; 2570A Coupler/Controller; 2911A Guarded Crossbar Scanner; 2911B Crossbar Scanner Controller. The machine with analogue recording and digital readout, scans each channel and prints the voltage on a tape. From the voltage readings voltage differentials can be determined and the strain computed as explained in paragraph 3.4. A test set up with all three yokes in position is shown in Plate No. 7. Plates No. 8 show some pieces of apparatus used for obtaining strain gauge information.

3.2 Testing of the specimens

Beam I, the most strongly reinforced and Beam IV which carried the largest number of strain gauges were tested last. Beam II which had the least amount of longitudinal reinforcement and which carried no strain gauges was the first to be tested. This provided the opportunity of assessing the performance of the testing equipment and making any necessary adjustments before carrying out the tests on the more complicated Beams I and IV.

3.2.1 Characteristic behaviour of the specimens

Each beam was subjected to pure torsion. The pattern of the cracks was approximately the same for each beam. The general trend of these cracks was at an inclination of about 40° to 50° to the longitudinal axis of the beam (Plate Nos. 9, 10, page 37). The number of cracks increased with loading. The encircled numbers on the plates indicate the order in which the cracks occurred.

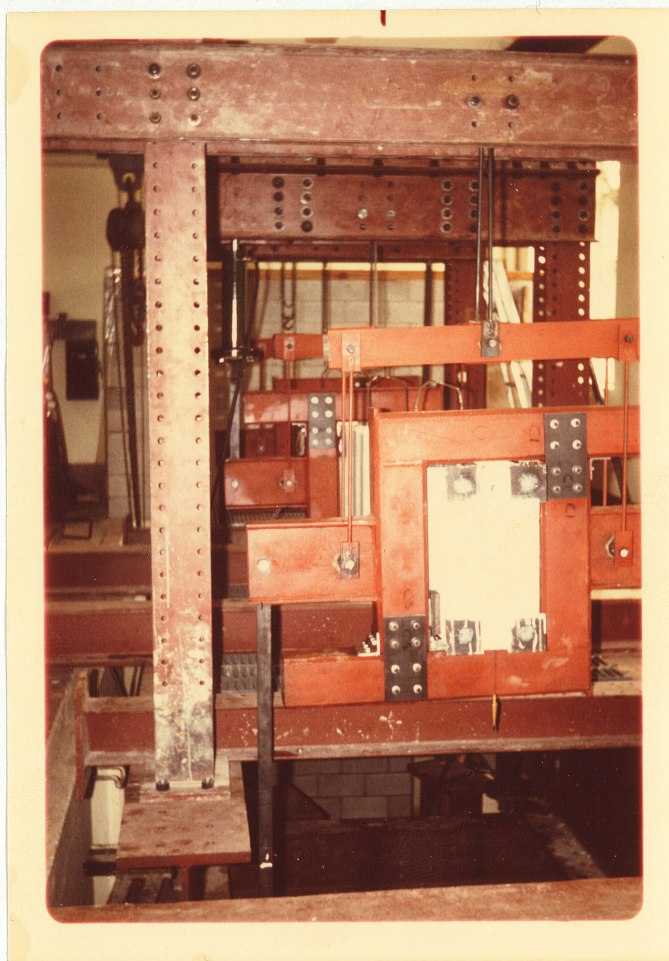
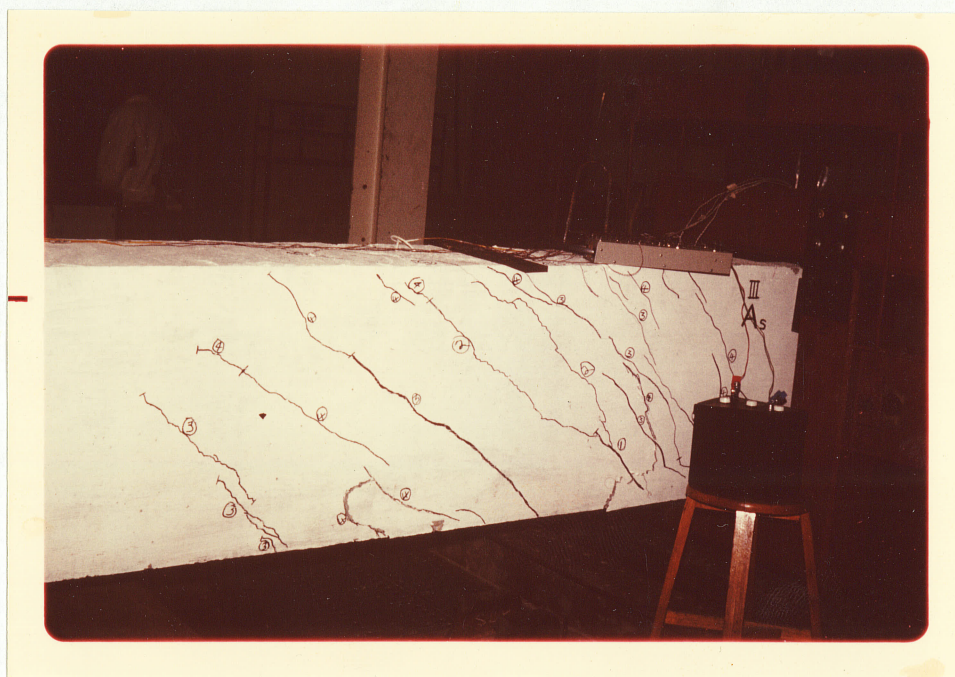


Plate No. 7

Test set up: all three
yokes in position



(a)



(b)

Plates No. 8

Some pieces of apparatus used for obtaining strain gauge information: (a) car battery, (b) data acquisition system

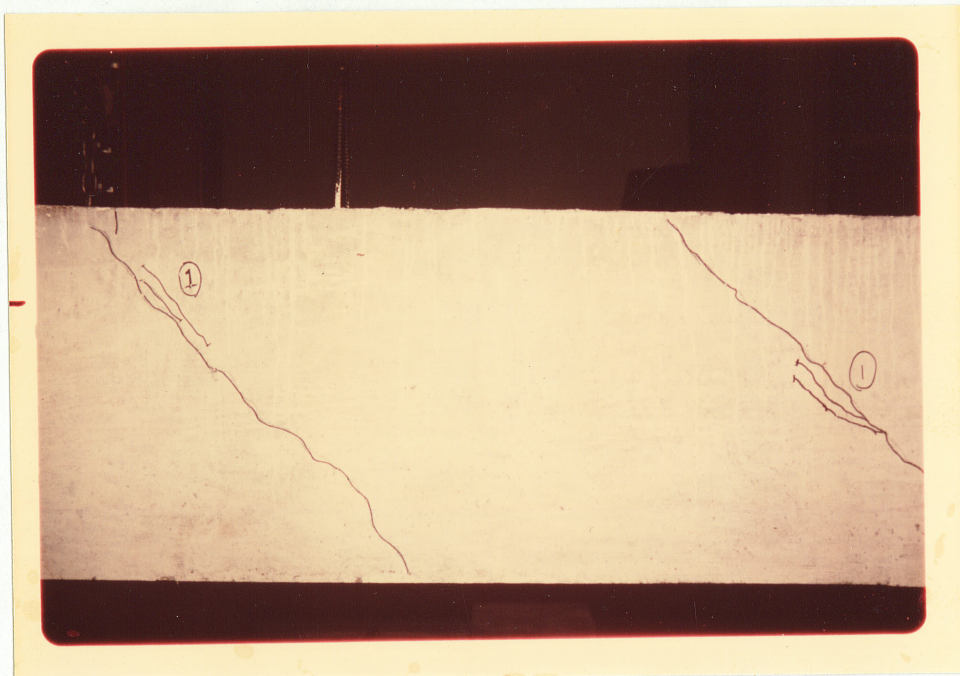


Plate No. 9

Typical torsion cracks

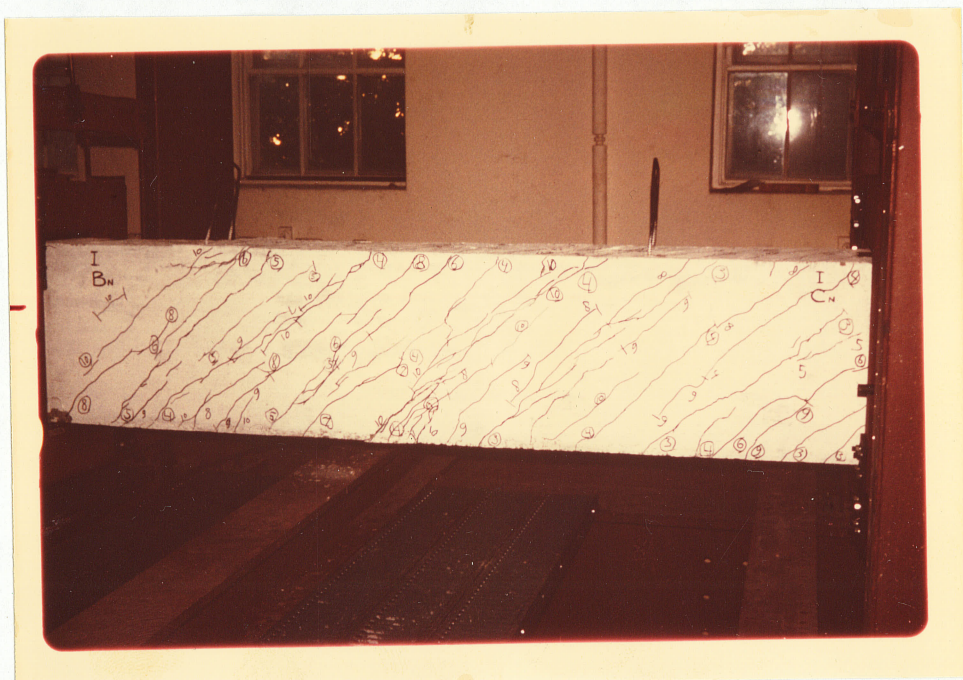


Plate No. 10

Beam I just before failure occurred

The load to be applied at each loading stage by means of the loading jacks was previously determined and indicated on the charts, which served as guides to the operators of the jacks (Fig. 13 and Fig. 14). The number against each arrow indicated the loading stage.

3.3 Evaluation of the strain gauge readings (Beam IV)

The strain gauges by means of which the creep and shrinkage effects were determined were placed in Beam IV only. With the percentage creep and shrinkage losses known for Beam IV, the percentage losses for the other three beams were determined from the factors computed in Appendix D.

Of the ten strain gauges attached to the prestressing wires of Beam IV, three developed faults at the early stages of the experiment. Four of the strain gauges attached to the reinforcing bars of this beam also become faulty. The readings from these gauges were either erratic or too high to be credible.

The rest of the strain gauges on Beam IV functioned well until the end of August (1972). This was about 130 days after the Beam had been prestressed. Early in September the strain gauges on the reinforcing bars in bond with concrete showed a sudden drop in their readings. About 14 days later all but one of the strain gauges on the prestressing wires also indicated a sudden drop in readings. The tensile strain

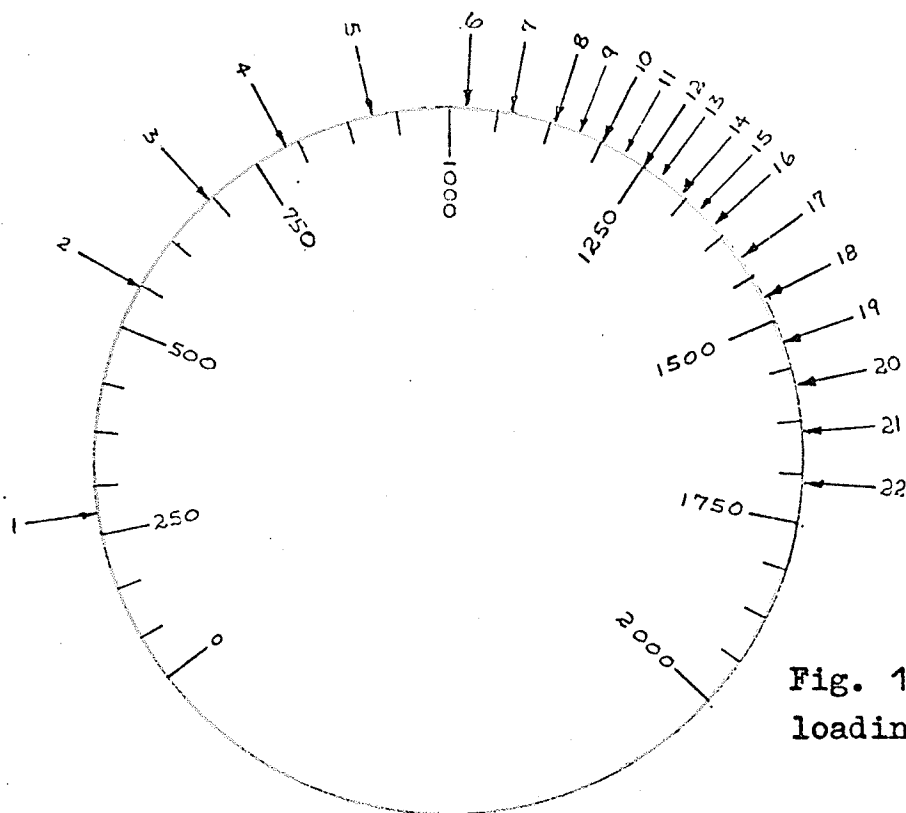


Fig. 13 Chart for loading jack 1

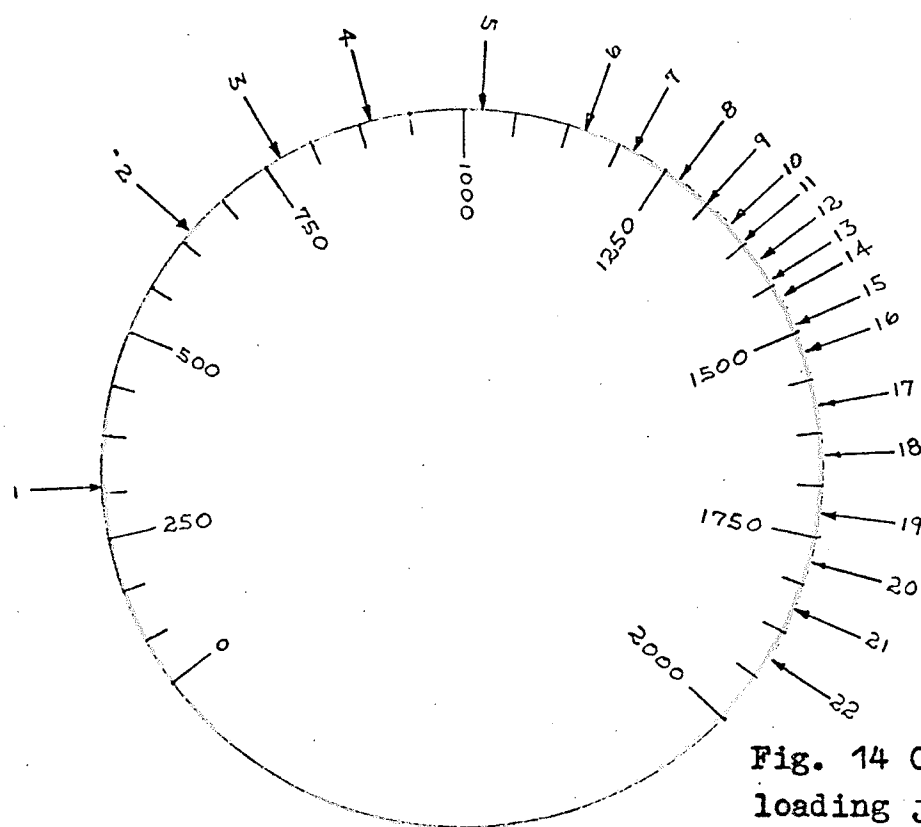


Fig. 14 Chart for loading jack 2

Charts for the operation of the loading jacks

indicated by strain gauge No. 10 on a prestressing wire dropped from 2165.0×10^{-6} in/in on September 6 to -1530.0×10^{-6} in/in on September 19. This was a drop of 3695.0×10^{-6} in/in. The compressive strain indicated by strain gauge No. 21 rose from -683.0×10^{-6} in/in on August 29 to -281.0×10^{-6} in/in on September 6 and showed a tensile strain of 102.0×10^{-6} in/in on September 19.

A probable explanation for this sudden change which set in about early September was the deterioration of the bond between the metalfilm strain gauges and the prestressing wires and the reinforcing bars. After about 130 days of sustained prestressing force which produced high strain in the tendons and the reinforcing bars the bond holding the metalfilm gauges to the wires and the bars could well have deteriorated. Another possible explanation for this deterioration could lie in the deterioration of water proofing of the gauges.

The graphs on pages 47 and 48 were plotted from the strain gauge readings up to the end of August. With a very few exceptions, the changes in strain up to that time were steady and predictable.

3.4 Strain Computation

The strains were computed separately for the shrinkage readings (February 29 to April 18) and the creep and shrinkage readings (April 18 to September 19).

The computation was done according to the following equation:

$$S = \frac{L}{K} \times \frac{dV}{2V}$$

where

S = strain in inch per inch

k = strain gauge factor

= 2.11 for 5 mm gauges

= 2.05 for high elongation gauges

dV = voltage differential

V = voltage of battery

Shrinkage strain, February 29 - April 18:

average voltage of battery V = 3.0644 Volts

$$S = \frac{L}{2.11 \times 2 \times 3.0644} \quad dV = 0.3087 \text{ dV}$$

Creep and shrinkage strain, April 18 - Sept. 19:

average voltage of battery V = 3.0125 Volts

For 5 mm gauges

$$S = \frac{L}{2.11 \times 2 \times 3.0125} \quad dV = 0.3142 \text{ dV}$$

For high elongation gauges

$$S = \frac{L}{2.05 \times 2 \times 3.0125} \quad dV = 0.3238 \text{ dV}$$

The voltage differential dV for any strain computation was obtained by subtracting the particular voltage reading from the initial or first voltage reading of the series.

Example: Computation of the creep and shrinkage strain on July 21 as indicated by strain gauge No. 10:

$$\text{voltage reading on April 18} = -18191.0 \times 10^{-6} \text{ Volt}$$

$$\text{voltage reading on July 21} = -24590.0 \times 10^{-6} \text{ Volt}$$

$$dV = + 6399.0 \times 10^{-6} \text{ Volt}$$

$$\text{Strain } S = +0.3238 \times 6399 \times 10^{-6} \text{ in/in}$$

$$= +2071 \times 10^{-6} \text{ in/in (tensile)}$$

The computed shrinkage strains and creep and shrinkage strains for Beam IV are shown in Tables 5 and 6 respectively. The strains indicated by the strain gauges on two of the stirrups of Beam III at different stages of the test loading are shown in Table 7. Figures 15 to 17 show the graphical representation of the strains for Beam IV.

Each beam was kept moist for a period of three weeks. During this period the beam was constantly watered, covered with water soaked jute material and in addition wrapped with plastic sheets. The positive portion of the shrinkage curve (Fig. 15 a) indicates that Beam IV instead of losing moisture did absorb water during that period.

The kink occurring in the curve of Fig. 15 c at the concrete age of about 65 days was due to the effect of prestressing, through which influence the creep shortening of the concrete commenced. This creep shortening became added to the shrinkage shortening already taking place.

Table 5 Shrinkage strain (Beam IV)

Strain $S = K (10^{-6})$ in/in $K =$ value shown in the table

Strain gauge number	Age of concrete in days	22	29	44	51	58	64
	Date 1972	March 7	March 14	March 29	April 5	April 12	April 18
Strain gauges attached on $\frac{3}{8}$ " ϕ reinforcing bars							
21		+ 96.0	+ 116.0	- 294.0	- 238.0	- 191.0	- 189.0
23		+ 63.0	+ 28.0	- 272.0	- 288.0	- 338.0	- 421.0
Σ		+ 159.0	+ 144.0	- 566.0	- 526.0	- 529.0	- 610.0
Average strain		+ 79.0	+ 72.0	- 283.0	- 263.0	- 265.0	- 305.0
Increase in strain		+ 79.0	+ 72.0	- 283.0	- 263.0	- 265.0	- 305.0

Table 6 Creep and shrinkage strain (Beam IV)

Strain $S = I (10^{-6})$ in/in $K =$ value shown in the table

Strain gauge number	Age of concrete in days	66	71	81	94	123	158	168	177	183	190	197	205	218
	Date 1972	Apr. 20	Apr. 25	May 5	May 18	June 16	July 21	July 31	Aug. 9	Aug. 15	Aug. 22	Aug. 29	Sept. 6	Sept. 19
Strain gauges attached on the tendons:														
10	2518	2500	2438	2387	2212	2071	2021	2038	1962	2005	1903	2165	-1530	
11	2880	2870	2763	2645	2588	2475	2475	2470	2440	2387	2324	2325	1564	
13	3355	3350	3285	3165	3125	2981	2963	2995	2968	2886	2825	2935	2130	
14	1988	1836	1756	1770	1722	1709	1699	1719	1728	1500	1440	1480	855	
15	2736	2634	2415	2359	2234	2160	2139	2132	2125	2110	2063	2116	1850	
16	2886	2829	2746	2735	2534	2475	2439	2421	2435	2436	2398	2475	1621	
18	2350	2309	2240	2235	2021	1946	1900	1889	1900	1900	1840	1948	2066	
	18713	18328	17643	17296	16436	15817	15624	15664	15558	15224	14793			
Average strain	2675	2616	2524	2464	2350	2263	2233	2235	2223	2175	2110			
Loss in strain		59	151	211	325	412	442	440	452	500	565			

Table 6 cont. Creep and shrinkage strain (Beam IV)

Strain $S = I (10^{-6})$ in/in $K =$ value shown in the table

Strain gauge number	Age of concrete in days	66	71	81	94	123	158	168	177	183	190	197	205	218
	Date 1972	Apr. 20	Apr. 25	May 5	May 18	June 16	July 21	July 31	Aug. 9	Aug. 15	Aug. 22	Aug. 29	Sept. 6	Sept. 19

Strain gauges attached on reinforcing No. 3 bars:

21	- 98	-155	-127	-138	-433	-591	-616	-577	-618	-616	-683	-281	+102
23	-146	-193	-212	-217	-486	-579	-572	-567	-562	-548	-592	-373	+328
	-244	-348	-339	-355	-919	-1170	-1188	-1144	-1180	-1164	-1275		
Average strain	-122	-174	-169	-178	-459	-585	-594	-572	-590	-582	-637		
Increase in strain		- 52	- 47	- 56	-337	-463	-472	-450	-468	-460	-515		

Table 7 Strain in the stirrups of (Beam III)

$S = K (10^{-6})$ in/in $K =$ value shown in the table

Strain gauge number \ Loading Stage	1	2	3	4	5	6	7	8	9
1	10.0	19.0	22.0	24.0	28.0	29.0	29.0	26.0	23.0
2	2.0	1.0	1.0	3.0	5.0	5.0	5.0	4.0	3.0
3	3.0	5.0	5.0	5.0	5.0	9.0	9.0	1.0	6.0
4	11.0	21.0	25.0	31.0	37.0	49.0	54.0	61.0	89.0
5	6.0	11.0	13.0	14.0	16.0	21.0	23.0	26.0	36.0
6	4.0	7.0	8.0	9.0	10.0	13.0	15.0		520.0
7	3.0	4.0	3.0	3.0	2.0	4.0	25.0	644.0	1320.0
8	3.0	3.0	2.0	2.0	2.0	4.0	14.0	32.0	208.0
9	0.0	1.0	2.0	4.0	6.0	5.0	5.0	5.0	1.0
10	3.0	2.0	1.0	1.0		1.0	3.0	6.0	28.0

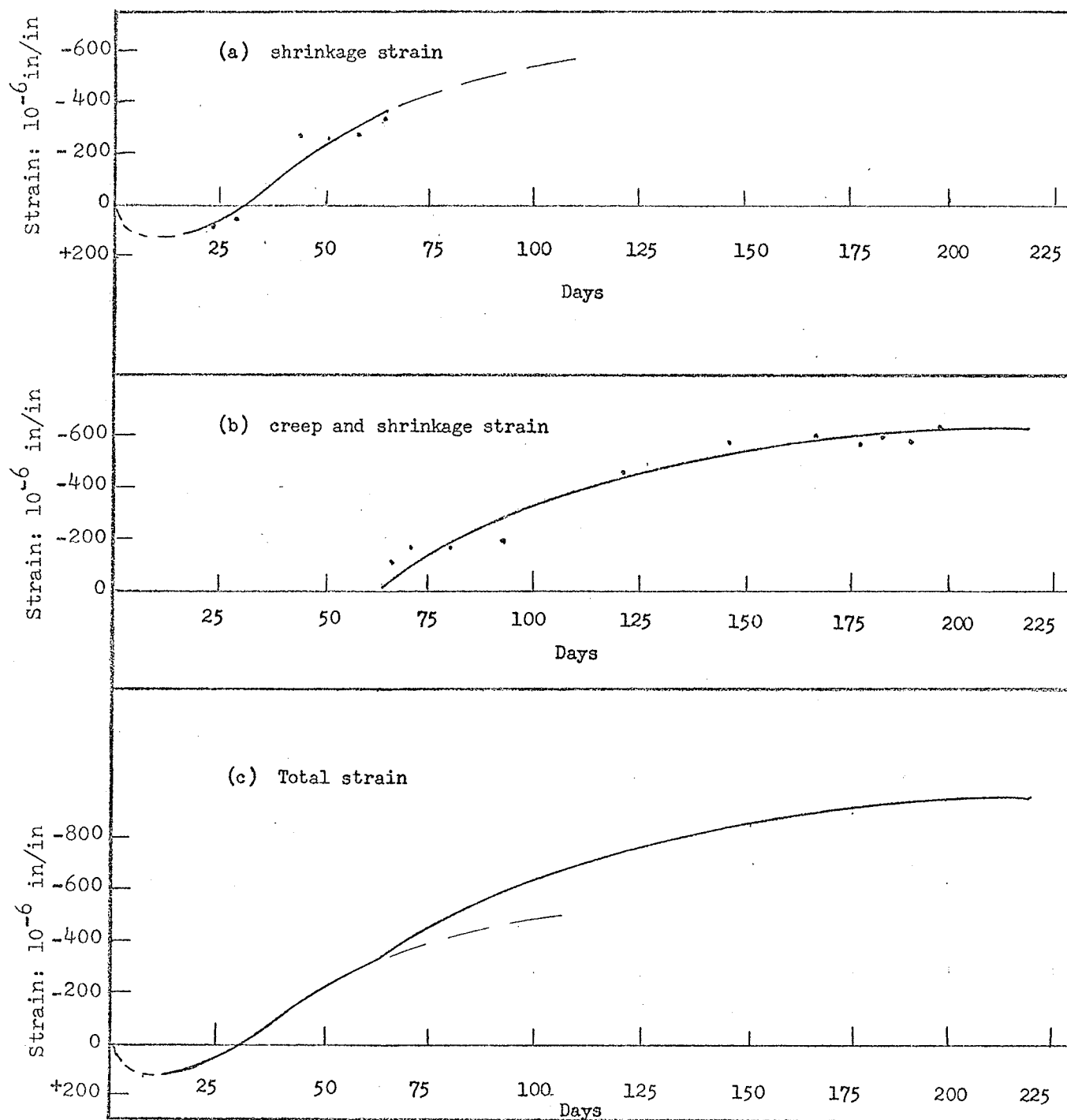
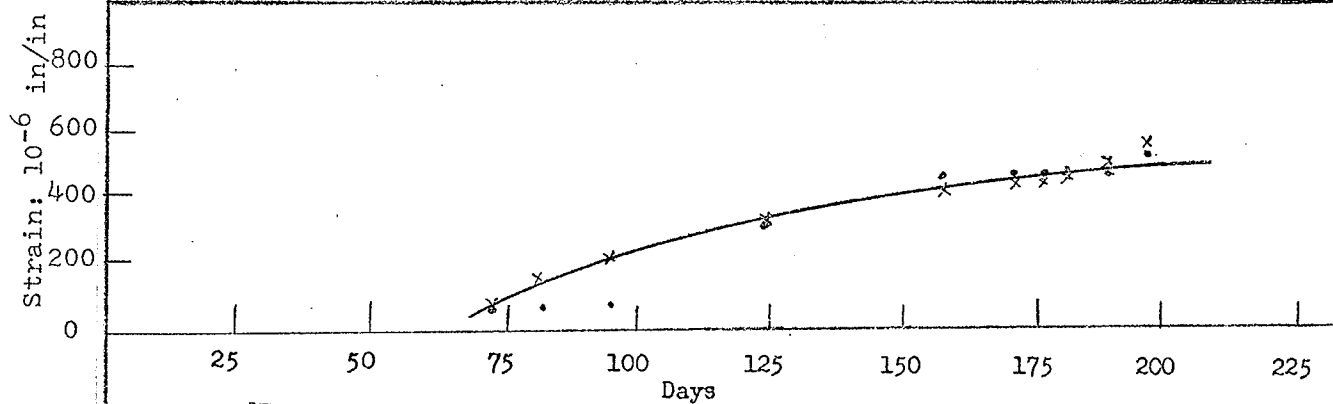
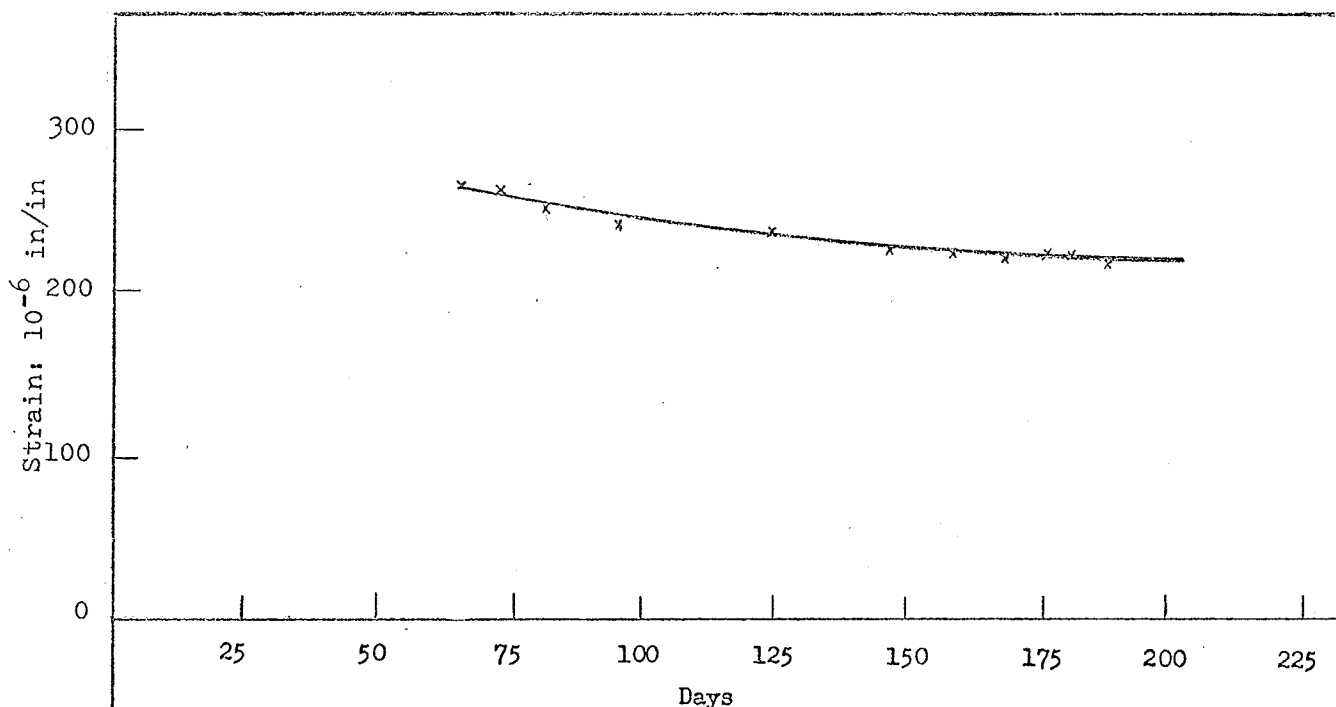


Fig. 15 Changes in the length of Beam IV due to the influences of shrinkage and creep
 + elongation -- shortening



• concrete
x tendon

3.5 Prestressing force

3.5.1 Initial prestressing

The magnitude of the initial prestressing applied to each beam was read from the dial gauge on the prestressing equipment supplied by BBR. These values are shown in Table 8.

3.5.2 Area of composite section

For the computation of the concrete stresses due to prestressing, the determination (Appendix C) of the area of composite section for each beam was necessary. The computed values are shown in Table 8.

Table 8 Initial prestressing; area of composite sections.

Beam No.	Prestressing force (Kips)	Area of composite section (sq. in)
I	72.0	293.50
II	24.0	293.39
III	58.4	285.56
IV	58.4	177.56

3.5.3 Computation of the losses in prestress

As stated earlier, the creep and shrinkage losses in prestress for Beam IV were determined by means of the

strains indicated by the strain gauges. The force in the tendons computed from the stress-strain equation were compared with the force applied by the stressing jack.

The usual causes of loss in prestress can be considered briefly as follow:

- (a) Creep and shrinkage losses. These were determined for Beam IV from strain gauge readings.
- (b) Friction losses. These did not arise in this experiment since the tendons were straight.
- (c) Elastic shortening. The beam was post-tensioned on April 18. The first creep and shrinkage reading was taken two days later (April 20), which was chosen as the initial date for the creep and shrinkage computation. The state of the strain in the tendons and the reinforcing bars on April 20 has already accounted for the elastic shortening of the beam.
- (d) Anchorage losses. The type of wedge or shims used with the BBR system allows for little or no anchorage loss in prestress. Moreover, any such losses have already been accounted for by the state of strain on April 20.
- (f) Relaxation losses. By definition relaxation is loss in stress without change in strain. Losses due to relaxation could not be determined by strain gauge readings. These losses were determined according to Libby (30).

3.5.4 Creep factors

-51-

For the computation of the losses in prestress for Beams I to III due to creep effect, creep factors "C" were determined for the beams, Appendix D.

C_1 = creep factor due to effective thickness of beam.

C_2 = creep factor due to the influence of age of concrete at loading (prestressing)

C_3 = creep factor due to the influence of concrete compressive strength.

The computed values are shown in Table 9.

Table 9 Creep factors

Beam No.	C_1	C_2	C_3
I	0.86	0.67	0.70
II	0.84	0.66	1.29
III	0.86	0.72	0.66
IV	1.07	0.78	1.00

3.5.5 Prestressing force on Beam IV determined from the strain gauge readings

Remark:

The tendon strain gauges indicated great strain differences between individual wires in some cases.

The strains indicated by the strain gauge numbers 13 and 14 on April 20, for instance, were 3355×10^{-6} in/in and 1988×10^{-6} in/in respectively. These gauges were attached on two wires placed in the same duct and had their button heads fitted to a common anchor head. Due to fabrication problems the wires were not originally of equal length. By the button head system of prestressing these inequalities in the fabrication length of the wires cause more strain to be placed on the shorter wires than on the longer ones. However, these differences in strain have no adverse effect on the strain computation as long as no wire has been strained beyond the elastic limit during prestressing.

The average strain indicated by the strain gauges in all 12 wires has been used for the computation of the prestressing force.

For Beam IV, tendon strain on April 20 = 2675×10^{-6} in/in

Stress in the tendons

$$f_s = ES$$

where E = modulus of elasticity of the prestressing wire in psi,

S = strain in tendon in/in.

$$f_s = 30.2 \times 10^6 \times 2675 \times 10^{-6} \text{ psi}$$

$$= 8.06 \times 10^4 \text{ psi} \quad = 80.6 \text{ Ksi}$$

Area of 12 prestressing wires in the 4 bundles

$$= 12 \times \frac{3.1416 \times 0.275^2}{4} = 0.7125 \text{ sq in}$$

Prestressing force (April 20)

$$= 80.6 \times 10^4 \times 0.7125 \text{ lb} = 57.5 \text{ Kips}$$

Prestressing force determined by the pressure gauge on the stressing jack on April 18 = 58.4 Kips (see page 49).

Loss in prestress from April 18 to April 20

$$= 58.4 - 57.5 = 0.90 \text{ Kip}$$

$$\text{Percentage loss} = \frac{0.90}{58.4} \times 100 = 1.54 \%$$

The shim system of wedging produces little anchorage loss in prestress. The difference of 900 lb is partly due to the fact that the reading of the pressure gauge on the stressing jack may not be exact, partly due to elastic shortening since the four tendons were not stressed all at once and partly due to creep and shrinkage loss in the two days between April 18 and 20.

The 1.54 % loss will be regarded as the initial loss in prestress (April 20) for the other three beams as well.

3.5.6 Loss in prestress from April 20 to Sept. 19

The strain loss in the tendons of Beam IV from April 20 to Sept. 19 was 505.0×10^{-6} in/in, Fig. 17.

Percentage loss $\frac{505.0}{2675.0} \times 100$ 18.9 %

Therefore, assuming elastic behaviour the percentage loss in prestress due to creep and shrinkage was 18.9 %. This will be taken as the percentage loss in prestress at the time of testing.

3.6 Experimental results

3.6.1 Torque twist

The angle of twist at various loading stages was read and recorded for each beam, Table 10. The torque-twist graphs are shown in Figs. 18 to 21.

Table 10 Angle of twist vs. loading			
Applied load (Kips)	Torsional mo- ment (Kip-in)	Rotation	Twist
		Degrees	$10^{-4} \frac{\text{rad}}{\text{in}}$
Beam I			
18.0	553.5	0.1 *	0.2 *
19.0	584.25	0.2 *	0.3 *
21.0	645.75	0.4	0.7
22.0	676.50	0.8	1.3
23.0	707.25	1.8	2.9
25.0	768.75	2.8	4.5
29.0	891.00	4.6	7.5

* These readings are at limit of resolution

Table 10 cont. Angle of twist vs. loading			
Applied load (Kips)	Torsional mo- ment (Kip-in)	Rotation	Twist
		Degrees	$10^{-4} \frac{\text{rad}}{\text{in}}$
Beam II			
10.0	307.50	0.1 *	0.2 *
14.0	430.50	0.2 *	0.3 *
16.0	492.00	0.6	1.0
18.0	553.50	0.8	1.3
19.0	584.25	1.0	1.6
20.5	630.00	1.4	2.3
Beam III			
12.0	369.00	0.1 *	0.2 *
16.0	492.00	0.2 *	0.3 *
18.0	553.50	0.4	0.7
19.0	584.25	0.6	1.0
20.0	615.00	0.8	1.3
21.0	645.50	1.6	2.6
Beam IV			
11.0	338.25	0.1 *	0.2 *
12.0	369.00	0.2 *	0.3 *
14.0	430.50	0.6	1.0
16.0	492.00	1.2	1.9
18.0	555.00	3.2	5.2

* These readings are at limit of resolution

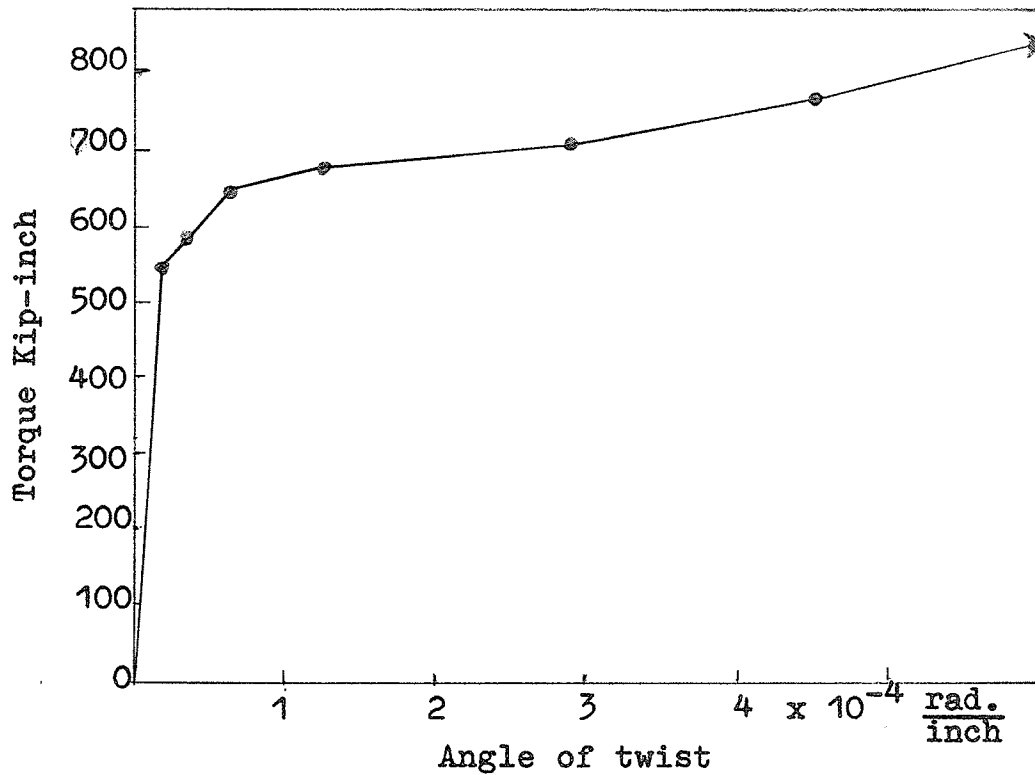


Fig. 18 Torque - Twist for Beam I

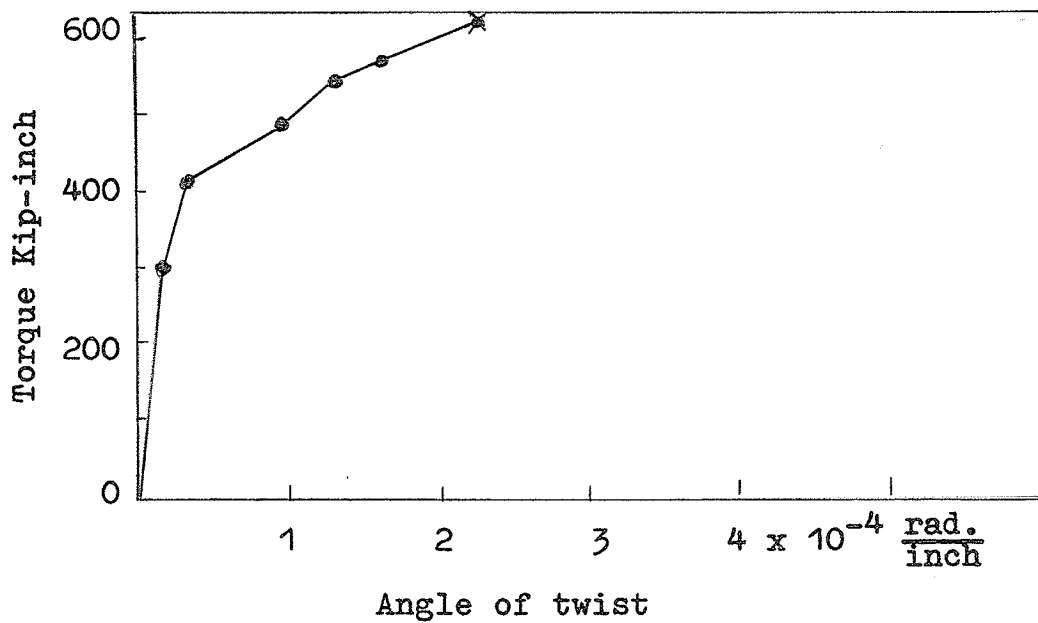


Fig. 19 Torque - Twist for Beam II

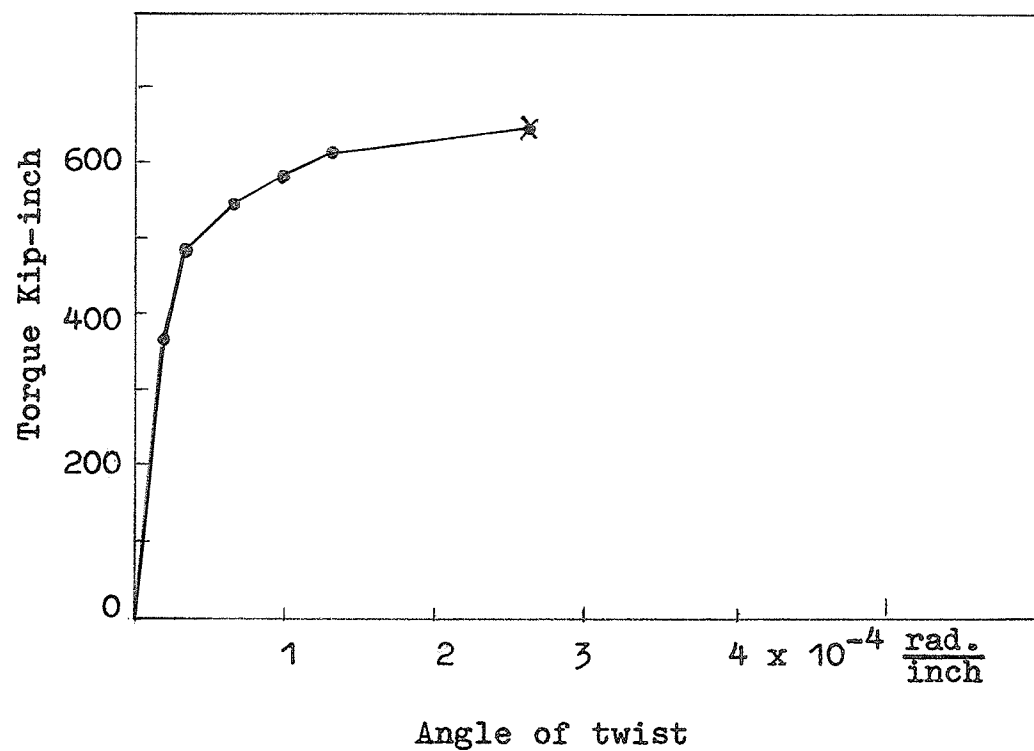


Fig. 20 Torque - Twist for Beam III

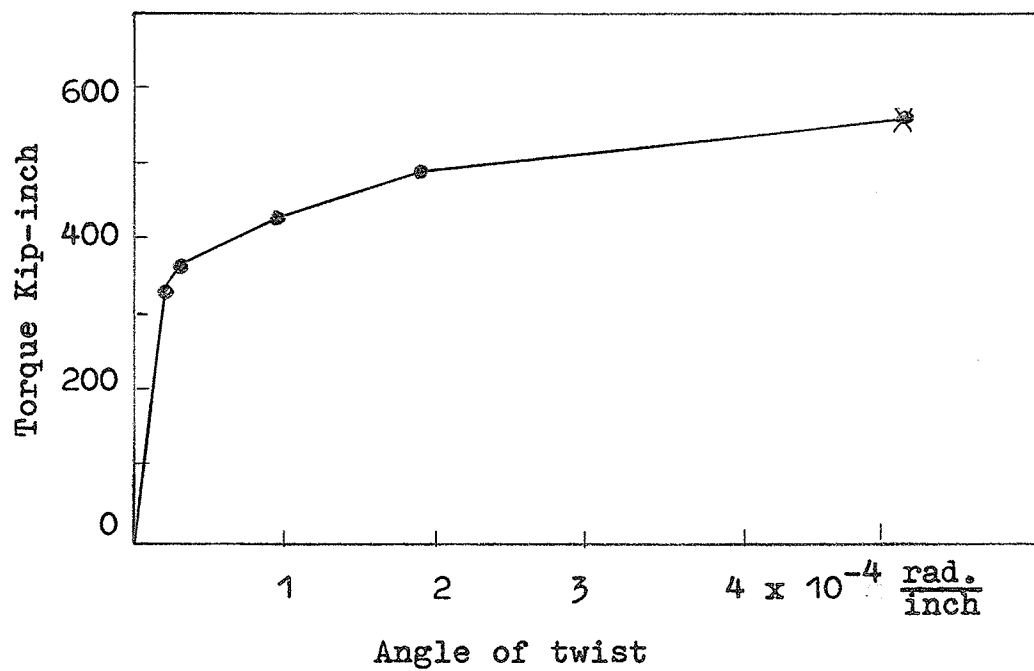
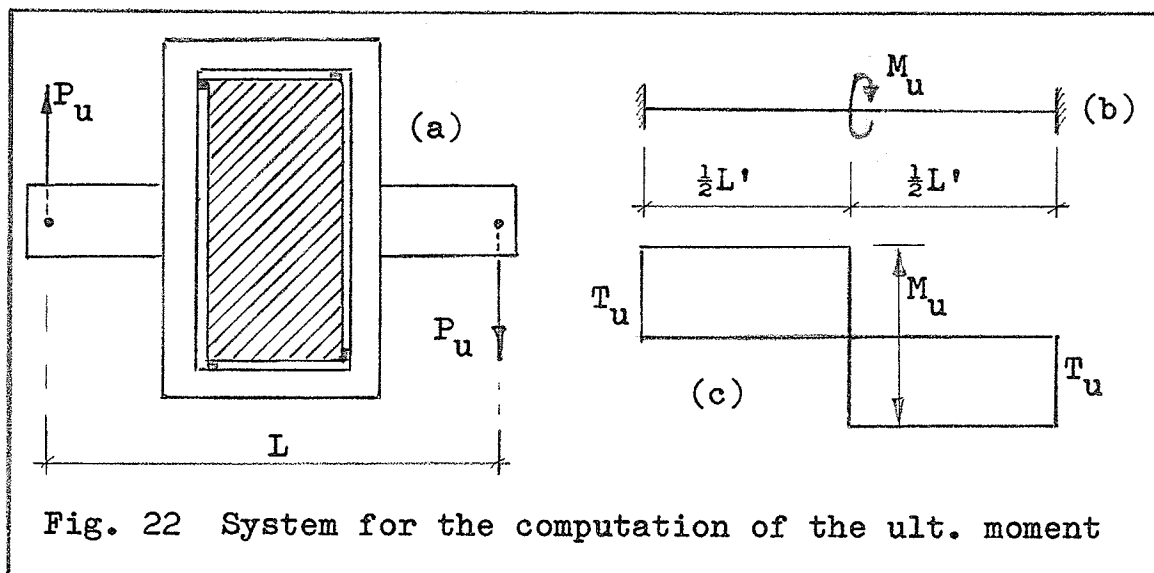


Fig. 21 Torque - Twist for Beam IV

The torsional moment was applied at the middle of each beam by means of jacks attached to pulling rods fitted to the lever arms of the middle yoke as described previously. The two ends of each beam were prevented from rotating by means of constraining yokes placed at those ends (Fig. 6).



Equal forces P applied to each arm of the yoke provided the pure torsional moment, eliminating any shear resultant on the beam.

$$\text{Applied ultimate moment } M_u = P_u \times L$$

$$\text{Ultimate torque } T_u = \frac{1}{2} M_u$$

The ultimate torque observed for each beam is shown in Table 11.

Table 11 Ultimate forces and moments

-59-

Beam No.	P_u (Kips)	M_u (Kip in.)	T_u (Kip in.)
I	29.0	1782.0	891.0
II	20.5	1260.0	630.0
III	21.0	1291.0	645.5
IV	18.0	1110.0	555.0

3.6.3 Ultimate torsional moment computed in
accordance with the equations of Dr. Hsu
and Dr. Lampert.

Before making the concluding remarks about the results of the tests, the ultimate torsional capacity of the beams will be computed in accordance with the ultimate torque equations put forward by the following authors:

(A) Thomas T.C. HSU and Eivind HOGNESTAD.

Dr. Hsu's equations are given partly in

"Torsion in Structural Concrete"

published by the ACI, and partly in

"Torsion in Structural Concrete: Ultimate Torque of Reinforced Rectangular Beams" contained in the PCA Bulletin of May 1967.

Dr. Hognestad's equations are given in

"Shear and Torsion in Prestressed Concrete" presented during the PCI Prestressed Concrete Design Seminar in Chicago on January 25 - 29, 1971. These equations are on the lines of Dr. Hsu's theory.

(B) Paul LAMPERT

Dr. Lampert's equation is contained in

"Bruchwiderstand von Stahlbetonbalken unter Torsion und Biegung" Institut fuer Baustatik, Eidgenoessische Technische Hochschule Zurich, Switzerland, and referred to in "Beton und Stahlbetonbau" of June 1973.

The detailed computation of the ultimate torsional moments according to Dr. Hsu and Dr. Lampert is shown in Appendix F. Table 12 shows the ultimate torsional moment determined by experimental test and also computed in accordance with Dr. Hsu's and Dr. Lampert's equations.

Table 12 Ultimate torsional moments (Kip in).

Beam	Experimental	Hsu/Hognestad	Lampert
I	891.0	639.7	907.0
II	630.0	539.2	575.0
III	645.5	538.5	703.0
IV	555.0	522.3	703.0

The ratios of the test results to those predicted by Hsu/Hognestad and Lampert equations are shown in Table 13.

Table 13 Comparison of the test results with the results predicted by Hsu/Hognestad and Lampert equations

Beam	$T_{up, test}$	$T_{up, test}$
	$T_{up, calc. (Hsu/Hognestad)}$	$T_{up, calc. (Lampert)}$
I	1.4	0.98
II	1.17	1.09
III	1.20	0.92
IV	1.06	0.79

CHAPTER IV

CONCLUSION

In this chapter, certain factors which proved to have significant influence on the test results are discussed. A comparison of the test results with the results predicted by some earlier investigators is also made and a suggestion for further research is presented.

The cross sections, reinforcement and the ultimate torsional strengths of the test beams are shown in Fig. 23.

4.1 The effect of a void central core

Beams III and IV with identical concrete cross sections were also identically reinforced and were both subjected to the same amount of prestressing force, Fig. 23 b, c, d. Some investigators (24, 28) state that the concrete core contributes little or nothing to the torsional resistance of rectangular beams. This would imply that the two beams tested have practically the same ultimate torsional strength. However, the exact size of the core relative to the overall size of the cross section for which this statement would hold true was not stipulated by the investigators. The concrete of the hollow beam (Beam IV) was 3 inches thick all round. This thickness was $1/4$ and $1/8$ of the width and the height of the beam respectively. Results from the tests showed that the ultimate torsional moment resisted by the hollow beam was 86 percent of that

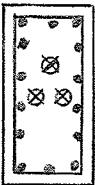
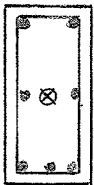


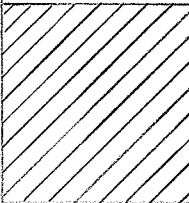

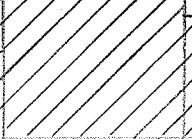
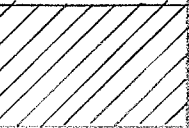
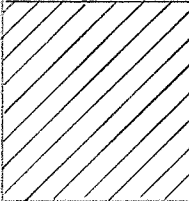
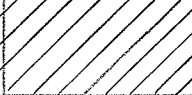

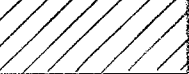
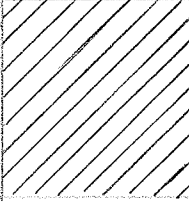
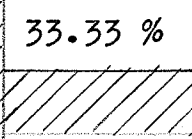
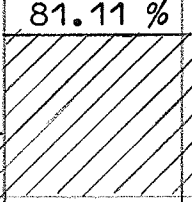
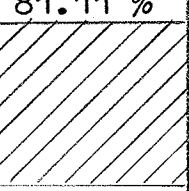
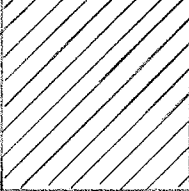
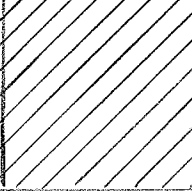
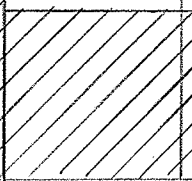
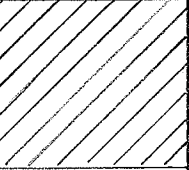
Beam No.	I	II	III	IV
Cross Section				
• longitudinal $\frac{3}{8}$ " ϕ rebar ⊗ prestressing tendon	solid	solid	solid	hollow
Longitudinal $\frac{3}{8}$ " ϕ rebars	14	7	6	6
Effective prestress	72.0 K	24.0 K	58.4 K	58.4 K
Spacing of $\frac{3}{8}$ " ϕ stirrups	4.75 in.	4.75 in.	5.5 in.	5.5 in.
Ultimate torsional strength	100 % 	70.71 % 	72.45 % 	62.29 % (a) 
Longitudinal $\frac{3}{8}$ " ϕ reinforcing bars	100 % 	50 % 	43 % 	43 % (b) 
Effective prestress	100 % 	33.33 % 	81.11 % 	81.11 % (c) 
Transverse reinforcement (stirrups)	100 % 	100 % 	86.38 % 	86.38 % (d) 

Fig. 23 Cross sections, reinforcement and ultimate torsional strengths of the test beams.

resisted by the solid Beam No. III, Fig. 23 a. From this it could be inferred that the void in Beam IV did lower its ultimate torsional capacity. Another factor that might have contributed to the lower torsional capacity was related to construction problems. The presence of the 6" x 18" styroform forming the core and lying close to the tendon duct at each corner of the beam might have presented some degree of obstruction in the application of vibration to the concrete. Such an obstruction could lead to variation in the local concrete strength which in turn could affect the load resisting capacity of the beam.

4.2 Influence of the longitudinal reinforcement

Beams I and II with identical overall concrete cross section had identical transverse reinforcement of $\frac{3}{8}$ " ϕ stirrups at 4.75" spacing. Beam I had twice the number of longitudinal reinforcing bars as Beam II and was subjected to thrice the amount of prestressing force, Fig. 23 b, c, d. The ultimate torsion resisted by Beam I was 41.4 % greater than that resisted by Beam II. This indicates that the longitudinal reinforcement, reinforcing bars and tendons, made a considerable contribution to the ultimate torsional strength of Beam I.

4.3 Influence of transverse reinforcement

The effective prestress applied to Beam III was approximately 2.7 times that applied to Beam II (Fig. 23 c). The test results indicated that Beam III had only

a negligible excess in ultimate torsional strength of about 2.4 % over Beam II Fig. 23 a. The main factor that probably made up for the relative deficiency in the amount of prestress in Beam II was the greater amount of transverse reinforcement. The spacing of the stirrups in Beams II and III was 4.75" and 5.5" respectively. This increase of about 16 % in the transverse reinforcement provided additional torsional strength for Beam II. Another factor that also provided additional torsional strength for the beam was the excess of one $\frac{3}{8}$ " ϕ rebar in its longitudinal reinforcement over that of Beam III.

4.4 Effect of prestress on the angle of twist

The angle of twist at different loading stages are shown in Figs. 18 to 21. The first straight portion of each of the four graphs corresponds to the observed angles of twist before cracking occurred. A significant effect of the prestressing was that it reduced the pre-cracking angle of twist. The pre-cracking angle of twist for Beam I subjected to a prestressing force of 61.6 Kips was much less than that for Beam II with a prestress of only 18.8 Kips. Beams II and III were both solid and had identical overall concrete cross sections. Although Beam III had less number of longitudinal deformed $\frac{3}{8}$ " ϕ bars and smaller amount of transverse reinforcement than Beam II, the observed pre-cracking angle of twist was

smaller for Beam III. This was probably due to the greater amount of prestressing applied to Beam III. The hollow Beam IV had a greater pre-cracking angle of twist than the solid Beam III, although both beams were identically reinforced and had the same width and depth dimensions. A major factor leading to the greater pre-cracking angle of twist for Beam IV could be the void in the beam. A possible obstruction mentioned earlier with respect to the application of vibration to the concrete of Beam IV might have also contributed to the greater pre-cracking angle of twist.

4.5 Strain in the stirrups

The strains indicated at different stages of the test loading by the strain gauges placed on two of the stirrups of Beam III were shown in Table 7. Tensile as well as compressive strains were registered. The only compressive strain indicated for a longer leg of a stirrup was that shown by the strain gauge No. 8 during the 8th and the 9th loading stages. This sudden reversal from tensile to compressive strain at the last stage of the test might be caused by a local concrete disruption at the stage when the concrete has badly cracked and the beam was almost at the point of failure.

The yield stress of the $\frac{3}{8}$ " ϕ bars used for both the longitudinal and the transverse reinforcement was

56.4 Ksi. This corresponds to a yield strain of 1880.0×10^{-6} in/in. The 1320.0×10^{-6} in/in strain indicated by strain gauge No. 7 at the failure of the beam was 70.2 % of the yield strain. The rest of the tensile strains shown were far less than the yield strain. This would give the impression that none of the stirrups carrying the strain gauges was strained to yielding. It was observed that the magnitudes of the strains indicated by these strain gauges attached to the stirrups were significantly less than even the creep and shrinkage strains of the longitudinal $\frac{3}{8}$ " ϕ reinforcing bars of Beam IV. With the exception of the strain readings for the strain gauge No. 7, no other stirrup strain gauge reading exceeded 90.0×10^{-6} in/in. This strain was about 14 % of the creep and shrinkage strain indicated by the strain gauges of the longitudinal rebars. The incredibly low strains in the stirrups could be due to faulty functioning of the strain gauges. A probable deterioration of the bond between the strain gauges and the reinforcement was mentioned earlier in this work.

4.6 Comparison with previous investigations

The ratios of the observed ultimate torques to those computed in accordance with the Hsu/Hognestad and Lampert ultimate torque equations are shown in Table 13. The ultimate torsional moment test results for Beams I to

III showed a closer agreement with the predictions of Dr. Lampert's equation. The predictions by Dr. Hsu's and Dr. Hognestad's equations were lower than the observed test results for the three beams. The test result for Beam IV showed a closer agreement with the result computed from the Hsu/Hognestad equations. But it was pointed out earlier that the effect of void and certain other factors might be responsible for a comparatively low torsional strength of Beam IV.

Something remarkable about Dr. Lampert's prediction expressed in equation (4) is that it assumes that the prestressing tendons are stressed to yield at the failure of the beam. Whether or not the prestressing tendons will be stressed to yielding at the failure of the test specimen depends on a number of factors including the degree of the strain in the tendons just before the testing and the percentage of the longitudinal reinforcement. The influence of these factors needs a closer investigation before any definite conclusion can be made. If the prestressing reinforcement is not strained to yielding point before the beam fails, then Dr. Lampert's equation would appear to be conservative.

The contributions made by the concrete, the non-prestressed reinforcement and the prestressing reinforcement to the ultimate torsional strength of Beams I to III

as determined by Dr. Hsu's and Dr. Hognestad's equations discussed on page 8 are shown in Table 14.

Table 14 Contributions to the ultimate torque

Beam	Ultimate torque	Concrete	Non-prestressed reinforcement	Prestressed reinforcement
I	639.7 Kip in.	182.4 Kip in.	427.5 Kip in.	29.8 Kip in.
	100 %	28.51 %	66.83 %	4.66 %
II	539.2 Kip in.	163.5 Kip in.	365.0 Kip in.	10.70 Kip in.
	100 %	30.30 %	67.70 %	2.0 %
III	538.5 Kip in.	200.0 Kip in.	314.5 Kip in.	24.0 Kip in.
	100 %	37.14 %	58.40 %	4.46 %

From the figures in the table it appears that the contribution made by prestressing according to Hsu and Hognestad was very small. Moreover, since Beams I and II had the same amount of transverse reinforcement (Fig. 23 d), by decreasing the number of reinforcing $\frac{3}{8}$ " ϕ bars from 14 for Beam I to 7 for Beam II, there was a decrease of 62.5 Kip in. in the contribution made by the non-prestressed reinforcement. This difference was due to the 7 longitudinal reinforcing $\frac{3}{8}$ " ϕ bars not added to Beam II. Simi-

larly a decrease in the amount of prestressing force of Beams II relative to Beam I produced a decrease of 19.1 Kip in. in the torsional strength provided by prestressing. Total decrease in the ultimate torsional strength due to the longitudinal reinforcement (rebars and tendons) not added to Beam II was 81.6 Kip in.

However, test results indicated that the ultimate torsional strength decreased from 891.0 Kip in. for Beam I to 630.0 Kip in. for Beam II. This difference of 261.0 Kip in. was brought about by the difference in the amount of the longitudinal reinforcing bars and tendons of Beams I and II. This difference was more than 3 times that predicted by Dr. Hsu's equations. It would appear therefore that Dr. Hsu's equations underrates the influence of the longitudinal reinforcing bars and also of prestressing.

The factor in Dr. Hsu's equation (1), page 8 which takes the effect of longitudinal reinforcement into consideration is the slope of that equation. Representing this factor by R gives

$$R = 0.66 m + 0.33 \frac{d_1}{b_1} \text{ - - - - - (5).}$$

This expression does not account for the effect of prestressing which forms a part of the longitudinal reinforcement. According to Dr. Hsu (28), the contribution of prestressing to the ultimate torsional strength of a rectangular reinforced concrete beam is directly pro-

portional to the contribution made by the concrete. This relationship is expressed by equation (2) page 8 . The equation is reproduced here to facilitate reading and comparison.

$$M_{tp}^* = M_{tp} \sqrt{1 + 10 \frac{f_{pa}}{f'_c}} \text{ --- (2)}$$

M_{tp} = contribution of the concrete to the strength of a member with web reinforcement;

f_{pa} = average effective prestress after all losses;

f'_c = compressive strength of concrete

The test results indicated that the longitudinal reinforcement made a considerable contribution to the ultimate torsional strength of Beam I. It was shown that the contribution predicted by Dr. Hsu's equations was much less, page 70. In attempt to throw some light on the discrepancies, a review of the equations (5) and (2) is made.

The term involving the longitudinal reinforcement in equation (5) is $0.66 m$, m being a ratio defined as follows:

$$m = \frac{\text{volume of longitudinal reinforcement}}{\text{volume of transverse reinforcement}}$$

The value of m obtained for a beam was not necessarily the value to be used for the computation of the ultimate torsional strength of the beam. Dr. Hsu suggested that for m less than 0.7 the value 0.7 should be used, and for

m greater than 1.5 the value 1.5 should be used.

$$\text{i. e. } 0.7 \leq m \leq 1.5$$

These limits which were set arbitrarily and which, according to Dr. Hsu, appeared to be a conservative range could be a factor leading to the underrating of the influence of the longitudinal reinforcing bars. If for example the limits were $1.0 \leq m \leq 1.5$, the ultimate torsional strengths of Beams II and III (all other conditions remaining unchanged), would be 601.72 Kip ft and 593.22 Kip in. respectively. The ratios of the ultimate torsional strengths would be

$$\text{Beam II : } \frac{T_{u, \text{ test}}}{T_{u, \text{ calc.}}} = \frac{630.0}{601.72} = 1.05$$

$$\text{Beam III: } \frac{T_{u, \text{ test}}}{T_{u, \text{ calc.}}} = \frac{645.0}{593.22} = 1.09.$$

Thus, a lower limit of 1.0 for m would bring the prediction by Dr. Hsu's equations close to the results obtained by the test.

The predictions by Dr. Hsu's equations indicated that the concrete contribution to the ultimate torsional strength averaged 32.0 % for Beams I to III, Table 14. This contribution, which corresponds to M_{tp} in equation (2), is considerable. However, the concrete contribution to the ultimate torsional strength of a reinforced concrete beam is a controversial issue. Some investigators

(28) hold the view that concrete contributes substantially to the ultimate torsional strength. other investigators (24) hold the view that, since the concrete is badly cracked near ultimate load, its ability to resist torque is greatly reduced and should be assumed to be zero. An investigation of the concrete contribution to the ultimate torsional strength of reinforced concrete beams was outside the scope of this work, in which the primary aim was to assess the influence of the longitudinal reinforcing bars and tendons. If, according to some investigators, the concrete contribution to the ultimate torsional strength is negligible, then the contribution made by prestress as predicted by Dr. Hsu's equation will have almost no significance at all.

In summary, from the results of the tests performed by the writer, he concludes that:

- (a) For a thin-walled rectangular hollow beam with the wall thickness equal to or less than $\frac{1}{4}$ of the smaller dimension of the cross section, the ultimate torsional capacity is less than that of a comparable solid beam with the same overall dimension. The buckling of the thin walls of the cross section under torsional loading, as well as higher concrete compression stresses in these walls can contribute to the failure of the beam.

- (b) The longitudinal reinforcement (reinforcing bars and prestressing tendons) makes a considerable contribution to the ultimate torsional strength of the beam. The test results show that, by doubling the amount of rebars and tripling the amount of prestressing force, there was a resultant increase of more than 35 % in the ultimate torsional strength.
- (c) By decreasing the stirrup spacing, thus providing more steel resistance to torsion per unit length of beam, the ultimate torsional strength of the beam is increased. An increase of 16 % in the amount of stirrups was approximately equivalent to doubling the amount of the prestressing force.
- (d) Prestressing reduces the pre-cracking angle of twist and increases the pre-cracking torsional load. The constraint in the lateral direction provided by the stirrups together with the compressive force from prestressing increase the initial modulus of elasticity of the concrete and therefore the beam's pre-cracking resistance to twisting.
- (e) The ultimate torsional moment test results showed fair agreement with the predictions of Dr. Lampert's equation, and were higher than the results

predicted by Dr. Hsu's equation. Dr. Hsu's equation appears to underrate the influence of the longitudinal reinforcement and of prestressing.

Remark

The ultimate torsional strength obtained in each of the single beam tests performed may not be an accurate value. If a group of beams each identical to the Beam No. I for instance were tested, the average ultimate torsional strength obtained for the group would represent a more satisfactory value than that obtained for the single Beam I.

4.7 Suggestions for further research

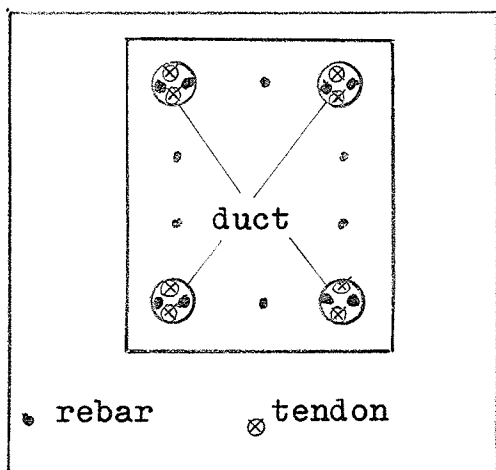
The ultimate torsional strength of structural concrete is influenced by several factors. A fuller understanding of the torsional capacity of reinforced concrete requires further investigation of some of these factors which are briefly stated in the following paragraphs.

- (a) Studies of the state of the strain in the prestressed and the non-prestressed reinforcement near and at ultimate load. The knowledge of the state of the strain will help to explain how the torsional resistance provided by the longitudinal reinforcement is shared between the prestressed and the non-prestressed reinforcement.
- (b) Studies of the effect of restraint on axial displacement of the ends of a beam subjected to torsional loading. This will help to explain to what extent the influence of prestressing on the ultimate torsional strength is due to the compressive force pro-

duced by prestressing, and to what extent it is due to the material properties of the prestressing steel.

- (c) Studies of the effectiveness of concrete to resist torsion near and at ultimate load where deformation is high. This will lead to a better understanding of the mechanism of torsional resistance of concrete at high strains, and throw more light onto the controversial issue of the concrete contribution to the ultimate torsional strength.

In particular, a method of conducting the investigation suggested in paragraph (a) is given.



The diagram illustrates a method that can be used to determine and compare the magnitudes of the strain in the deformed reinforcing bars and in the prestressing tendons at different loading stages. The device, by

means of which the effect of concrete bond on these strains can be eliminated, was partly employed in the present work. For the suggested further research, tendon and rebars are enclosed in flexible steel ducts which will not be grouted. The ends of the prestressed tendons are supported or wedged on the anchor plates at the ends of the beams, and the ends

of the non-prestressed bars anchored in the concrete. Any openings made in the ducts to facilitate the placing of the strain gauges on the tendons and the rebars will be carefully taped so that concrete is prevented from entering the ducts. With the concrete bond effect absent in the ducts, an accurate comparative study of the strains in the tendons and in the rebars in the duct for different loadings can be made.

HISTORICAL BIBLIOGRAPHY

- (1) Bach, C., and Graf, O. "Versuche ueber die Widerstandsfestigkeit von Beton und Eisenbeton gegen Verdrehung." Deutscher Ausschuss fuer Eisenbeton, Heft 16 Wilhelm Ernst, Berlin, 1912.
- (2) Young C.R., Sagar, W.L., and Hughes, C.A.. "Torsional Strength of Rectangular Sections of Concrete, Plain and Reinforced" University of Toronto, School of Engineering, Bulletin No. 9, 1922.
- (3) Nylander, H. "Vridning och Vridningsinspanning vid Betong Konstruktioner." (Torsion and Torsional Restraint by Concrete Structures), Statens Kommittee for Byggnadsforskning, Stockholm, Bulletin No. 3, 1945.
- (4) Turner, L., and Davies, V.C. "Plain and Reinforced Concrete in Torsion, with Particular Reference to Reinforced Concrete Beams." The Institute of Civil Engineers, London, Selected Engineering Papers No. 165, 1934.
- (5) Miyamoto, T. "Torsional Strength of Reinforced Concrete." Concrete and Constructional Engineering (London), V. 22, 1927 p. 637.
- (6) Ernst, G. "Ultimate Torsional Properties of Rectangular Reinforced Concrete Beams." ACI Journal, V. 29, No. 4, Oct. 1957, p. 341.
- (7) Lessig, N.N. "Determination of the Load-Bearing Capacity of Reinforced Concrete Elements with Rectangular Cross-Section Subjected to Flexure with Torsion." Trudy, No. 5, Concrete and Reinforced Concrete Institute (Moscow), 1959, p. 5 - 28.

- (8) Yudin, V.K. "Determination of the Load Bearing Capacity of Reinforced Concrete Elements of Rectangular Cross-Section Under Combined Torsion and Bending," Beton i Zhelezobeton, No. 6, June 1962, p. 265 - 268.
- (9) Gesund, H., and Boston, L.A. "Ultimate Strength in Combined Bending and Torsion of Concrete Beams Containing only Longitudinal Reinforcement." ACI JOURNAL, V. 61, No. 11, Nov. 1964
- (10) Gesund, H., Schuette, R.J., Buchanan, G.R., and Gray, G.A. " Ultimate strength in Combined Bending and Torsion of Concrete Beams Containing Both Longitudinal and Transverse Reinforcement." ACI JOURNAL, Vol. 61, No. 12, Dec. 1964.
- (11) Pandit, G.S., and Warwark, J. "Torsional Strength and Behavior of Concrete Beams in Combined Loading." published by the University of Alberta, Edmonton, Alberta, July 1965.
- (12) Iyalin, I.M. "Experimental Investigation of Behavior of Rectangular Reinforced Concrete Beams Subjected to Combined Shear and Torsion." Proceedings of the Concrete and Reinforced Concrete Institute, Moscow, V.5, 1959 (in Russian).
- (13) Lessig, N.N. "Study of Cases of Failure of Concrete Subjected to Combined Flexure and Torsion." Design of Reinforced Concrete Structures, edited by A.A. Gvozdev, State Publishing Office of Literature on Structural Engineering, Architecture and Structural Materials (Moscow), 1961, pp. 229 - 271.
- (14) Yudin, V.K. "Behavior of Reinforced Concrete Beams with Rectangular Cross-Section Subjected to Combined Torsion with Flexure." Beton i Zhelezobeton, No. 1, Moscow, 1964, pp. 30 -35. (English Translation by Margaret Corbin as Foreign Literature Study No. 431, Portland Cement Association, Skokie, Ill.)

- (15) Farmer, L.E. "Reinforced Concrete Semi-Continuous T-Beams Under Combined Bending, Shear and Torsion." PhD Dissertation, University of Texas, May 1965.
- (16) Ersoy, U. "Combined Torsion in Semi-Continuous Concrete L-Beams without Stirrups." Ph D Dissertation, University of Texas, Aug. 1965.
- (17) Cowan, H. J. "The Strength of Plain, Reinforced and Prestressed Concrete Under the Action of Combined Stresses, with Particular Reference to the Combined Bending and Torsion of Rectangular Sections." Magazine of Concrete Research (London), V. 5, No. 14, Dec. 1953, p. 86.
- (18) Humphreys, R. "Torsional Properties of Prestressed Concrete." The Structural Engineer, London, V. 35, No. 6, June 1957, pp. 213 - 224.
- (19) Zia, P. "Torsional Strength of Prestressed Concrete Members." ACI JOURNAL, V. 32, No. 10, Apr. 1961.
- (20) Gardner, R.P.M. "The Behavior of Prestressed Concrete I-Beams Under Combined Bending and Torsion." Technical Report TRA/329, Cement and Concrete Association (London), Feb. 1960.
- (21) Reeves, J.S. "Prestressed Concrete Tee Beams Under Combined Bending and Torsion." Technical Report TRA/364, Cement and Concrete Association (London), Dec. 1962.
- (22) Swamy, N. "The Behavior and Ultimate Strength of Prestressed Concrete Hollow Beams Under Combined Bending and Torsion." Magazine of Concrete Research (London), V. 14, No. 40, Mar. 1962.
- (23) Lampert, P. "Bruchwiderstand von Stahlbetonbalken unter Torsion und Biegung." Institut fuer Baustatik, Eidgenoessische Technische Hochschule Zurich, Switzerland, January 1970.

- (24) Lampert, P. "Torsion und Biegung von Stahlbetonbalken." Schweizerische Bauzeitung, Jan. 1970, pp. 85 - 95.
- (25) Leonhardt, f. "Schub und Torsion im Spannbeton (Shear and Torsion in Prestressed Concrete)." 6th FIP Congress, Prague, June 1970.
- (26) Hognestad, E. "Shear and Torsion in Prestressed Concrete." Presented during PCI Prestressed Concrete Design Seminar, Chicago, January 25 - 29, 1971.
- (27) Brown, E.I. "Strength of Reinforced Concrete T-Beams Under Combined Direct Shear and Torsion." ACI JOURNAL, V. 51, No. 9, May 1955.
- (28) Hsu, T.T.C. "Torsion of Structural Concrete-Ultimate Torque of Reinforced Rectangular Beams." Portland Cement Association, Research and Development Division, Skokie, Illinois, May 1967.
- (29) ACI "Torsion of Structural Concrete" Publication SP - 18, American Concrete Institute, Detroit, Michigan, 1966.
- (30) Libby J.R. "Modern Prestressed Concrete, Design Principles and Construction Methods." Van Nostrand Reinhold Company New York.
- (31) Lehrstuhl fuer Massivbau, Technische Universitaet Munich "Einfluss von Kriechen und Schwinden des Betons auf Schnittgroessen und Spannungen."
- (32) Portland Cement Association "Design and Control of Concrete Mixtures." PCA Engineering Bulletin.
- (33) Stiglat/Wippel "Platten" Verlag von Wilhelm Ernst & Sohn, Berlin 1973.
- (34) Franz, G. "Konstruktionslehre des Stahlbetons." Springer-Verlag, Berlin, 1964.

DESIGN OF THE FORM WORK FOR THE CASTING OF THE CONCRETE BEAMS

A1 Concrete pressure on the form work

The pressure exerted by fresh concrete on the walls of the form work could cause the latter to deform appreciably. These deformations would result to bulging and irregular cross sectional properties of the concrete specimen. The purpose of this detailed design was to prevent such irregularities.

The lateral concrete pressure on the wall of the form work is influenced to a certain extent by the friction on the wall surface (34). This influence is illustrated in Fig 24.

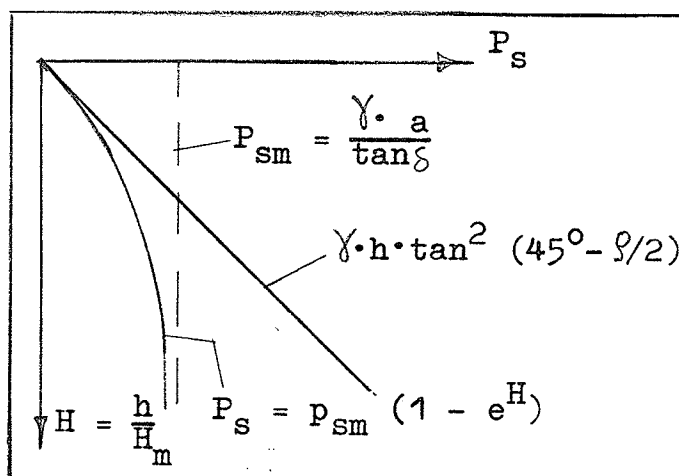


Fig. 24 Influence of the wall surface friction on the lateral concrete pressure.

$$a = \frac{A}{U} ; H_m = \frac{a}{k} ; k = \tan \delta \cdot \tan^2 (45^\circ - \delta/2);$$

A = cross sectional area of concrete in the form work;

U = perimeter of the form work;

γ = specific gravity of concrete;

δ = angle of friction on the wall surface;

ϕ = angle of internal friction;

The lateral pressure $p_s = p_{sm} (1 - e^H)$, where $p_{sm} = \frac{\gamma \cdot a}{\tan \delta}$, represents the "silo effect" which results when the space between the walls of the form work is small relative to the height of the cast concrete. The height of each test beam was only twice the width. The equation for the lateral pressure for the "silo effect" condition is not used in the design. The following more conservative equation for the lateral pressure will be used.

$$p = \gamma \cdot h \cdot \tan^2 (45^\circ - \phi/2), \text{ Fig. 24}$$

h = height of the cast concrete.

$$\text{For } \phi = 17.5^\circ \tan^2 (45^\circ - 8.75^\circ) = 0.537$$

$$p = 150 \times 2.0 \times 0.537 = 161.0 \text{ lb/sq.ft.}$$

Since the effect of the vibration of the concrete could greatly reduce the value of ϕ , or even make $\phi = 0$, and since there are uncertainties with regard to the effects of temperature, roughness of the form work and of the aggregate, the value of p obtained above will be doubled to

$$2 \times 161.0 = 322.0 \text{ lb/sq.ft.} = 2.24 \text{ psi.}$$

Modulus of elasticity (timber):

$$\text{Glued laminated timber } E_{pl} = 1.69 \times 10^6 \text{ psi}$$

$$\text{Sawn timber } E_{st} = 1.12 \times 10^6 \text{ psi}$$

$$n = \frac{E_{st}}{E_{pl}} = \frac{1.12}{1.69} = 0.66.$$

A 2 Details of the form work

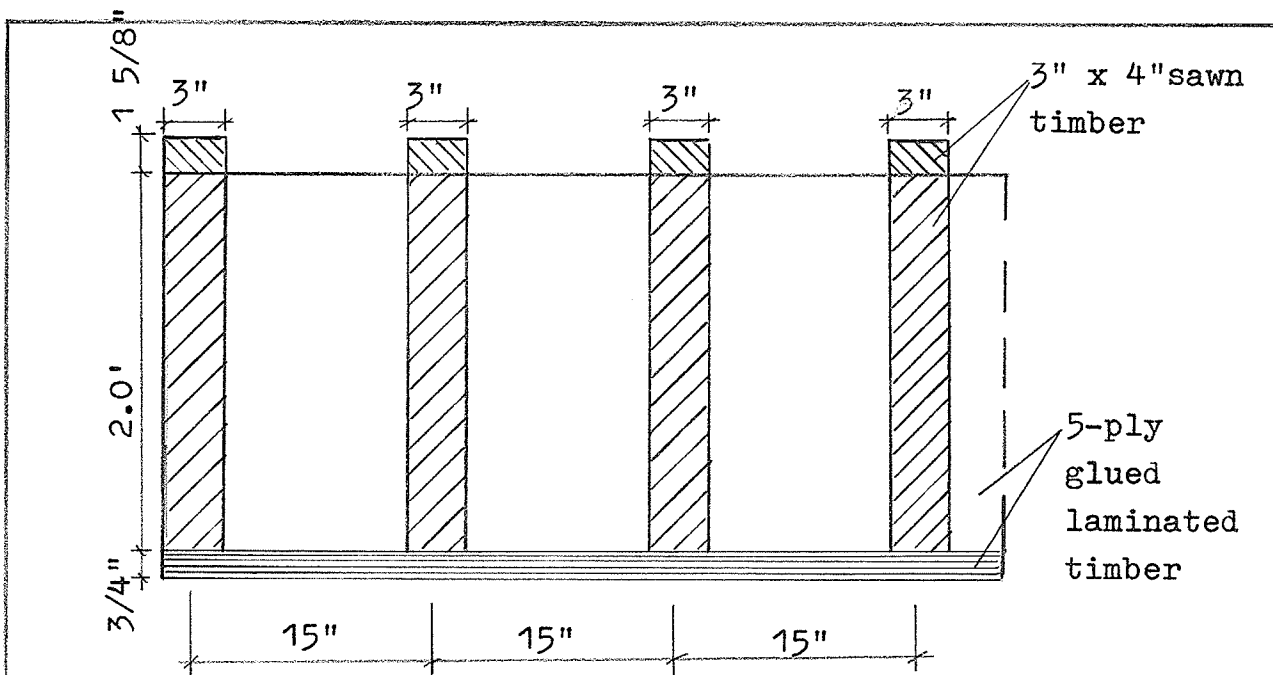


Fig. 25 Form work (elevation)

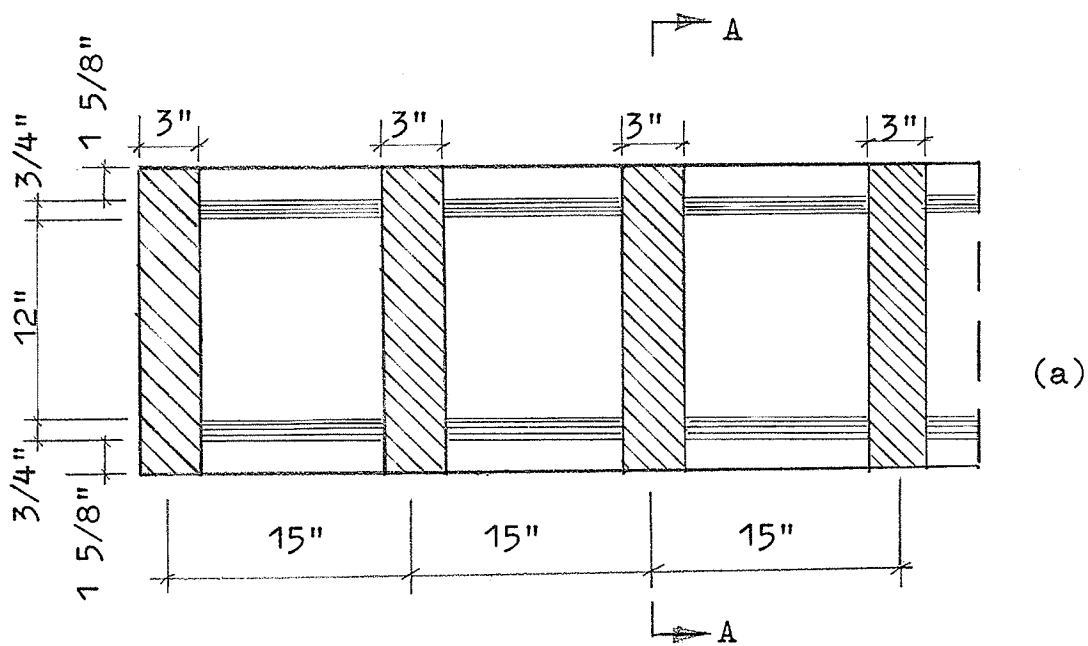


Fig. 26 Form work (plan)

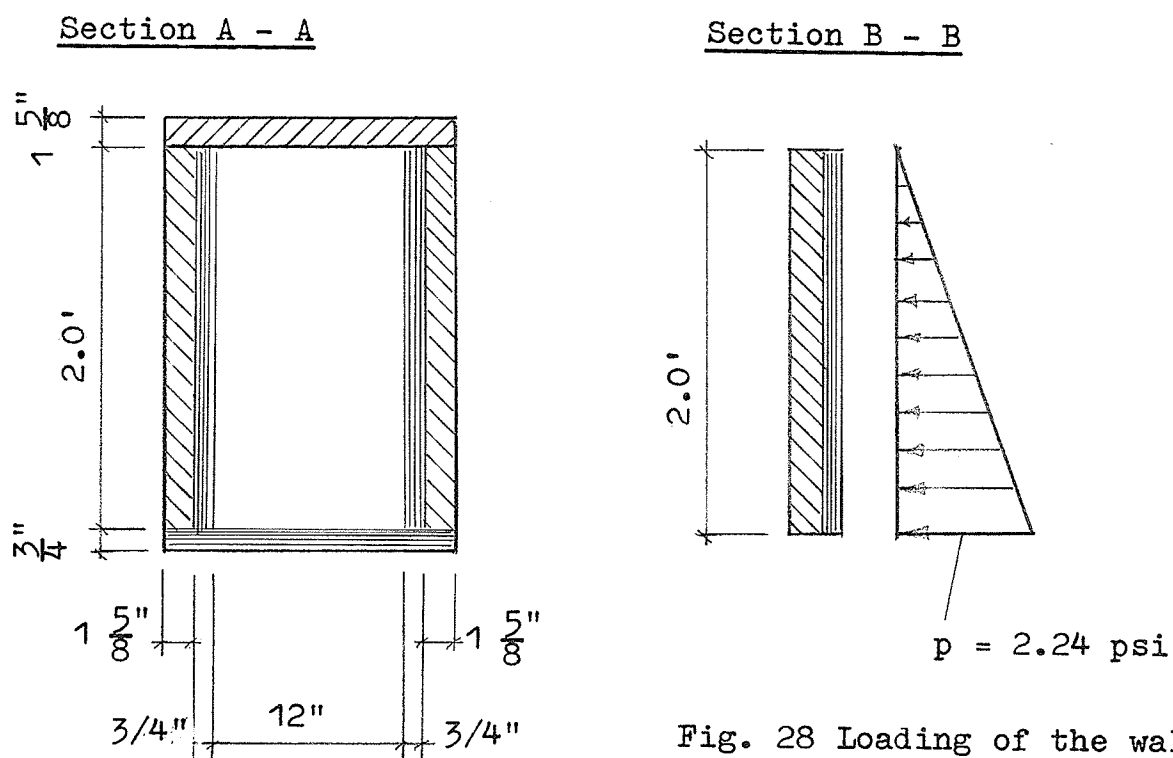


Fig. 28 Loading of the wall

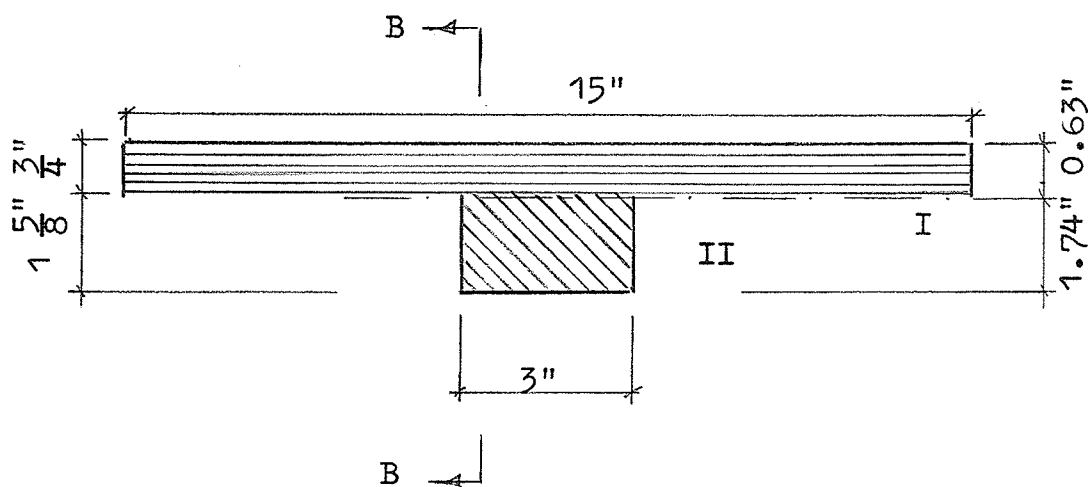


Fig. 27 A portion of the wall with stiffner (plan)

A3 Composite section properties

Part	Area A (in ²)	a(in)	Axa (in ³)	e(in)	I (in ⁴)	Axe ² (in ⁴)
I	11.25	2.0	22.50	0.26	0.53	0.76
II	3.22	0.81	2.61	0.93	0.70	2.78
Σ	14.47		25.11		1.23	3.54

$$e_{ib} = \frac{25.11}{14.47} = 1.74 \text{ in.}$$

$$e_{it} = 2.37 - 1.74 = 0.63 \text{ in.}$$

$$e_I = 2.0 - 1.74 = 0.26 \text{ in.}$$

$$e_{II} = 0.81 - 1.74 = 0.93 \text{ in.}$$

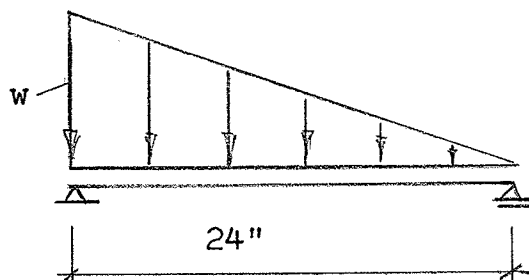
$$I_i = 1.23 + 3.54 = \underline{4.77 \text{ in}^4}$$

$$S_{ib} = \frac{I_i}{e_{ib}} = \underline{2.74 \text{ in}^3}$$

$$S_{it} = \frac{4.77}{0.63} = \underline{7.57 \text{ in}^3}$$

A4 Computation of the stresses

System with loading



$$p = 2.24 \text{ psi}$$

$$w = 2.24 \times 15 = 33.6 \text{ lb/in.}$$

$$\text{max. moment} = \frac{w \cdot l^2}{9 (3)^{1/2}} = \frac{33.6 \times 24^2}{9 \times 1.73} = 1243.0 \text{ lb.in.}$$

Stresses:

$$\text{Laminated timber } f_{pl} = \frac{\text{max. } M}{Z_{it}} = \frac{1243.0}{7.57} = \underline{164.2 \text{ psi}} \\ (\text{compression})$$

$$\text{Sawn timber } f_{st} = n \times \frac{\text{max. } M}{Z_{ib}} = 0.66 \frac{1243.0}{2.74} = \underline{299.4 \text{ psi}} \\ (\text{tension})$$

A5 Deflection

Deflection at the stiffening support:

$$\Delta_1 = 0.00652 \frac{w l^4}{E I}$$

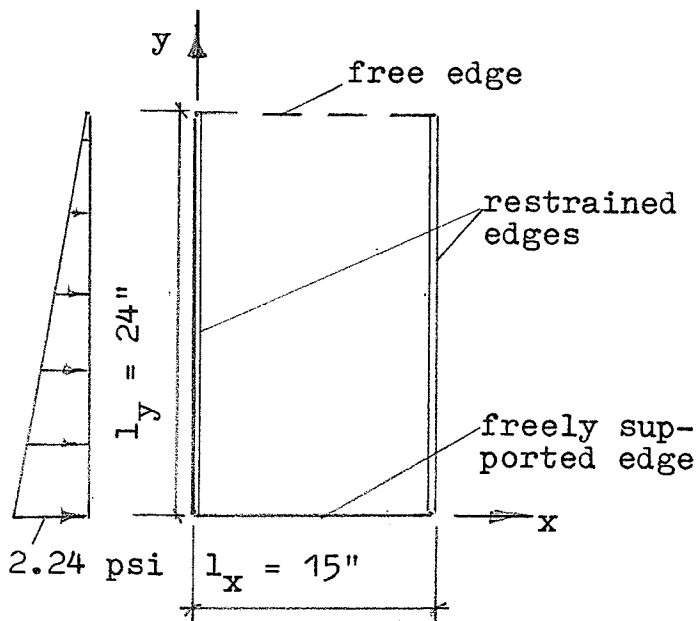
Calculating with the smaller of the two values of

E (E_{st}):

$$\Delta_1 = \frac{0.00652 \times 33.6 \times 24^4}{1.120 \times 10^6 \times 5.85} = \underline{0.011 \text{ in.}}$$

The deflection at the stiffening support is insignificant.

Deflection of the plywood between two stiffening supports:



$$\Delta_2 = \frac{K \cdot l_x^2}{k_w \cdot N}$$

$$K = \frac{p \cdot l_x \cdot l_y}{2}$$

$$N = \frac{d^3 \cdot E}{12} \quad (= \text{plate stiffness})$$

d = thickness of plate

k_w = deflection coefficient
given in (33)

$$K = \frac{2.24 \times 15.0 \times 24}{2} = 403.2 \text{ lb.}$$

$$N = \frac{0.75^3 \times 1.69 \times 10^6}{12} = 0.059 \times 10^6 \text{ lb-in.}$$

$$\frac{I_y}{I_x} = \frac{24}{15} = 1.6$$

From Tables (33) $k_w = 2100$

$$\Delta_2 = \frac{403.2 \times 15^2}{2100 \times 0.059 \times 10^6} = 0.0007 \text{ in.}$$

Total deflection $\Delta = 0.011 + 0.0007 = 0.0117 \text{ in.}$

The total deflection is also insignificant.

APPENDIX B

DESIGN OF THE STEEL YOKE

B. 1 Introductory remark

The primary purpose of the three steel yokes was to provide the means of applying the torsional loading to the test beams in the manner explained in Chapter III. The nature of the laboratory investigation made it necessary to test reinforced concrete beams of a fairly big size. A steel yoke strong enough to provide the necessary torsional moments and at the same time suffering no appreciable deformation was necessary. Another purpose of the steel yokes was to provide the means of testing beams of bigger cross sections such as reinforced or prestressed concrete box girders for pure torsion or for torsion combined with bending and shear. With regard to the size of the testing frame available in the Heavy Structures Laboratory the yoke was designed for beams with overall dimensions of not more than 24 inch square, Fig. 29. Each yoke could be adjusted and used for smaller test specimens. To facilitate such adjustment, each yoke comprised two parts, each part being rigidly welded together. The component pieces numbered 1, 2, 3 in Fig. 30 form one part; the pieces numbered 4, 5, 6 form the other part. The two parts are connected by bolts for a chosen test specimen size. Shims could be used when the height or width of a test specimen is less than 12 inches.

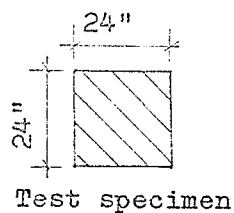
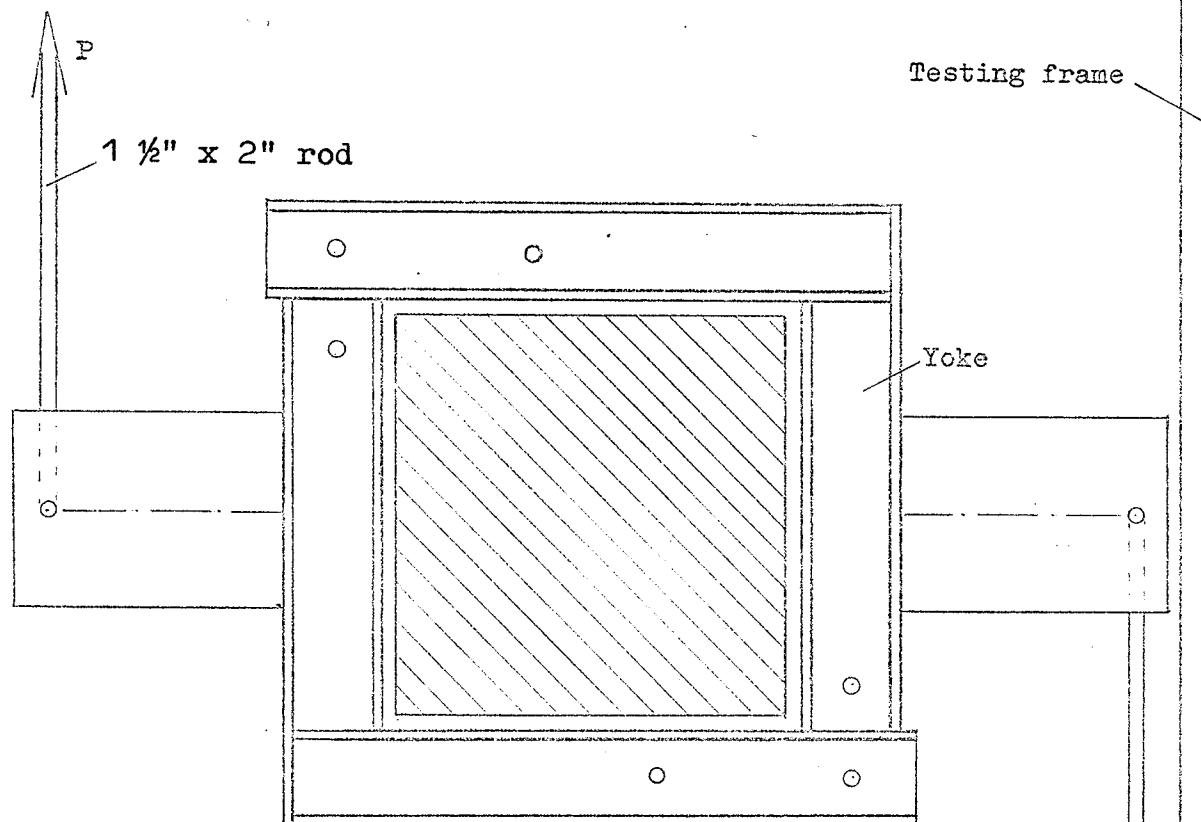


Fig. 29 Yoke set-up for large test specimen

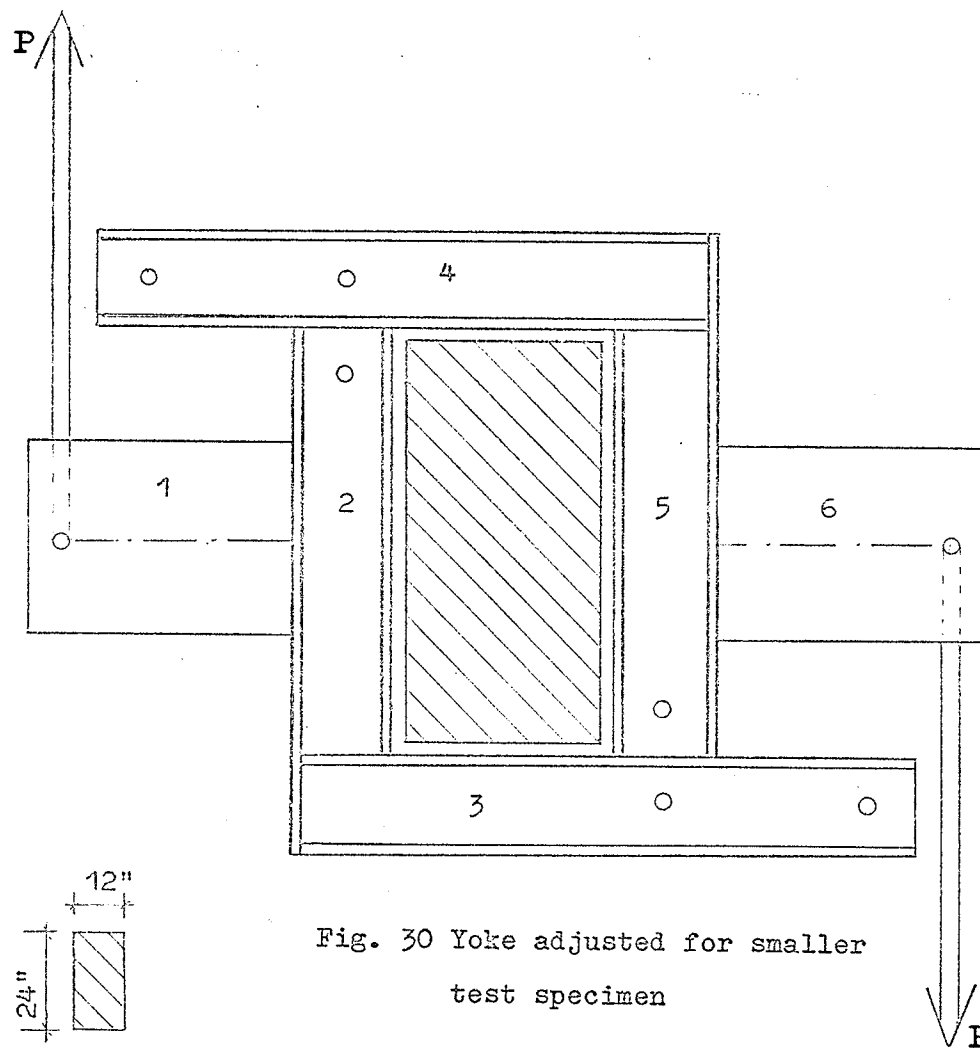


Fig. 30 Yoke adjusted for smaller
test specimen

Test specimen

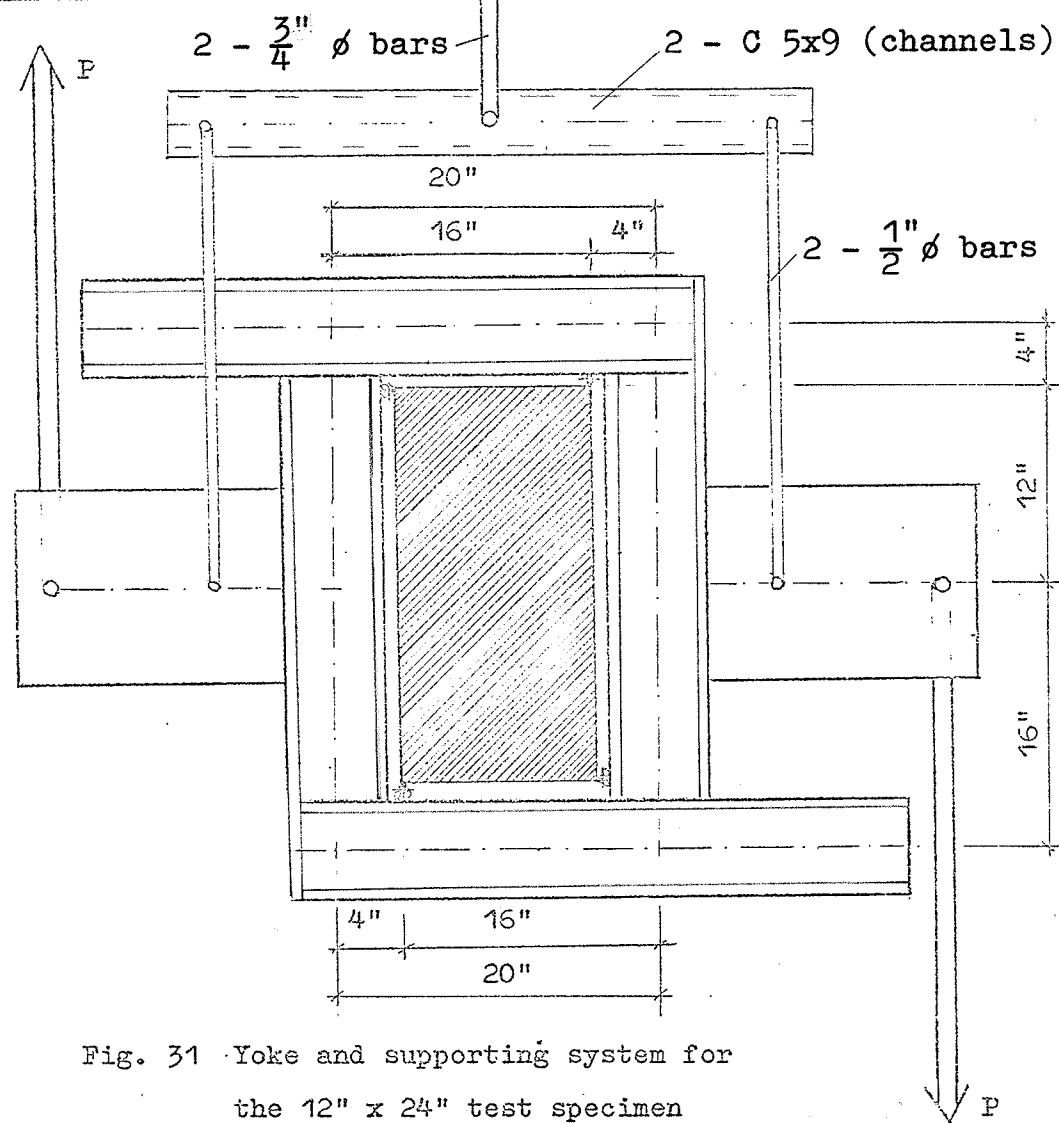
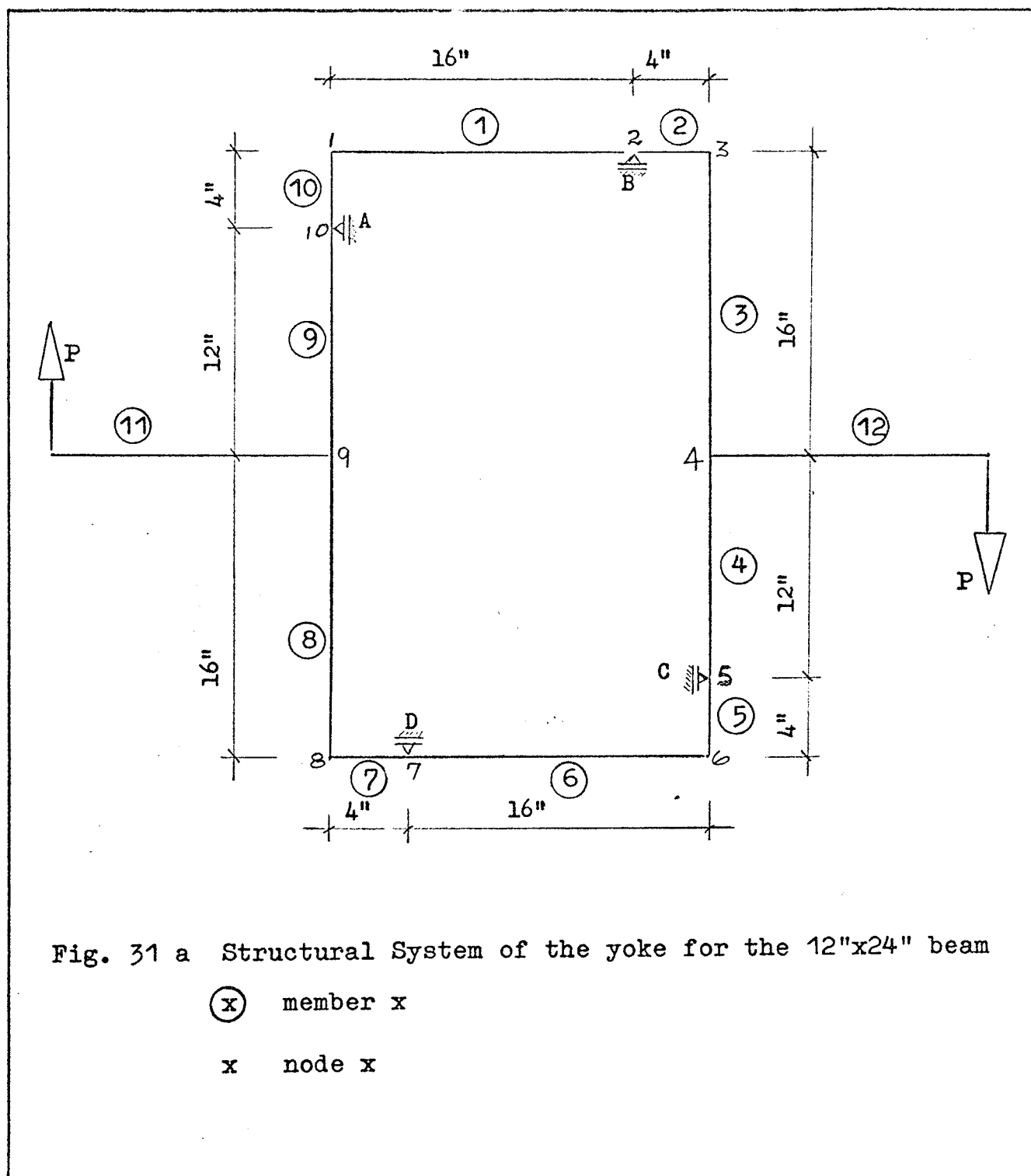


Fig. 31 Yoke and supporting system for
the 12" x 24" test specimen



B 2 Analysis of the yoke

The three yokes were identical. Each was designed for two equal loads $P = 50$ Kips applied simultaneously as shown in Fig. 29 and in the structural system on page 93. The determination of the forces acting on the system for the chosen design load was done by means of the plane frame computer program incorporated in the University of Manitoba Computer System. Two computations were made for two structural systems corresponding to two yoke adjustments for test specimens of 12" x 24" and 24" x 24". The determined member end forces are shown in Tables B 1 and B 2.

Table B 1 Member end forces for the yoke adjusted
for 12" x 24" test specimen.

Member	Start			End		
	Axial	Shear	Moment	Axial	Shear	Moment
1	-42.972	-2.046	-3.316	42.972	2.046	0.588
2	-42.972	51.101	-0.588	42.972	-51.101	17.605
3	-51.101	-42.972	-39.848	51.101	42.972	-17.605
4	-2.641	-42.972	-11.016	2.641	42.972	-31.956
5	-2.641	44.185	3.698	2.641	-44.185	11.016
6	-44.185	-2.641	0.178	44.185	2.641	-3.698
7	-44.185	53.586	18.022	44.185	-53.586	-0.178

Member	Start			End		
	Axial	Shear	Moment	Axial	Shear	Moment
8	-53.586	-44.185	-18.022	53.586	44.185	-40.876
9	-2.046	-44.185	-33.020	2.046	44.185	-11.165
10	-2.046	42.971	11.165	2.046	-42.971	3.316
11	-0.000	-51.540	-73.896	0.000	50.000	-0.000
12	-0.000	48.460	71.804	0.000	-50.000	0.000

Table B 2 Member end forces for the yoke adjusted
for 24" x 24" test specimen.

Member	Start			End		
	Axial	Shear	Moment	Axial	Shear	Moment
1	-41.427	-2.543	-4.406	41.427	2.543	-1.527
2	-41.428	51.339	1.527	41.428	-51.339	15.569
3	-51.339	-41.428	-39.820	51.339	41.428	-15.569
4	-2.879	-41.428	-9.443	2.879	41.428	-31.985
5	-2.879	42.651	4.760	2.879	-42.651	9.443
6	-42.651	-2.879	-1.957	42.651	2.879	-4.760

Member	Start			End		
	Axial	Shear	Moment	Axial	Shear	Moment
7	-42.651	54.083	16.053	42.651	-54.083	1.957
8	-54.083	-42.651	-16.053	54.083	42.651	-40.800
9	-2.543	-42.651	-33.096	2.543	42.651	-9.555
10	-2.543	41.427	9.555	2.543	-41.427	4.406
11	-0.000	-51.540	-73.896	0.000	50.000	0.000
12	-0.000	48.460	71.804	0.000	-50.000	-0.000

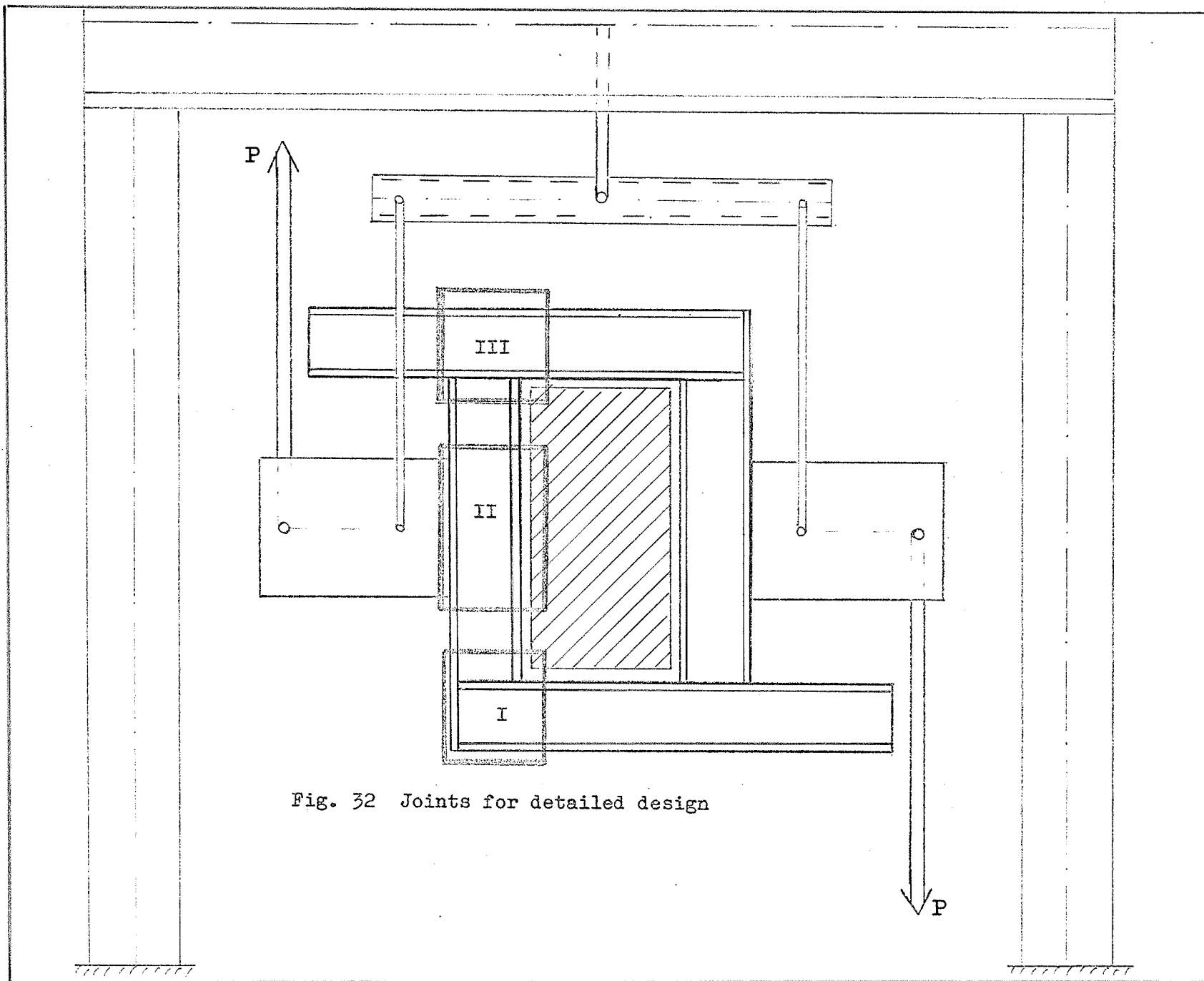
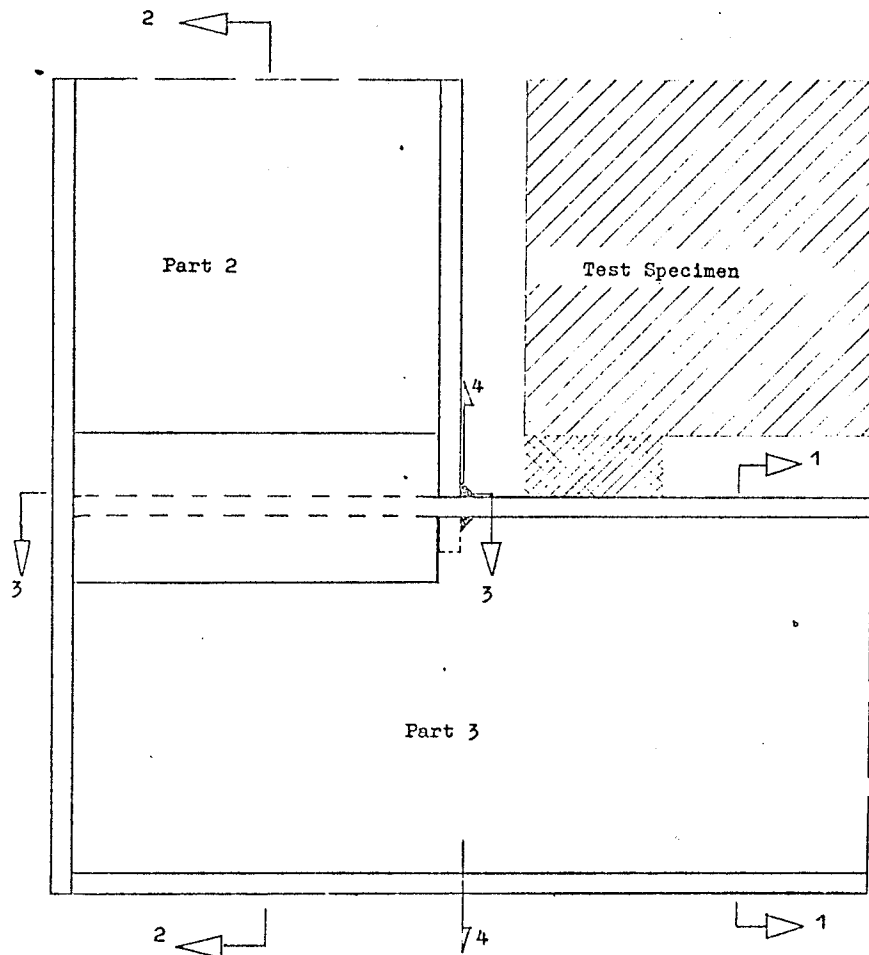


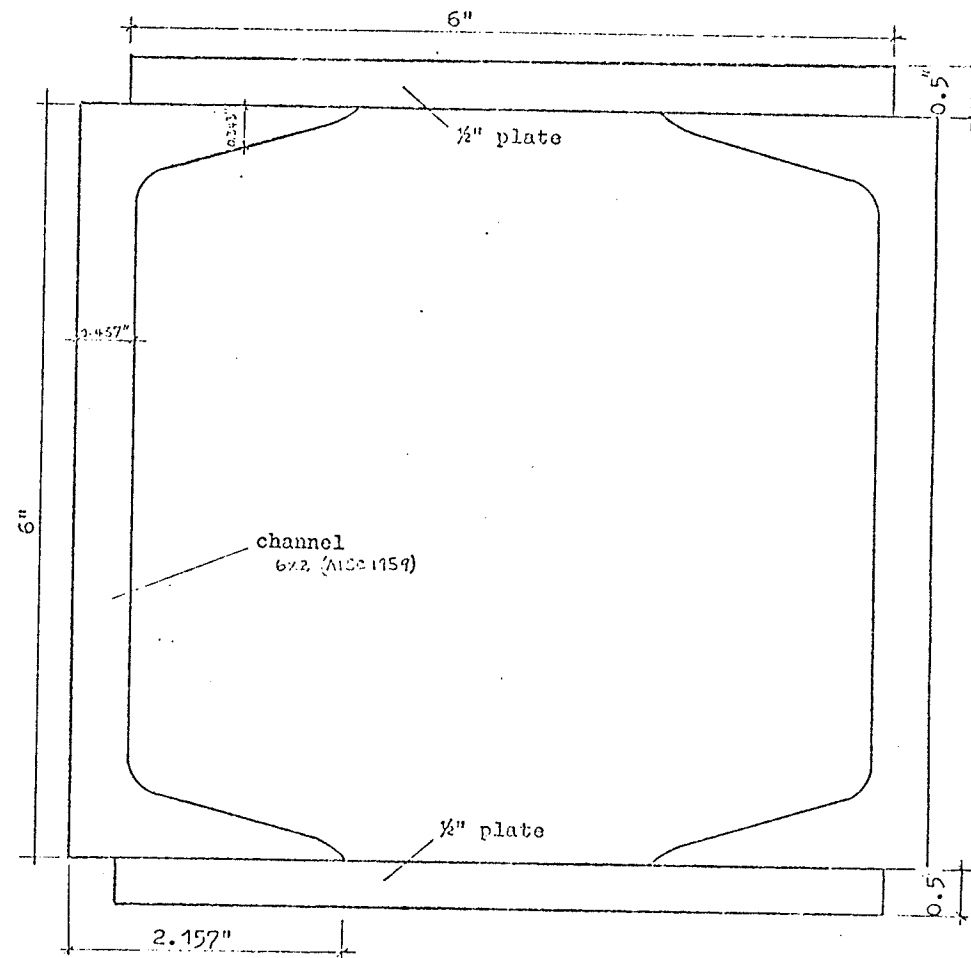
Fig. 32 Joints for detailed design

Detail I (Elevation)

Connection of the pieces 2 and 3 of Fig. 30.



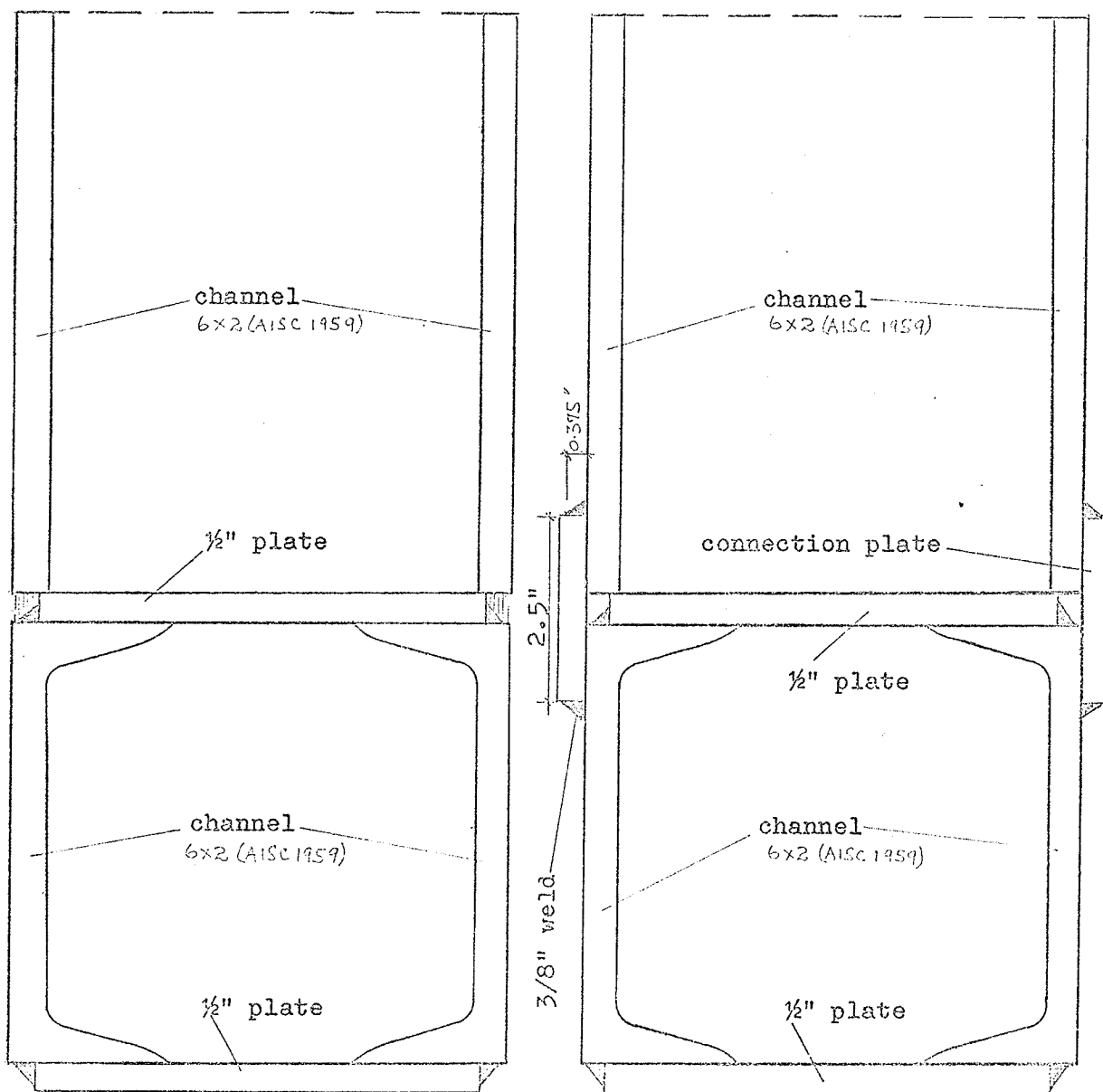
Section 1 - 1



Section 2 - 2

a) Without side connection plate

b) With side connection plate

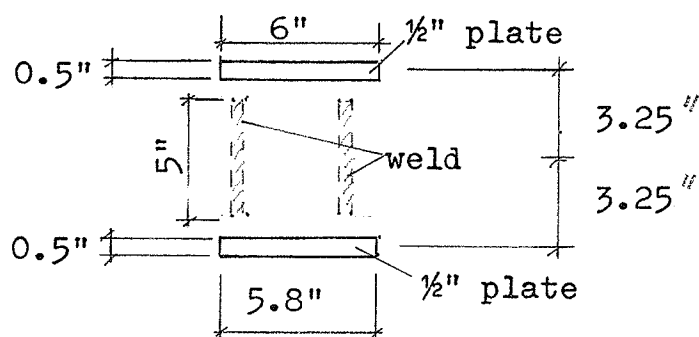


Connection type (a) is chosen for the design

B. 3 Check for stresses

The stress check is made for the portions marked I to III in Fig. 32.

Section 3 - 3



Section properties:

$$I_{pl} = \frac{6.0 \times 0.5^3}{12} + 6 \times 0.5 \times 3.25^2 + \frac{5.8 \times 0.5^3}{12} + 5.8 \times 0.5 \times 3.25^2 = 62.44 \text{ in.}^4$$

$$I_{weld} = 2 \times \frac{0.25 \times 5^3}{12} = \underline{5.08 \text{ in.}^4}$$

$$= 67.65 \text{ in.}^4$$

$$S^{top} \approx S^{bott.} = \frac{67.65}{3.5} = 19.33 \text{ in.}^3$$

$$A = 0.5 (6.0 + 5.8) + 2 \times 0.25 \times 5.0 = 8.40 \text{ in.}^2$$

Forces:

$$M = 18.02 \text{ Kip ft.} \quad (\text{system 1})$$

$$N = 54.08 \text{ K} \quad (\text{system 2})$$

$$V = 44.19 \text{ K} \quad (\text{system 1})$$

Stresses:

-101-

$$f^{\text{top}} \quad (\text{at the outside of the frame})$$

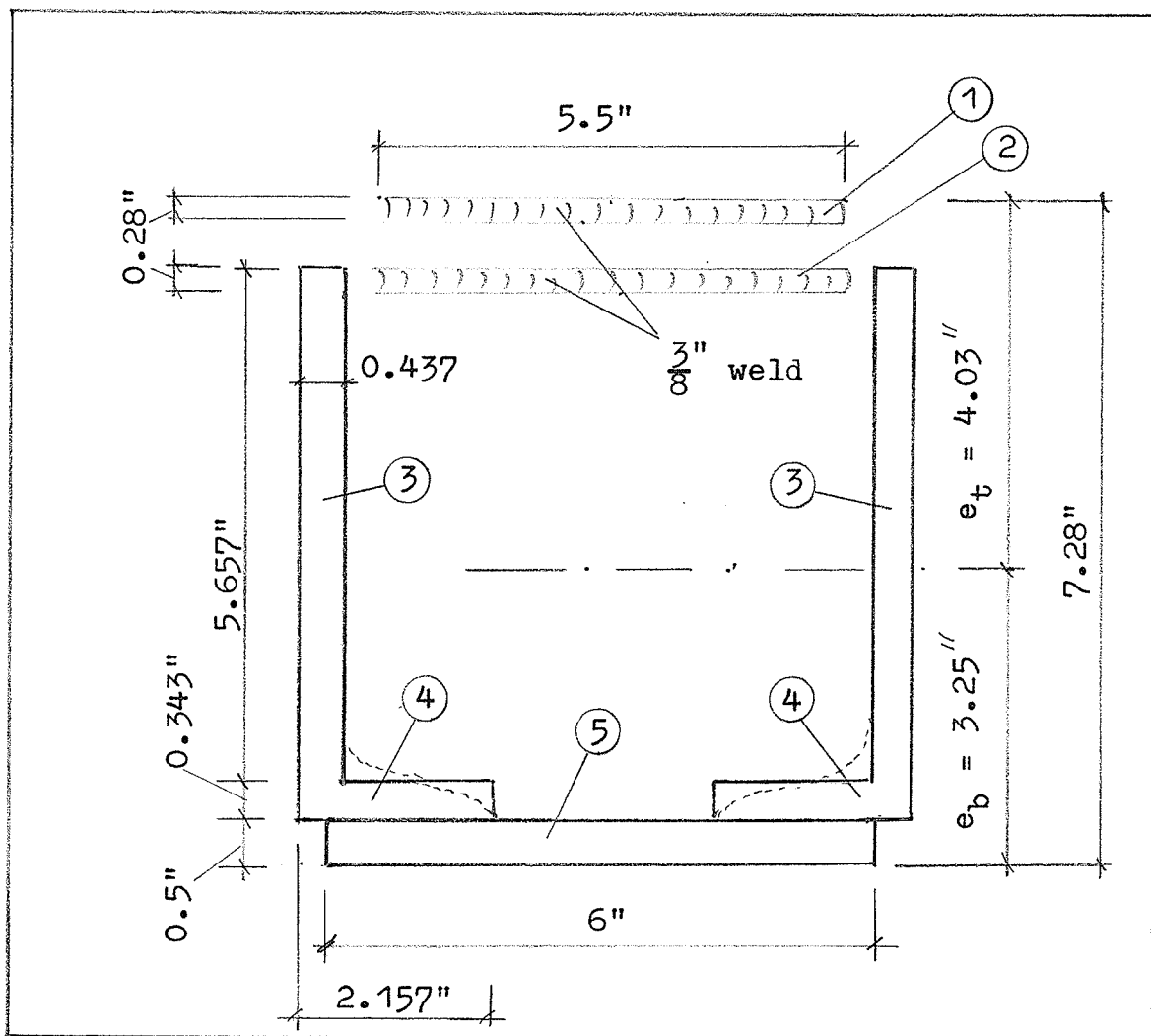
$$= \frac{54.08}{8.40} - \frac{18.02 \times 12}{19.33} = \underline{-4.75 \text{ Ksi}} \quad (\text{compression})$$

$$f^{\text{bott.}} \quad (\text{at the inside of the frame})$$

$$= 6.44 + 11.19 = \underline{17.63 \text{ Ksi}} \quad (\text{tension})$$

$$v = \frac{44.19}{8.40} = \underline{5.26 \text{ Ksi}}$$

Section 4 - 4



Section properties:

Part	Area A(in ²)	a(in)	Axa (in ³)	e(in)	I (in ⁴)	Axe ² (in ⁴)
1	1.54	7.14	11.00	3.89	≈ 0	23.30
2	1.54	6.36	9.80	3.11	≈ 0	14.90
3	4.94	3.67	18.13	0.42	6.59	0.87
4	1.48	0.67	0.99	-2.58	≈ 0	9.85
5	3.00	0.25	0.75	-3.00	0.06	27.00
Σ	12.50		40.67		6.65	75.92

$$e_b = \frac{40.67}{12.50} = 3.25 \text{ in.}$$

$$e_t = 7.28 - 3.25 = 4.03 \text{ in.}$$

$$e_1 = 7.14 - 3.25 = 3.89 \text{ in.}$$

$$e_2 = 6.36 - 3.25 = 3.11 \text{ in.}$$

$$e_3 = 0.42 \text{ in. ; } e_4 = -2.58 \text{ in. ; } e_5 = -3.00 \text{ in.}$$

$$I_i = I + A \cdot e^2 = 82.57 \text{ in}^4$$

$$s^{\text{top}} = \frac{82.57}{4.03} = 20.49 \text{ in}^3$$

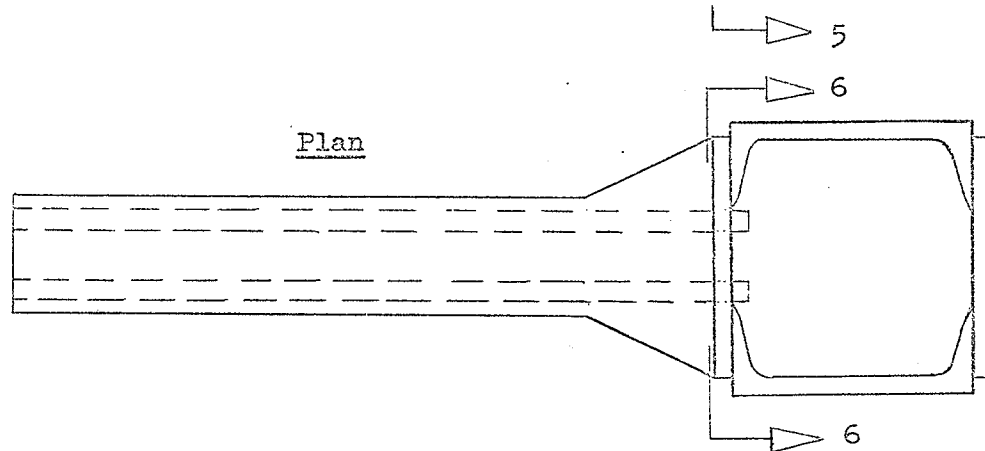
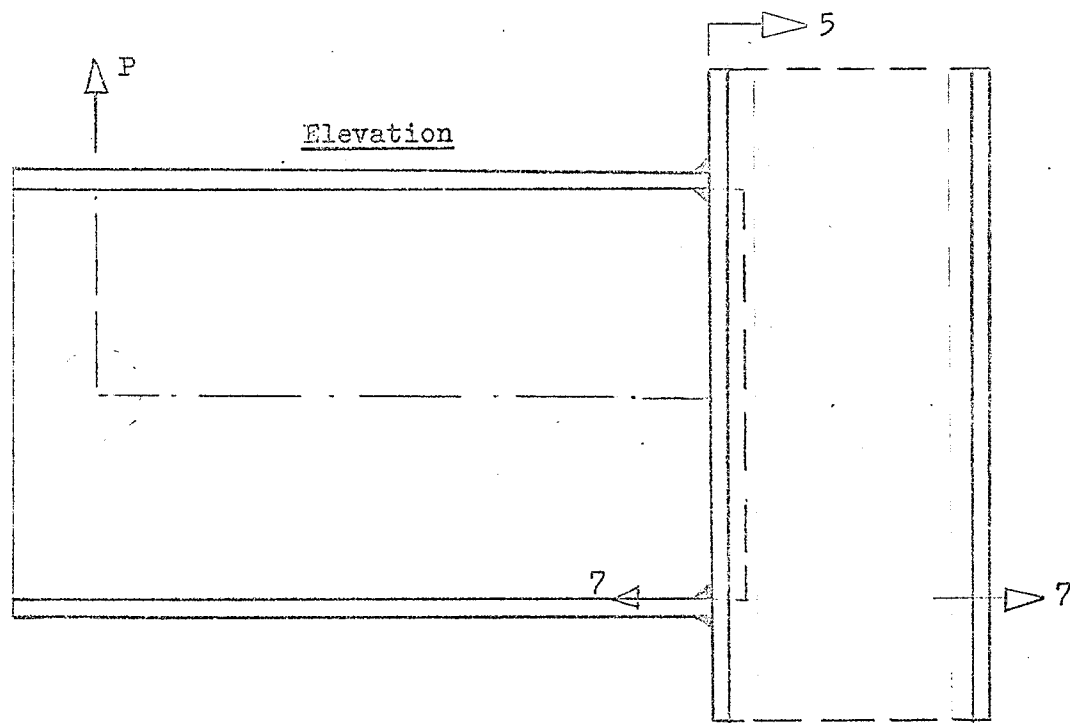
$$s^{\text{bott.}} = \frac{82.57}{3.25} = 25.41 \text{ in}^3$$

Forces:

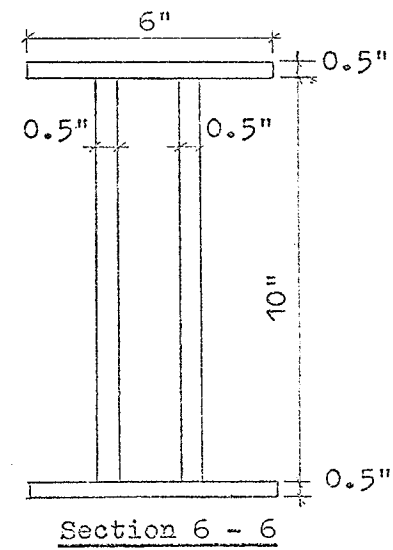
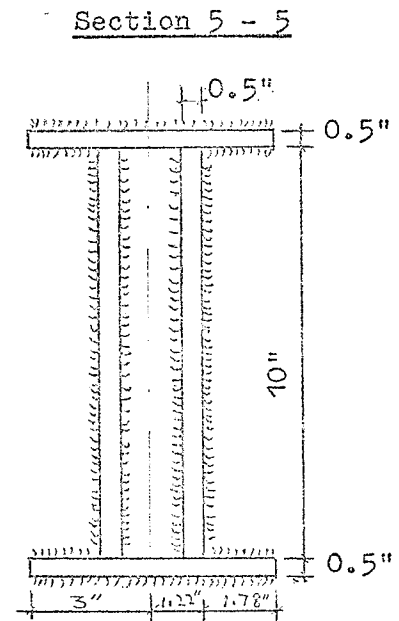
$$M = 18.02 \text{ Kip ft.}$$

$$N = 44.19 \text{ K}$$

$$V = 54.08 \text{ K}$$



Detail II



Stresses:

-104-

$$\begin{aligned} f^{\text{top}} & \quad (\text{at the inside of the frame}) \\ & = \frac{44.19}{12.50} + \frac{18.02 \times 12}{20.49} = \underline{14.09 \text{ Ksi}} \\ f^{\text{bott.}} & = 3.54 - \frac{18.02 \times 12}{25.41} = - \underline{4.97 \text{ Ksi}} \\ v & = \frac{54.08}{12.50} = \underline{4.33 \text{ Ksi}} \end{aligned}$$

Section 5 - 5

The Stresses are carried by the weld and the web plates

Section moment or inertia:

$$\begin{aligned} \text{web plates: } & \frac{2 \times 0.5 \times 10^3}{12} = 83.33 \text{ in.}^4 \\ \text{web weld: } & \frac{4 \times 0.26 \times 9^3}{12} = 63.18 \text{ in.}^4 \\ \text{flange weld: } & 2\left(\frac{6 \times 0.26^3}{12} + 6 \times 0.26 \times 5.63^2\right) = 98.91 \text{ in.}^4 \\ & 4\left(\frac{1.4 \times 0.26^2}{12} + 1.4 \times 0.26 \times 5.13^2\right) = \underline{38.33 \text{ in.}^4} \\ & \quad \quad \quad 283.75 \text{ in.}^4 \end{aligned}$$

$$S^{\text{top}} = S^{\text{bott.}} = \frac{283.75}{5.76} = 49.26 \text{ in.}^3$$

$$A = 2 \times 0.5 \times 10 + 0.26(4 \times 9 + 2 \times 5.5 + 4 \times 1.4) = 23.68 \text{ in.}^2$$

$$M = 71.80 \text{ Kip ft.}$$

$$N = 0.0 \text{ K}$$

$$V = 48.46 \text{ K}$$

Stresses:

$$\begin{aligned} f^{\text{top}} = f^{\text{bott.}} & = \frac{71.80 \times 12}{49.26} = \underline{17.49 \text{ Ksi}} \\ v & = \frac{48.46}{10.0} = \underline{4.85 \text{ Ksi}} \end{aligned}$$

Section 6 - 6

Section moment of inertia:

$$\text{Web plates : } \frac{2 \times 0.5 \times 10^3}{12} = 83.33 \text{ in.}^4$$

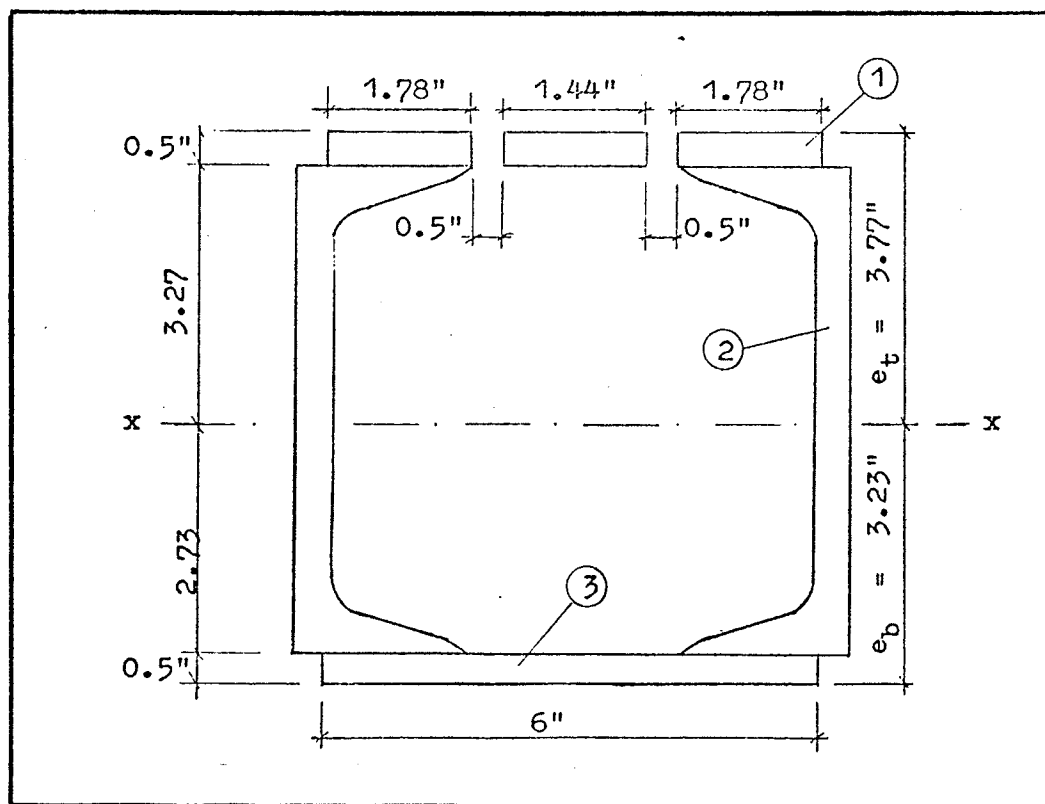
$$\text{flanges: } 2\left(\frac{6 \times 0.5^3}{12} + 6 \times 0.5 \times 5.25^2\right) = \frac{165.50 \text{ in.}^4}{248.83 \text{ in.}^4}$$

$$S = \frac{248.83}{5.5} = 45.24 \text{ in.}^3$$

$$f = \frac{71.80 \times 12}{45.24} = \underline{19.0 \text{ Ksi}}$$

Section 7 - 7

Section properties:



Part	Area A(in ²)	a (in)	Axa (in ³)	e(in)	I (in ⁴)	Axe ² (in ²)
1	2.50	6.75	16.88	3.52	0.05	30.98
2	7.62	3.25	24.77	0.02	34.60	0
3	3.00	0.25	0.75	2.98	0.06	26.64
	13.12		42.40		34.71	57.62

$$e_b = \frac{42.40}{13.12} = 3.23 \text{ in.}$$

$$e_t = 7.0 - 3.23 = 3.77 \text{ in.}$$

$$e_1 = 6.75 - 3.23 = 3.52 \text{ in.}$$

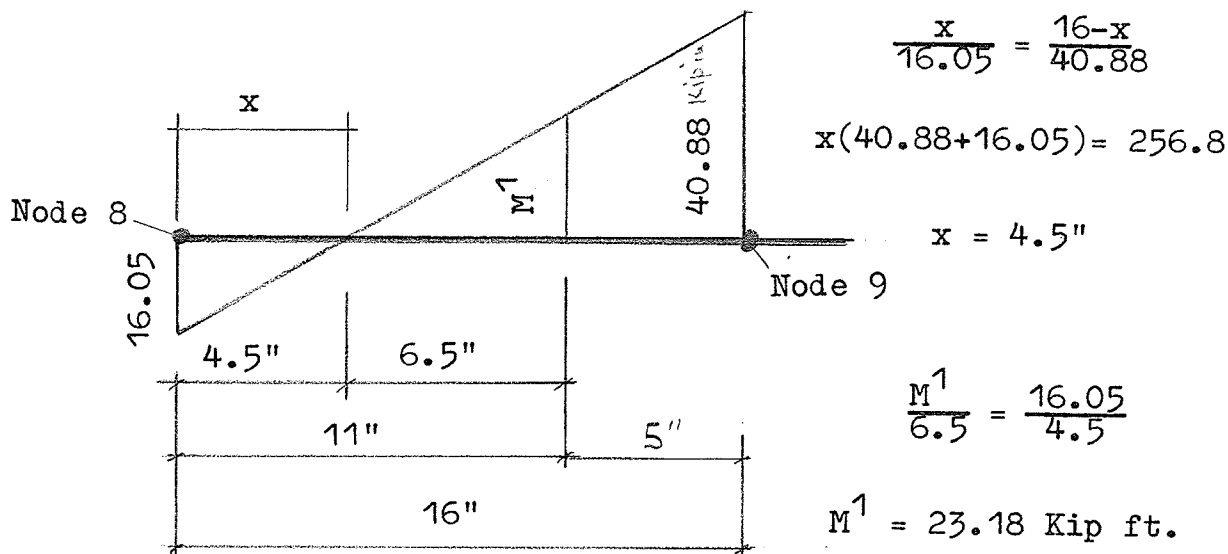
$$e_2 = 0.02 \text{ in ; } e_3 = - 2.98$$

$$I_i = 34.71 + 57.62 = 92.33$$

$$S^{\text{top}} = \frac{92.33}{3.77} = 24.49 \text{ in}^3$$

$$S^{\text{bott.}} = 28.59 \text{ in}^3$$

$$\left. \begin{array}{l} M = 40.88 \text{ Kip ft.} \\ N = 54.08 \text{ K} \\ V = 44.19 \text{ K} \end{array} \right\} \text{ at node 9}$$



$$f^{\text{top}} = \frac{54.08}{13.12} + \frac{23.18 \times 12}{24.49} = \underline{15.48 \text{ Ksi}}$$

$$f^{\text{bott.}} = 4.12 - \frac{23.18 \times 12}{28.59} = \underline{-5.61 \text{ Ksi}}$$

Section 8 - 8 (page 109)

Forces:

$$M = 4.41 \text{ Kip ft.}$$

$$N = 2.54 \text{ K}$$

$$V = 41.43 \text{ K}$$

Section moment of inertia:

$$\text{Two channels } 1 : 2 \times 17.3 = 34.60 \text{ in.}^4$$

$$\text{Flange plates } 2 : 2\left(\frac{6 \times 0.5^3}{12} + 6 \times 0.5 \times 3.25^2\right) = \frac{63.50 \text{ in.}^4}{98.10 \text{ in.}^4}$$

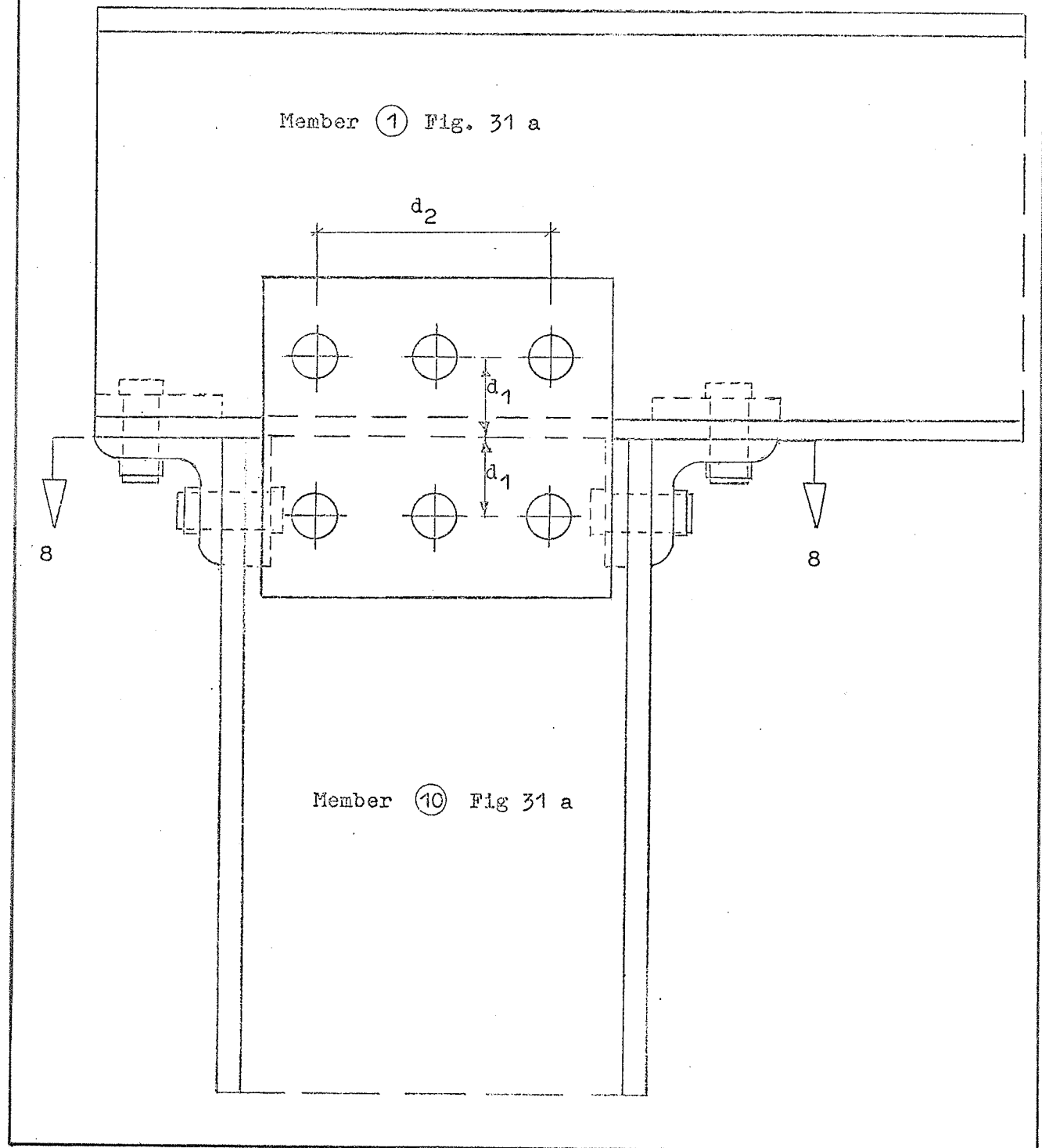
Moment of inertia of connection plates 2a :

$$2 \left(\frac{0.5 \times 5.5^3}{12} \right) = 13.86 \text{ in.}^4$$

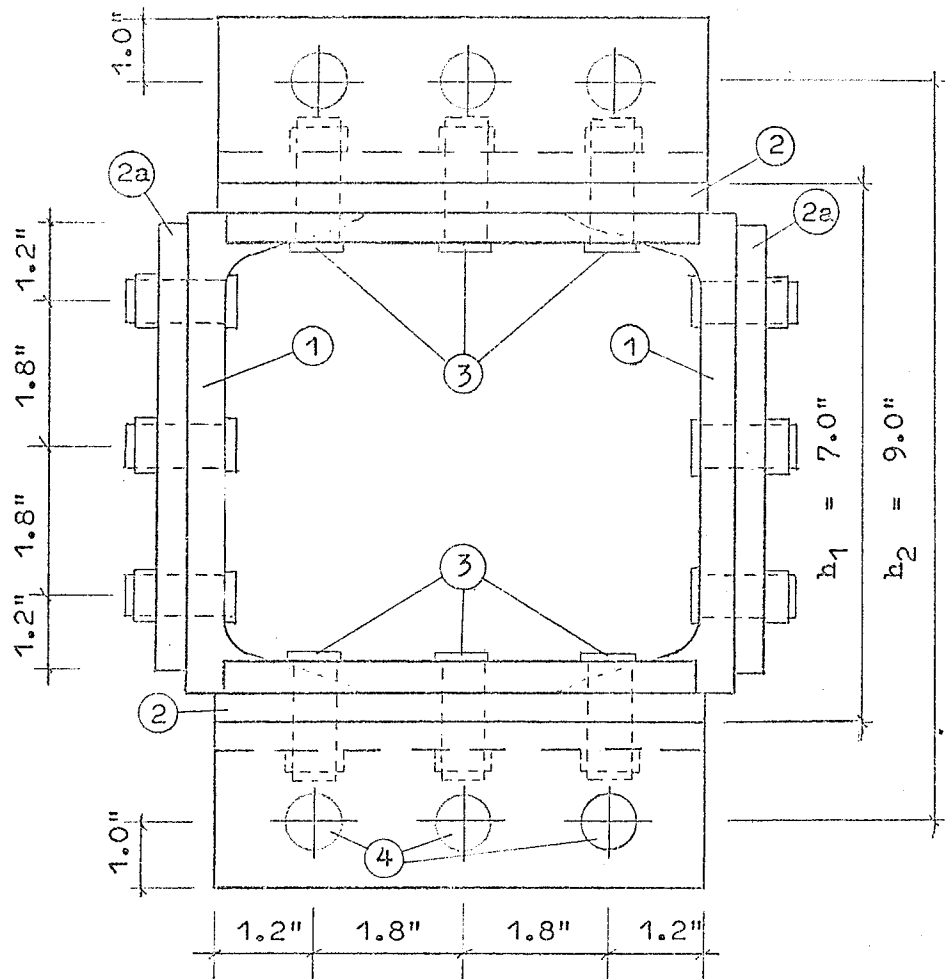
$$S = \frac{13.86}{3} = 4.62 \text{ in.}^3$$

$$\frac{34.60}{98.10} = 0.352$$

Detail III



Section 8 - 8



Moment carried by connection plates 2a :

$$M_1 = 0.352 \times 41.43 = 1.55 \text{ Kip ft.}$$

Computation of the stresses

(1) Bolts 3 :

Moment carried by the bolts $M_2 = 4.41 - 1.55 = 2.86 \text{ Kip ft.}$

Tensile force in the bolts due to M_2

$$= \frac{M_2}{h_1} = \frac{2.86 \times 12}{7.0} = 4.90 \text{ K}$$

$\frac{1}{2}$ " ϕ bolts with $A = 0.196 \text{ in}^2$

$$\text{Tensile stress } f_1 = \frac{4.90}{3 \times 0.196} = 8.33 \text{ Ksi}$$

Part of the axial force in member 10 carried by bolts 3 :

$$N_1 = \frac{6}{12} \times 2.54 = 1.27 \text{ K}$$

$$f_2 = \frac{1.27}{6 \times 0.196} = 1.08 \text{ Ksi}$$

$$f_1 + f_2 = \underline{9.41 \text{ Ksi}}$$

(2) Bolts 4 :

Tensile force in the bolts due to M_2 :

$$N_2 = \frac{M_2}{h_2} = \frac{34.32}{9.0} = 3.81 \text{ K}$$

$$\text{Tensile stress } f_3 = \frac{3.81}{3 \times 0.196} = 6.48 \text{ Ksi}$$

$$\text{Tensile stress due to } N_1 \quad f_4 = \frac{1.27}{6 \times 0.196} = 1.08$$

$$f_3 + f_4 = \underline{7.56 \text{ Ksi}}$$

Shear force from axial force in member 1

$$N_2 = \frac{6}{12} \times 41.43 = 20.72 \text{ K}$$

$$\text{Shear stress } v = \frac{20.72}{6 \times 0.196} = 17.62 \text{ Ksi}$$

For $\frac{5}{8}$ " ϕ bolts each of area 0.336 in²

$$v = \frac{20.72}{6 \times 0.336} = \underline{10.28 \text{ Ksi}}$$

(3) Connection plates 2a :

Moment in the plates due to shear in member 10

$$\frac{1}{2} V \cdot d_1 = \frac{1}{2}(41.43 \times 1.25) = 25.89 \text{ Kip in.}$$

Total moment resisted by connection plates

$$M_3 = 1.55 \times 12 + 25.89 = 44.49 \text{ Kip in.}$$

$$\text{Bending moment stress } f_5 = \frac{44.49}{4.62} = \underline{9.63 \text{ Ksi}}$$

Shear force in the bolts of the connecting plates:

$$\text{parallel to member 10: } \max H_1 = \frac{M_3}{d_2} \text{ k}$$

For the bolt arrangement chosen, $k = 1.0$

$$\text{For one side } \max H_1 = \frac{1}{2} \left(\frac{44.49}{3.6} \right) = 6.18 \text{ K}$$

$$\text{parallel to member 1 : } H_2 = \frac{V}{n} = \frac{41.43}{12} = 3.45 \text{ K}$$

$$\text{Resultant bolt force} = (H_1^2 + H_2^2)^{\frac{1}{2}} = 7.08 \text{ K}$$

$$\max \text{ shear stress} = v_{\max} = \frac{7.08}{0.307} = \underline{23.06 \text{ Ksi}}$$

For all bolt connections use $\frac{5}{8}$ " ASTM A 490X with allowable shear stress of 32 Ksi. A more conservative approach for the bolt connection was adopted by increasing the number of bolts of each connection plate from 6 to 8, see (photograph) Plate 7.

CROSS-SECTION AREAS FOR STRESS COMPUTATION

Modular ratio $n = 8$ Beam I (not grouted)

$$\text{Area of 3 tendon ducts} = 3 \times \frac{3.1416 \times 1.5^2}{4} = 5.30 \text{ sq.in.}$$

$$\text{Net area} = 288 - 5.30 = 282.70 \text{ sq.in.}$$

Additional equivalent area from reinforcing

$$\text{bars} = (8 - 1) \times 0.11 \times 14 = 10.80 \text{ sq.in.}$$

$$\text{Area of composite section} = \underline{293.50 \text{ sq.in.}}$$

Beam II (grouted)

$$\text{Gross area} = 12 \times 24 = 288.00 \text{ sq.in.}$$

$$\text{From reinf. bars } (8 - 1) \times 0.11 \times 7 = 5.39 \text{ sq.in.}$$

$$\text{Area of composite section} = \underline{293.39 \text{ sq.in.}}$$

Beam III (not grouted)

$$\text{Area of 4 tendon ducts} = 4 \left(\frac{3.1416 \times 1.5^2}{4} \right) = 7.06 \text{ sq.in.}$$

$$\text{Net area} = 288 - 7.06 = 280.94 \text{ sq.in.}$$

$$\text{From reinf. bars } 7 \times 0.11 \times 6 = 4.62 \text{ sq.in.}$$

$$\text{Area of composite section} = \underline{285.56 \text{ sq.in.}}$$

Beam IV (not grouted)

$$\text{Area of 4 ducts} = 7.06 \text{ sq.in.}$$

$$\begin{aligned} \text{Area of styroform} &= 6 \times 18 = 108.00 \text{ sq.in.} \\ &115.06 \text{ sq.in.} \end{aligned}$$

$$\text{Net area} = 288.0 - 115.06 = 172.94 \text{ sq.in.}$$

$$\text{From reinf. bars } 7 \times 0.11 \times 6 = 4.62 \text{ sq.in.}$$

$$\text{Area of composite section} = 177.56 \text{ sq.in.}$$

APPENDIX D

-113-

DETERMINATION OF THE CREEP FACTORS

The creep factors were determined with respect to the influence of the effective thickness of the beams, the age of concrete at loading and the concrete compressive strength.

(a) Influence of effective thickness

The effective thickness was determined according to Ruesch (31).

$$d_w = \frac{2F}{U}$$

where

d_w = effective thickness

F = area of concrete in the cross-section

U = circumference exposed to desiccation

The ratios of the effective thicknesses were used for the computation of the percentage creep and shrinkage losses in the prestress of Beams I to III. Beam IV was used as the reference beam.

Beam IV (Hollow beam)

$$\text{Area of 4 tendon ducts} = 4 \times 3.1416 \times 1.5^2 = 7.0 \text{ sq.in.}$$

$$\text{Area of reinf. bars} = 6 \times 0.11 = 0.66 \text{ sq.in.}$$

$$\text{Area of styroform} = 6 \times 18 = \frac{108.00 \text{ sq.in.}}{115.66 \text{ sq.in.}}$$

$$F = 288 - 115.66 = 172.28 \text{ sq.in.}$$

$$U = 2 (12+24+6+18) = 120 \text{ in.}$$

$$d_w = \frac{2 \times 172.28}{120} = 2.87 \text{ in.}$$

From Figure 7 in (31) the creep factor due to effective thickness

$$C_{a4} = 1.07$$

Beam III

-114-

$$\text{Area of 4 ducts} = 7.06 \text{ sq.in.}$$

$$\begin{aligned} \text{Area of reinf. bars } 6 \times 0.11 &= \underline{0.66 \text{ sq.in.}} \\ &7.72 \text{ sq.in.} \end{aligned}$$

$$F = 288 - 7.72 = 280.28 \text{ sq.in.}$$

$$U = 2 (12+24) = 72.0 \text{ in.}$$

$$d_w = \frac{2 \times 280.28}{72} = 7.78 \text{ in.}$$

$$C_{a3} = 0.86$$

Beam II

$$\text{Area of duct} = 1.76 \text{ sq.in.}$$

$$\begin{aligned} \text{Area of reinf. bars } = 7 \times 0.11 &= \underline{0.77 \text{ sq.in.}} \\ &2.53 \text{ sq.in.} \end{aligned}$$

$$F = 288 - 2.53 = 285.47 \text{ sq.in.}$$

$$U = 2 (12+24) = 72 \text{ in.}$$

$$d_w = \frac{2 \times 285.47}{72} = 7.92 \text{ in.}$$

$$C_{a2} = 0.84$$

Beam I

$$\text{Area of 3 ducts} = 5.30 \text{ sq.in.}$$

$$\begin{aligned} \text{Area of reinf. bars } = 14 \times 0.11 &= \underline{1.54 \text{ sq.in.}} \\ &6.84 \text{ sq.in.} \end{aligned}$$

$$F = 288 - 6.84 = 281.16 \text{ sq.in.}$$

$$U = 72 \text{ in.}$$

$$d_w = \frac{2 \times 281.16}{72} = 7.8 \text{ in.}$$

$$C_{a1} = 0.86$$

(b) Influence of age of concrete at Loading (prestressing)

Beam IV

Age at prestressing 66 days

Creep factor determined according to (31),

$$C_{b4} = 0.78$$

Beam III

Age at prestressing 99 days

$$C_{b3} = 0.72$$

Beam II

Age at prestressing 155 days

$$C_{b2} = 0.66$$

Beam I

Age at prestressing 145 days

$$C_{b1} = 0.671$$

(c) Influence of concrete compressive strength

A most important factor which influences the compressive strength of concrete is the water/cement ratio. The computation of creep factor due to the influence of compressive strength of concrete was based on the water/cement ratio. This ratio was determined according to (32). The compressive strength of Beam IV was used as the base.

Beam IV

$$C_{c4} = 1.0$$

Beam III

From compression tests performed in the laboratory,

strength of concrete for Beam IV = 5000 psi

strength of concrete for Beam III = 6930 psi

$$\text{Ratio of compressive strength} = \frac{6930}{5000} = 1.385$$

From Fig. 23 of (32), compressive strength ratio of $\frac{4300}{2900} = 1.48$ is produced by difference in water/cement ratio of 0.150. Therefore the ratio 1.385 will be produced by a difference in water/cement ratio of

$$\frac{1.385}{1.48} \times 0.150 = 0.140.$$

From Fig. 6 in (31) the creep factor $C_{c3} = 0.66$

Beam II

Compressive strength of concrete for Beam II = 4640 psi

$$\frac{5000}{4640} = 1.08$$

$$\text{Difference in water/cement ratio} = \frac{1.08}{1.48} \times 0.150 = 0.109$$

$$\text{Creep factor } C_{c2} = 1.29$$

Beam I

Compressive strength of concrete = 5770 psi

$$\frac{5770}{5000} = 1.152$$

$$\text{Difference in water/cement ratio} = \frac{1.152}{1.48} \times 0.150 = 0.117$$

$$\text{Creep factor } C_{c1} = 0.7$$

ULTIMATE TORSIONAL STRENGTHS OF 4 BEAMS DETERMINED IN
ACCORDANCE WITH THE EQUATIONS OF DR. HSU AND DR. LAMPERT.

In this illustrative example the torsional capacities of the non-prestressed equal volume beams are first determined. The effect of prestressing was then considered.

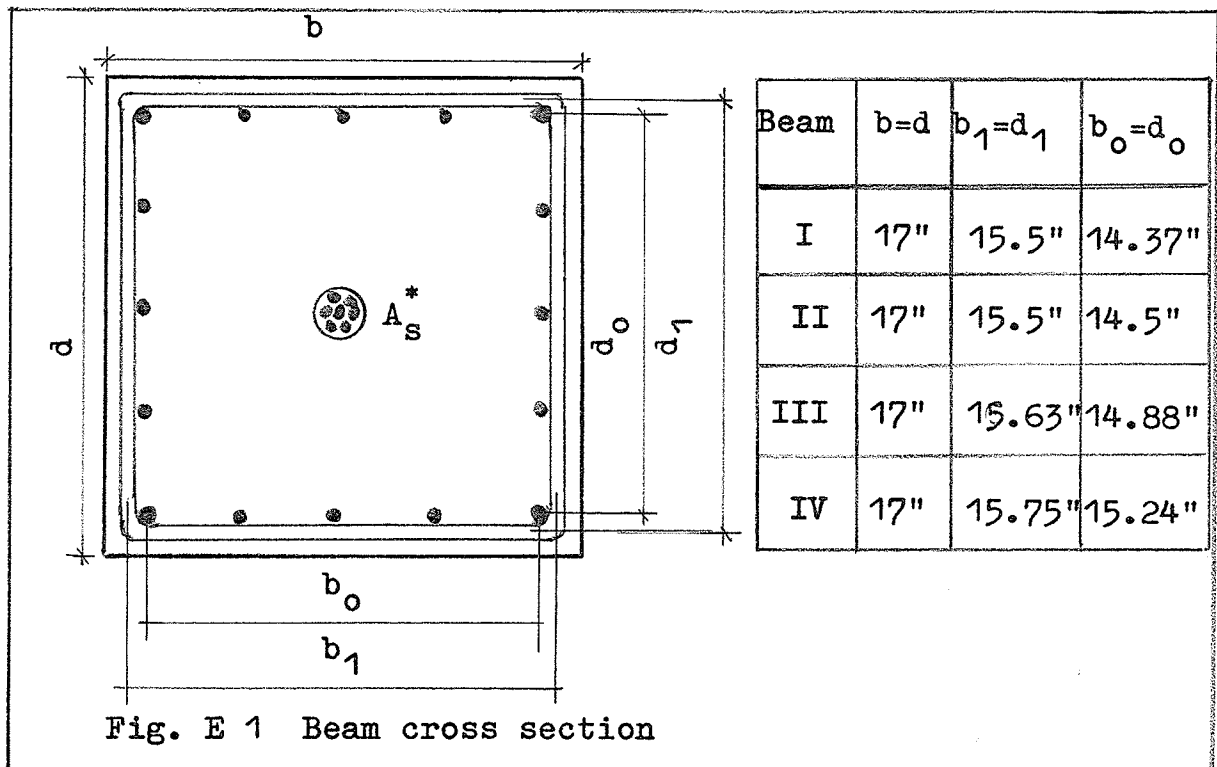


Table E1 Properties of the non-prestressed reinforcement.

Reinforcement	ϕ (in)	Area (in ²)	f_y (Ksi)
$\frac{5}{8}$ " ϕ bars	0.625	0.304	46.0
$\frac{1}{2}$ " ϕ bars	0.50	0.196	45.4
$\frac{3}{8}$ " ϕ bars	0.375	0.11	47.8
$\frac{1}{4}$ " ϕ bars	0.25	0.05	59.2

Table E2 Reinforcement of the beams

Beam	Longitudinal	Transverse	Prestress	
			concr. stress	Area A_s^*
I	16 $\frac{5}{8}$ " ϕ bars	$\frac{1}{2}$ " ϕ stirrups, $s=2.5$ "	250 psi	0.482 in ²
II	16 $\frac{1}{2}$ " ϕ bars	$\frac{1}{2}$ " ϕ stirrups, $s=3.88$ "	250 psi	0.482 in ²
III	16 $\frac{3}{8}$ " ϕ bars	$\frac{3}{8}$ " ϕ stirrups, $s=3.9$ "	250 psi	0.482 in ²
IV	16 $\frac{1}{4}$ " ϕ bars	$\frac{1}{4}$ " ϕ stirrups, $s=3.94$ "	250 psi	0.482 in ²

Determination of the stirrup spacing to make each beam
have equal volume reinforcement

For equal volume reinforcement $m = \frac{A_l \times s}{A_t \times s} = 1$

Beam I : $\frac{16 \times 0.304 \times s_1}{0.196 \times 4 (15.5)} = 1 ; s_1 = 2.5 \text{ in.}$

Beam II : $\frac{16 \times 0.196 \times s_2}{0.196 \times 4 (15.5)} = 1 ; s_2 = 3.88 \text{ in.}$

Beam III : $\frac{16 \times 0.11 \times s_3}{0.11 \times 4 (15.63)} = 1 ; s_3 = 3.90 \text{ in.}$

Beam IV : $\frac{16 \times 0.05 \times s_4}{0.05 \times 4 (15.75)} = 1 ; s_4 = 3.94 \text{ in.}$

Determination of the area of prestressing steel to produce
a chosen concrete compression stress of 250 psi

Concrete stress due to prestress $f_{cp} = 250 \text{ psi}$

Total concrete compressive force $F = 0.25 \times 17^2 = 72.25 \text{ K}$

Yield stress in tendon = 250 Ksi

Effective stress after losses = $0.6 f'_s$

$$\frac{72.25}{A_s^*} = 250 \times 0.60$$

$$A_s^* = \frac{72.25}{250 \times 0.60} = 0.482 \text{ in}^2$$

Computation of the ultimate torque for the non-prestressed beams

(a) Computation according to equation (1)

$$\text{Beam I} \quad \frac{f_{ly}}{f_{ty}} = \frac{46.0}{45.4} = 1.01$$

$$\begin{aligned} T_u &= \frac{2.4}{17} \times 17.0^2 \times 17 \quad 3600 \\ &\quad + (0.66 \times 1.01 + 0.33) \frac{15.5^2 \times 0.196 \times 45.4}{2.5} \\ &= 171.6 + 0.997 \times 855.14 = \underline{1024.17 \text{ Kip in.}} \end{aligned}$$

$$\text{Beam II} \quad \frac{f_{ly}}{f_{ty}} = \frac{45.4}{45.4} = 1$$

$$\begin{aligned} T_u &= 171.6 + (0.66 \times 1.0 + 0.33) \frac{15.5^2 \times 0.196 \times 45.4}{3.88} \\ &= \underline{717.10 \text{ Kip in.}} \end{aligned}$$

$$\text{Beam III} \quad \frac{f_{ly}}{f_{ty}} = 1$$

$$T_u = 171.6 + 0.99 \frac{15.63^2 \times 0.11 \times 47.8}{3.9} = \underline{497.67 \text{ Kip in.}}$$

Beam IV

$$T_u = 171.6 + 0.99 \frac{15.75^2 \times 0.05 \times 59.2}{3.94} = \underline{356.01 \text{ Kip in.}}$$

(b) Computation according to equation (4)

Beam I

$$Z_y = 16 \times 0.304 \times 46.0 = 223.74 \text{ K}$$

$$B_y = 0.196 \times 45.4 = 8.90 \text{ K}$$

$$T_{uo} = 2 \times 14.37^2 \frac{8.90 \times 223.74}{2.5 \times 4 (14.37)} = \underline{1537.16 \text{ Kip in.}}$$

Beam II

$$Z_y = 16 \times 0.196 \times 45.4 = 142.37 \text{ K}$$

$$B_y = 8.9 \text{ K}$$

$$T_{uo} = 2 \times 14.5^2 \frac{8.9 \times 142.37}{3.88 \times 4 (14.5)} = \underline{997.85 \text{ Kip in.}}$$

Beam III

$$Z_y = 16 \times 0.11 \times 47.8 = 84.13 \text{ K}$$

$$B_y = 0.11 \times 47.8 = 5.26 \text{ K}$$

$$T_{uo} = 2 \times 14.88^2 \frac{5.26 \times 84.13}{3.9 \times 4 (14.88)} = \underline{611.55 \text{ Kip in.}}$$

Beam IV

$$Z_y = 16 \times 0.05 \times 59.2 = 47.36 \text{ K}$$

$$B_y = 0.05 \times 59.2 = 2.96 \text{ K}$$

$$T_{uo} = 2 \times 15.24^2 \frac{2.96 \times 47.36}{3.94 \times 4 (15.24)} = \underline{354.89 \text{ Kip in.}}$$

Computation of the ultimate torque with the effect of pre-stress added

(a) Computation according to equation (2), page 8

$$f_{pa} = 250 \text{ psi}$$

$$M_{tp} = 171.6$$

-121-

$$\begin{aligned} M_{tp}^* &= M_{tp} \left(1 + 10 \frac{250}{3600} \right) \\ &= 1.302 M_{tp} \end{aligned}$$

Contribution made by prestress

$$= 0.302 M_{tp} = 0.302 \times 171.6 = \underline{51.82 \text{ Kip in.}}$$

Sum of the ultimate torques for each beam:

$$\text{Beam I} \quad T_{up} = 1024.17 + 51.82 = \underline{1075.99 \text{ Kip in.}}$$

$$\text{Beam II} \quad T_{up} = 717.10 + 51.82 = \underline{768.92 \text{ Kip in.}}$$

$$\text{Beam III} \quad T_{up} = 497.67 + 51.82 = \underline{549.49 \text{ Kip in.}}$$

$$\text{Beam IV} \quad T_{up} = 356.01 + 51.82 = \underline{407.83 \text{ Kip in.}}$$

(b) Effect of prestress taken into consideration,
using equation (4), page 11

Beam I

$$\begin{aligned} Z_y &= 223.74 + 0.482 \times 250 \\ &= 223.74 + 120.5 = 344.24 \text{ K} \end{aligned}$$

$$B_y = 8.9 \text{ K}$$

$$T_{uo} = 2 \times 14.37^2 \frac{8.9 \times 344.24}{2.5 \times 4 (14.37)} = \underline{1906.79 \text{ Kip in.}}$$

Beam II

$$Z_y = 142.37 + 120.5 = 262.87 \text{ K}$$

$$B_y = 8.9 \text{ K}$$

$$T_{uo} = 2 \times 14.5^2 \frac{8.9 \times 262.87}{3.88 \times 4 (14.5)} = \underline{1355.69 \text{ Kip in.}}$$

Beam III

-122-

$$Z_y = 84.13 + 120.5 = 204.63 \text{ K}$$

$$T_{uo} = 2 \times 14.88^2 \frac{5.26 \times 204.63}{3.9 \times 4 (14.88)} = \underline{953.85 \text{ Kip in.}}$$

Beam IV

$$Z_y = 43.36 + 120.5 = 163.86 \text{ K}$$

$$T_{uo} = 2 \times 15.24^2 \frac{2.96 \times 163.86}{3.94 \times 4 (15.24)} = \underline{660.08 \text{ Kip in.}}$$

The computed ultimate torsional moments are represented graphically in Fig. 5, page 13

ULTIMATE TORSIONAL MOMENT OF THE TEST BEAMS COMPUTED IN
ACCORDANCE WITH THE EQUATIONS OF DR. HSU AND DR. LAMPERT

(a) Ultimate torsional moment according to HSU/HOGNESTAD

$$M_{tp}^* = M_{tp} \sqrt{1 + 10 \frac{f_{pa}}{f_c}}$$

$\sqrt{1 + 10 \frac{f_{pa}}{f_c}}$ accounts for the effect of
prestress.

The ultimate torque equation for nonprestressed beam is

$$T_u = \frac{2.4}{\sqrt{b}} b^2 d \sqrt{f'_c} + (0.66 m \frac{f_{ly}}{f_{ty}} + 0.33 \frac{d_1}{b_1}) \frac{b_1 d_1 A_t f_{ty}}{S}$$

The first term on the right hand side is the contribution made by the concrete. The second term is the contribution made by the non/prestressed reinforcement.

$$\frac{2.4}{\sqrt{b}} b^2 d \sqrt{f'_c} \text{ in pound-inch. (b and d in inches, } f'_c \text{ in lb/sq.in).}$$

Beam IV

$$P_l = 6 \times 0.11 \times 5.5 = 3.63 \text{ cu. in.}$$

$$P_t = 0.11 \times 2 (10.62 + 22.62) = 7.32 \text{ cu.in.}$$

$$\frac{f_{ly}}{f_{ty}} = 1$$

$$m = \frac{3.63}{7.32} = 0.50 ; \text{ use } m = 0.7$$

$$\frac{2.4}{\sqrt{12}} \times 12^2 \times 24 \sqrt{5000} = 169.0 \text{ Kip in.}$$

-124-

This is the contribution made by the concrete.

$$(0.66 \times 0.7 + 0.33 \times \frac{22.62}{10.62}) \frac{10.62 \times 22.62 \times 0.11 \times 56.4}{5.5} \\ = 1.164 \times 271.0 = 315.0 \text{ Kip in.}$$

This is the contribution made by the non-prestressed reinforcement.

$$T_u = 169.0 + 315.0 = 484.0 \text{ Kip in.}$$

Determination of the effect of prestress.

$$\text{Total loss in prestress} = 18.90 + 3.84 = 22.74 \%$$

Prestressing force on Sept. 19 (testing date)

$$\frac{100 - 22.74}{100} \times 57.5 = 44.5 \text{ Kips}$$

$$f_{pa} = \frac{44.5 \times 1000}{177.56} = 250.6 \text{ psi}$$

$$\sqrt{1 + 10 \frac{250.6}{5000}} = 1.225$$

$$M_{tp} = 169.0 \text{ Kip in.}$$

$$M_{tp}^* = 169.0 \times 1.225 = 207.3 \text{ Kip in.}$$

$$\text{Contribution by prestress} = 207.3 - 169.0 = 38.3 \text{ Kip in.}$$

$$T_{up} = 484.0 + 38.3 = \underline{522.3 \text{ Kip in.}}$$

Beam I

$$P_1 = 14 \times 0.11 \times 4.75 = 7.31 \text{ cu.in.}$$

$$P_t = 0.11 \times 2 (10.62 + 22.62) = 7.31 \text{ cu.in.}$$

$$m = \frac{p_l}{p_t} = 1$$

-125-

Contribution by the concrete

$$= \frac{2.4}{3.46} \times 144 \times 24 \sqrt{5770} \text{ lb in.} = 2.4 \sqrt{5770} \text{ Kip in.}$$

$$= 182.4 \text{ Kip in.}$$

$$(0.66 \times 1.0 + 0.33 \times 2.13) \frac{1490.0}{8} = 1.363 \times \frac{1490.0}{4.75}$$

$$= 427.5 \text{ Kip in.}$$

$$T_u = 182.4 + 427.5 = 609.9 \text{ Kip in.}$$

Creep and shrinkage losses (Beam IV as reference beam):

$$\text{Creep factor for Beam IV } C_{a1} \times C_{b1} \times C_{c1}$$

$$= 1.07 \times 0.78 \times 1.0 = 0.835$$

$$\text{For Beam I } C = 0.86 \times 0.671 \times 0.70 = 0.404$$

Creep and shrinkage loss for Beam IV determined by strain gauge reading = 18.9 % (page 54).

Creep and shrinkage loss for Beam I

$$= 18.9 \times \frac{0.404}{0.835} = 9.15 \%$$

$$\text{Initial losses (page 53)} = 1.54 \%$$

$$\text{Relaxation losses} = 3.84 \%$$

$$\text{Total loss in prestress} = 14.53 \%$$

Prestressing force at testing

$$= \frac{85.47}{100} \times 72.0 \text{ Kips} = 61.6 \text{ Kips}$$

$$f_{pa} = \frac{61.6 \times 1000}{293.50} = 210.2 \text{ psi}$$

$$\sqrt{1 + 10 \frac{210.2}{5770.0}} = 1.167$$

$$M_{tp}^* = 182.4 \times 1.167 = 212.2 \text{ Kip in.}$$

$$\text{Contribution by prestress} = 212.2 - 182.4 = 29.8 \text{ Kip in.}$$

$$T_{up} = 609.9 + 29.8 = \underline{639.7 \text{ Kip in.}}$$

Beam II

$$P_l = 7 \times 0.11 \times 4.75 = 3.66 \text{ cu.in.}$$

$$P_t = 0.11 \times 2 (10.62 + 22.62) = 7.32 \text{ cu.in.}$$

$$m = \frac{3.66}{7.32} = 0.50 ; \text{ use } 0.70$$

Contribution by the concrete

$$= 2.4 \quad 4640 \text{ Kip in.} = 163.5 \text{ Kip in.}$$

$$(0.66 \times 0.7 + 0.33 \times 2.13) \frac{1490.0}{4.75} = 365.0 \text{ Kip in.}$$

$$T_u = 163.5 + 365.0 = 528.5 \text{ Kip in.}$$

$$\text{Creep factor } C = C_{b1} \times C_{b2} \times C_{b3}$$

$$= 0.84 \times 0.66 \times 1.29 = 0.715$$

$$\text{Creep and shrinkage loss} = \frac{0.715}{0.835} \times 18.9 = 16.20 \%$$

$$\text{Initial losses} = 1.54 \%$$

$$\text{Relaxation losses} = 3.84 \%$$

$$\text{Total loss in prestress} = 21.58 \%$$

Prestressing force at testing

$$= \frac{78.42}{100} \times 24.0 = 18.8 \text{ Kips}$$

$$f_{pa} = \frac{18.8 \times 1000}{293.39} = 64.1 \text{ psi}$$

$$\sqrt{1 + \frac{641.0}{4640}} = 1.067$$

$$M_{tp}^* = 163.5 \times 1.067 = 174.2 \text{ Kip in.}$$

Contribution by prestress = $174.2 - 163.5 = 10.70$ Kip in.

$$T_{up} = 528.5 + 10.70 = \underline{539.20 \text{ Kip in.}}$$

Beam III

$$P_1 = 6 \times 0.11 \times 5.5 = 3.63 \text{ cu.in.}$$

$$P_t = 0.11 \times 2 (10.62 + 22.62) = 7.32 \text{ cu.in.}$$

$$m = \frac{3.63}{7.32} = 0.5 ; \text{ use } m = 0.7$$

Contribution made by concrete

$$= 2.4 \quad 6930 \text{ Kip in} \quad = 200.0 \text{ Kip in.}$$

$$(0.66 \times 0.7 + 0.33 \times 2.13) \frac{1490}{5.5} = 314.5 \text{ Kip in.}$$

$$T_u = 200.0 + 314.5 = 514.5 \text{ Kip in.}$$

$$\text{Creep factor } C = 0.86 \times 0.72 \times 0.66 = 0.409$$

$$\text{Creep and shrinkage loss} = \frac{0.409}{0.835} \times 18.9 = 9.26 \%$$

$$\text{Initial losses} = 1.54 \%$$

$$\text{Relaxation losses} = 3.84 \%$$

$$\text{Total loss in prestress} = 14.64 \%$$

Prestressing force at testing

$$= \frac{85.36}{100} \times 58.4 = 49.8 \text{ Kips}$$

$$f_{pa} = \frac{49.8 \times 1000}{285.56} = 175.0 \text{ psi}$$

$$\sqrt{1 + \frac{1750.0}{6930}} = 1.12$$

$$M_{tp}^* = 200.0 \times 1.12 = 224.0 \text{ Kip in.}$$

Contribution by prestress = $224.0 - 200 = 24.0$ Kip in.

$$T_{up} = 514.5 + 24.0 = \underline{538.5 \text{ Kip in.}}$$

(b) Ultimate torsional moment computed according to LAMPERT

$$T_{uo} = 2 A_o \sqrt{\frac{B_y Z_y}{su}} \text{ - - - - - (4)}$$

Beam IV

$$2 A_o = 2 \times 8.5 \times 20.5 = 348.2 \text{ sq. in.}$$

$$u = 2 (8.5 + 20.5) = 58.0 \text{ in.}$$

$$B_y = 0.11 \times 56.4 = 6.2 \text{ Kips}$$

$$Z_y = 6 \times 0.11 \times 56.4 + 12 \times 0.0594 \times 241.3 = 209.2 \text{ Kips}$$

$$T_{uo} = 348.2 \left(\frac{6.2 \times 209.2}{5.5 \times 58.0} \right)^{\frac{1}{2}} = \underline{703.0 \text{ Kip in.}}$$

Beam I

$$2 A_o = 2 \times 9.87 \times 21.87 = 431.5 \text{ sq. in.}$$

$$u = 2 (9.87 + 21.87) = 63.48 \text{ in.}$$

$$Z_y = 14 \times 0.11 \times 56.4 + 9 \times 0.0594 \times 241.3 = 215.7 \text{ Kips}$$

$$T_{uo} = 431.5 \left(\frac{6.2 \times 215.7}{4.75 \times 63.48} \right)^{\frac{1}{2}} = \underline{907.0 \text{ Kip in.}}$$

Beam II

$$2 A_o = 431.5 \text{ sq.in.}$$

$$u = 63.48 \text{ in.}$$

$$Z_y = 7 \times 0.11 \times 56.4 + 3 \times 0.0594 \times 241.3 = 86.3 \text{ Kips}$$

$$T_{uo} = 431.5 \left(\frac{6.2 \times 86.3}{4.75 \times 63.48} \right)^{\frac{1}{2}} = \underline{575.0 \text{ Kip in.}}$$

Beam III

$$2 A_o = 348.2 \text{ sq.in.}$$

$$u = 58.0 \text{ in.}$$

$$Z_y = 209.2 \text{ Kips}$$

$$T_{uo} = \underline{703.0 \text{ Kip in.}}$$